University of Santiago de Compostela

PhD Thesis

Numerical solution of the Boltzmann transport equation for photons and of some equations derived from the Fokker-Planck approximation for electrons. Application to radiotherapy.

Author:
Taposh Kumar Das

Supervisor:
Óscar López Pouso

July 27, 2012

Contents

Introduction

The aim of radiotherapy treatment is the elimination of tumor cells by the concentration of high doses of radiation in the tumor tissue while not damaging healthy tissue. In external radiotherapy, ionizing radiation is applied from an external source.

In the present time we use radiation therapy (also called radiotherapy, X-ray therapy, or irradiation) to destroy the cancer cells and shrink tumors, by destroying the genetic materials of those cells in such a way that they are not able to continue to grow and divide [38]. Although some normal ambient cells will be destroyed by the radiotherapy, most of them can recover from the effects of radiation and function properly [38]. Finally the result of radiotherapy will be to damage as many cancer cells as possible but minimum number of normal cells should be affected by the radiation therapy.

The treatment of radiotherapy is usually applied via a linear accelerator in which electrons are accelerated to high energies using high frequency electromagnetic waves. These electrons strike a target such as tungsten, which produces X-rays in the bremsstrahlung process. X-rays are the first form of photon radiation to be used to treat cancer. The rays can be used to destroy cancer cells on the surface of an area, or penetrate to tissues deeper in the body. In the treatment of radiotherapy, one has to find the best alternatives for the photon beam orientation, as well as determining the value of different fields in order to achieve the desired distribution dose in the tumor site [23].

The cancer patients take therapies with high energy ionizing radiation in this time and, for maximum recovery of patients, it is most important to deposit a sufficient amount of energy in tumor or in cancer area [26]. So, it is very important to apply the correct dose distribution for the success of such radiation treatment.

“In principle an exact dose calculation for photon and electron radiation is possible and well known. Based on the known physical principles of interaction of radiation with human tissue the transport of energy into the patients body can be modelled and calculated by an appropriate Monte Carlo (MC) algorithm (Andreo 1991). If the modelling has been

done carefully this leads to exact results of the dose distribution in arbitrary geometries and nowadays highly developed MC codes for dose calculations are available. The drawback of MC algorithms lies in their high computation times which still makes them unattractive for everyday clinical use" [15]. "Monte Carlo methods provide approximate solutions to a variety of mathematical problems by performing statistical sampling experiments. They can be loosely defined as statistical simulation methods, where statistical simulation is defined in quite general terms to be any method that utilizes sequences of random numbers to perform the simulation" [40].

The Boltzmann transport equation (BTE) is the base of most of the dose calculation models. The Fokker-Planck and Fermi equations can be viewed as approximations of the BTE. In its original form, the BTE takes rigorously into account the inhomogeneities of the patient and the dispersive effects of the particles. The BTE is a integro-differential equation which is studied in many fields of physics, for example, in nuclear reactor physics, astrophysics, optical tomography, X-ray spectra and analysis of electron microbeams. Since the high energy particles move at speeds that are very close to the speed of light, it is the stationary BTE the one be used in radiotherapy. In this stationary case it has six variables: three spatial, two angular and one energy variable. One should seek a numerical solution, which can be stochastic or deterministic. Monte Carlo (MC) would be an example of stochastic method to solve the BTE [23].

Some advantages and disadvantages of the MC method

We show in this section some advantages and drawbacks of Monte Carlo methods which have been taken from reference [39] and [23].

Advantages of the MC method:

1. Algorithms are simple, coding and debugging efforts are minimised.

2. If the sampling algorithms are faithful, the accuracy of the code is determined by the accuracy of the fundamental cross section data.

3. They know quite well all physical interactions.

4. Geometries can be used for general 1-D, 2-D and 3-D.

Drawbacks of MC method:

1. Since the algorithms are microscopic, there is little theoretical insight derived in consideration of the macroscopic characteristics of radiation fields.
2. Monte Carlo calculations consume great amounts of computing resources, too much to be of practical use at this time in day-to-day radiotherapy, such as routine treatment planning.
3. We need a lot of calculation time to remove statistics uncertainties.
4. Due to these statistic it can be difficult to statistics to determine the effect of small variations in the parameters.
5. A Monte Carlo code should be treated as a black box and it is not always easy to get the right answers. The parameters to define the ranges of energy and length of particle paths must be chosen carefully. The algorithm need to be modified and adapted to the particular problem.

Some advantages and disadvantages of the Boltzmann transport equation

We show in this section some advantages and drawbacks of BTE which have been taken reference ([23]).

Advantages of the BTE:

1. The solutions can be replicated in different computer executions.
2. The method is quite well adapted for making changes in the parameters for a given application.
3. It may be faster than the Monte Carlo method.
4. Generates a solution for all points in phase space.

Drawbacks of the BTE:

1. Errors in the solution usually are not easy to estimate.
2. Some physics can be difficult to model.

3. It may require a very fine mesh to obtain solutions with a sufficient accuracy.

Contents

In this section we explain shortly the contents of our work.

The purpose of this memory is to describe the main interactions happening in the physical body in a radiation treatment, also to present numerical solution of Boltzmann transport equation (BTE) in three dimensional case for application in radiotherapy and to give some numerical results of photons on some planes. One differential equation related to the Fokker-Planck approximation of the BTE for electrons is solved as well by means of a finite difference method.

Following [15], the BTE model consists of two transport equations, one to describe the transport of photons and another one to describe the transport of electrons. A more complete model could include a third equation for positrons, but we have not considered it in this memory.

We get the formulation for dose calculation from [15] which is

$$D(\mathbf{r}) = \frac{mc^2}{\rho(r)} T \int_{\epsilon_{\mathsf{s}}}^{\infty} S_{\mathrm{M}}(\mathbf{r}, \epsilon'_{\mathsf{e}}) \Phi(\mathbf{r}, \epsilon'_{\mathsf{e}}) \mathrm{d}\epsilon'_{\mathsf{e}}, \tag{1}$$

where $\Phi(\mathbf{r}, \epsilon_{\mathsf{e}}) := \int_{S^2} \psi_{\mathsf{e}}(\mathbf{r}, \mathbf{\Omega}'_{\mathsf{e}}, \epsilon_{\mathsf{e}}) \mathrm{d}\mathbf{\Omega}'_{\mathsf{e}}$.

Here m is the mass of particle, c is the velocity of light in vacuum, ρ the local density of the medium and T the duration of the irradiation. To compute the dose from (1) we need the number of electrons (ψ_{e}) and the stopping power (S_{M}), but the stopping power is given, so we have to find only the number of electrons. And we get those electrons by solving the following Boltzmann transport equation.

The Boltzmann transport equation for electrons is

$$\begin{aligned}
\boldsymbol{\Omega}_{\mathsf{e}} \cdot \nabla \psi_{\mathsf{e}}(\mathbf{r}, \boldsymbol{\Omega}_{\mathsf{e}}, \epsilon_{\mathsf{e}}) =& \rho_{\mathsf{e}}(\mathbf{r}) \int_0^{\infty} \int_{S^2_{\frac{1}{2}}} \tilde{\sigma}_{C,\mathsf{e}}(\epsilon'_\gamma, \epsilon_{\mathsf{e}}, \boldsymbol{\Omega}'_\gamma \cdot \boldsymbol{\Omega}_{\mathsf{e}}) \psi_\gamma(\mathbf{r}, \boldsymbol{\Omega}'_\gamma, \epsilon'_\gamma) \, \mathrm{d}\boldsymbol{\Omega}'_\gamma \, \mathrm{d}\epsilon'_\gamma \\
&+ \rho_{\mathsf{e}}(\mathbf{r}) \int_{\epsilon_s}^{\infty} \int_{S^2_{\frac{1}{4}}} \tilde{\sigma}_{\mathrm{M}}(\epsilon'_{\mathsf{e}}, \epsilon_{\mathsf{e}}, \boldsymbol{\Omega}'_{\mathsf{e}} \cdot \boldsymbol{\Omega}_{\mathsf{e}}) \psi_{\mathsf{e}}(\mathbf{r}, \boldsymbol{\Omega}'_{\mathsf{e}}, \epsilon'_{\mathsf{e}}) \, \mathrm{d}\boldsymbol{\Omega}'_{\mathsf{e}} \, \mathrm{d}\epsilon'_{\mathsf{e}} \\
&+ \rho_{\mathsf{e}}(\mathbf{r}) \int_{\epsilon_s}^{\infty} \int_{S^2_{\frac{2}{4}}} \tilde{\sigma}_{\mathrm{M},\delta}(\epsilon'_{\mathsf{e}}, \epsilon_{\mathsf{e}}, \boldsymbol{\Omega}'_{\mathsf{e}} \cdot \boldsymbol{\Omega}_{\mathsf{e}}) \psi_{\mathsf{e}}(\mathbf{r}, \boldsymbol{\Omega}'_{\mathsf{e}}, \epsilon'_{\mathsf{e}}) \, \mathrm{d}\boldsymbol{\Omega}'_{\mathsf{e}} \, \mathrm{d}\epsilon'_{\mathsf{e}} \\
&+ \rho_{\mathsf{c}}(\mathbf{r}) \int_{S^2} \sigma_{\mathrm{Mott}}(\mathbf{r}, \epsilon_{\mathsf{e}}, \boldsymbol{\Omega}'_{\mathsf{e}} \cdot \boldsymbol{\Omega}_{\mathsf{e}}) \psi_{\mathsf{e}}(\mathbf{r}, \boldsymbol{\Omega}'_{\mathsf{e}}, \epsilon_{\mathsf{e}}) \, \mathrm{d}\boldsymbol{\Omega}'_{\mathsf{e}} \\
&- \rho_{\mathsf{e}}(\mathbf{r}) \sigma^{\mathrm{tot}}_{\mathrm{M}}(\epsilon_{\mathsf{e}}) \psi_{\mathsf{e}}(\mathbf{r}, \boldsymbol{\Omega}_{\mathsf{e}}, \epsilon_{\mathsf{e}}) \\
&- \rho_{\mathsf{c}}(\mathbf{r}) \sigma^{\mathrm{tot}}_{\mathrm{Mott}}(\mathbf{r}, \epsilon_{\mathsf{e}}) \psi_{\mathsf{e}}(\mathbf{r}, \boldsymbol{\Omega}_{\mathsf{e}}, \epsilon_{\mathsf{e}}), \qquad (2)
\end{aligned}$$

where ρ_{c} is the density of atomic cores in the medium and $\tilde{\sigma}_{C,\mathsf{e}}$ is the scattering cross section of electrons differential in angle and energy for Compton scattering of electrons. $\tilde{\sigma}_{\mathrm{M}}$ is the scattering cross section for primary electrons differential in angle and energy for Møller scattering and $\tilde{\sigma}_{\mathrm{M},\delta}$ is the cross section for secondary electrons (delta-rays) . The scattering cross section for Mott scattering σ_{Mott} is only differential in angle, because Mott scattering is an elastic scattering. The total cross section for Møller and Mott scattering are $\sigma^{\mathrm{tot}}_{\mathrm{M}}$ and $\sigma^{\mathrm{tot}}_{\mathrm{Mott}}$ respectively.

To solve the above BTE for electrons (2) we need the flux of photons (ψ_γ) because all other things are given (see [15]), so we have to find only the number of photons. And we get those photons by solving the following Boltzmann transport equation.
The Boltzmann transport equation for photons is

$$\begin{aligned}
\boldsymbol{\Omega}_\gamma \cdot \nabla \psi_\gamma(\mathbf{r}, \boldsymbol{\Omega}_\gamma, \epsilon_\gamma) =& \rho_{\mathsf{e}}(\mathbf{r}) \int_0^{\infty} \int_{S^2} \tilde{\sigma}_{C,\gamma}(\epsilon'_\gamma, \epsilon_\gamma, \boldsymbol{\Omega}'_\gamma . \boldsymbol{\Omega}_\gamma) \psi_\gamma(\mathbf{r}, \boldsymbol{\Omega}'_\gamma, \epsilon'_\gamma) \, \mathrm{d}\boldsymbol{\Omega}'_\gamma \, \mathrm{d}\epsilon'_\gamma \\
&- \rho_{\mathsf{e}}(\mathbf{r}) \sigma^{\mathrm{tot}}_{C,\gamma}(\epsilon_\gamma) \psi_\gamma(\mathbf{r}, \boldsymbol{\Omega}_\gamma, \epsilon_\gamma), \qquad (3)
\end{aligned}$$

where ρ_{e} is the electron density of the medium and $\tilde{\sigma}_{c,\gamma}$ is the scattering cross section of the photons, differential in angle and energy for Compton scattering of photons and $\sigma^{\mathrm{tot}}_{C,\gamma}(\epsilon_\gamma)$ is the total Compton scattering cross section of photons.

To solve the integro-differential equation (3) directly is very difficult, so we have thought of some other different way to solve it. We have got an idea from [11]. It is very interesting

process and we explain some of this process in here.

We consider a domain and a point R inside the domain. Let us consider that we have to find the number of photons in a fixed direction at R. Since we know the boundary value of incoming photons we can find directly the number of non-interacting photons at R in a fixed direction.

Then, when we go to find the number of one time interacting photon then the number of non-interacting photons will be the source term of the integro-differential equation (3). When we use this non-interacting photons then the equation (3) become a simple differential equation and we can solve it easily.

Similarly, for finding two time interacting photons, one time interacting photons will be the source of photons and applying this, the integro-differential equation became a simple differential equation and so on. But we have seen that the number of three time interacting photons is much smaller than the previous finding number of photons. So we have considered only non-interacting, one time interacting and two time interacting photons in here.

We have made a MATLAB code for solving the integro-differential equation (3) and some results are given in Chapter 4 in this memory.

The Boltzmann transport equation for electrons is much more difficult to solve directly than the BTE for photons. The reason is that the mean free path of electrons is much smaller than the mean free path of photons [15]. So, we cannot find an approximate solution for electron equation like as photon equation.

One possibility for solving the electron transport is to consider instead (the BTE) the so-called Fokker-Planck equation which reads as follows ([15], [27]):

$$\begin{aligned}\boldsymbol{\Omega}_{\mathsf{e}} \cdot \nabla \psi_{\mathsf{e}}(\mathbf{r}, \boldsymbol{\Omega}_{\mathsf{e}}, \epsilon_{\mathsf{e}}) - [T_{\mathrm{Mott}}(\mathbf{r}, \epsilon_{\mathsf{e}}) + T_{\mathrm{M}}(\mathbf{r}, \epsilon_{\mathsf{e}})] L\psi_{\mathsf{e}} \\ - \frac{\partial}{\partial \epsilon_{\mathsf{e}}}[S_{\mathrm{M}}(\mathbf{r}, \epsilon_{\mathsf{e}})\psi_{\mathsf{e}}] = Q(\mathbf{r}, \boldsymbol{\Omega}_{\mathsf{e}}, \epsilon_{\mathsf{e}}),\end{aligned} \tag{4}$$

where L is the Laplace operator on the sphere which is given by

$$L = \frac{\partial}{\partial \mu_{\mathsf{e}}}(1-\mu_{\mathsf{e}}^2)\frac{\partial}{\partial \mu_{\mathsf{e}}} + \frac{1}{1-\mu_{\mathsf{e}}^2}\frac{\partial^2}{\partial \varphi_{\mathsf{e}}^2}, \qquad \mu_{\mathsf{e}} = \cos\vartheta_{\mathsf{e}}. \tag{5}$$

$$where;\ \ 0 \le \vartheta_{\mathsf{e}} \le \pi. \tag{6}$$

Here, Q is the Compton source term

$$\begin{aligned} Q(\mathbf{r}, \mathbf{\Omega}_{\mathsf{e}}, \epsilon_{\mathsf{e}}) =& \rho_{\mathsf{e}}(\mathbf{r}) \int_0^\infty \int_{S^2_{1/2}} \tilde{\sigma}_{C,\mathsf{e}}(\epsilon'_\gamma, \epsilon_{\mathsf{e}}, \mathbf{\Omega}_\gamma \cdot \mathbf{\Omega}'_{\mathsf{e}}) \psi_\gamma(\mathbf{r}, \mathbf{\Omega}'_\gamma, \epsilon'_\gamma)\, \mathrm{d}\mathbf{\Omega}'_\gamma\, \mathrm{d}\epsilon'_\gamma \\ =& \rho_{\mathsf{e}}(\mathbf{r}) \int_{S^2_{1/2}} \int_0^\infty \tilde{\sigma}_{C,\mathsf{e}}(\epsilon'_\gamma, \epsilon_{\mathsf{e}}, \mathbf{\Omega}_\gamma \cdot \mathbf{\Omega}'_{\mathsf{e}}) \psi_\gamma(\mathbf{r}, \mathbf{\Omega}'_\gamma, \epsilon'_\gamma)\, \mathrm{d}\epsilon'_\gamma\, \mathrm{d}\mathbf{\Omega}'_\gamma. \end{aligned} \tag{7}$$

To solve numerically the equation (4), we need an appropriate method. For looking it we have separately solved some differential equations having to do with Fokker-Planck by a finite difference method.

Content of work

In Chapter 1 we recall some history about the treatment by radiotherapy and the effect of radiotherapy on the cell of the human body. In Chapter 2, we give some basic and physical concepts about the interaction of radiation with matter which is needed for understanding the Boltzmann transport equation. In Chapter 3, we write the BTE for photons and electrons, as well as the boundary conditions, and we describe the way in which energy is deposited in the molecules for making the formulation of the absorbed dose. In Chapter 4, we show numerically and graphically the result of BTE for photons and also we discuss details about the solution of BTE for photons. In the last Chapter 5, we show the Fokker-Planck approximation of the BTE for electrons and also we solve differential equation with a finite difference method; errors are computed for test cases with known exact solution.

Chapter 1

Principles of Radiobiology

In the medical science, generally the radiotherapy is used for killing the cancer cells. When a high energy ray hits a molecule then the molecule may be broken. Radiation can be produced by a special machine (linear accelerator), where a metal element is hit to produce electrons. Now, we have discovered more powerful X-ray sources. The more powerful an X-ray, the further into the body it penetrates and the less damage it does to the skin. X-ray energies are measured in kiloelectronvolts (keV) or Megaelectronvolts (MeV; 1 MeV = 1000 keV) [41].

Engineers developed an 8 MeV X-ray generator (or 'linear accelerator') in 1950s. Nowadays we use about 10 MeV X-ray energy in hospital. This technology has been developed very much since then, allowing the radiologists to guide the X-ray beam in order to target more accurately and avoid damaging normal tissue.

"Radiotherapy is usually required for one of the following reasons:

1. As a standalone treatment to cure cancer.

2. To shrink a cancer before surgery.

3. To reduce the risk of a cancer coming back after surgery.

4. To complement chemotherapy.

5. To control symptoms and improve quality of life if a cancer is too advanced to cure", [41].

1.1 Historical perspective

This section is included to provide the reader with a general idea of the origin of radiotherapy. The information has been taken for the cited references, and it is not our intention to state that all dates and names are the only true ones. One can find differences between our explanation and others, and we have made no research in order to find out or to decide which is the best or the correct explanation.

The German Physics professor Wilhelm Röntgen discovered X-rays in 1895. He gave a lecture called "Concerning a New Type Of Ray" which was a revolution in the scientific community. After one week Emil Grubbé a student doctor in Chicago, used radiation to treat cancer and that was the first time for cancer treatment. After three years, two Swedish doctors used radiotherapy to cure several cases of head and neck cancer. Röntgen was awarded the Nobel prize in 1901 for his discovery [41].

H. L. Smith took the first X-rays photograph on 12^{th}, January 1896. Two French physicians, Oudin and Barthélemy, submitted an X-ray photograph of the bones of the hand before the Académie Française on 20^{th}, January 1896. The first medical X-rays radiograph was made in 1896. "History was made in military medicine when portable X-rays machines were deployed with Kitchener's Army of the Sudan in 1898 and were used routinely for diagnostic assistance in traumatic injury. In 1898 the Medical Record (New York) carried 28 references on radiological diagnoses and procedures. The field of radiation therapy began to grow in the early 1900s largely due to the ground breaking work of Nobel Prize-winning scientist Marie Curie, who discovered the radioactive elements polonium and radium. This began a new era in medical treatment and research. Radium was used in various forms until the mid-1900s when cobalt and caesium units came into use. Medical linear accelerators have been used as a sources of radiation from 1940s", [19].

1.1.1 Types of radiotherapy

Generally for the cancer treatment by X-rays we follow the Coutard's fractionated process today, while the radiated rods are used in brachytherapy.
The three main divisions of radiation therapy are external beam radiation therapy or teletherapy, brachytherapy or sealed source radiation therapy and systemic radioisotope therapy or unsealed source radiotherapy. The differences among them lie in the position of

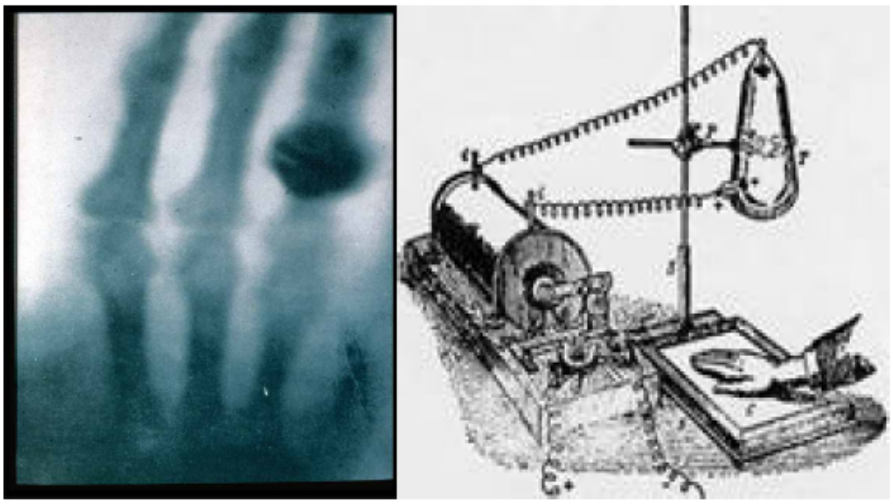

Figure 1.1: On the left, the first X-rays image, thought to be a radiograph of the hand of Röntgen's wife. On the right, experimental apparatus used by Professor Röntgen.

the radiation source [42].

1. **External beam radiotherapy (teletherapy):** The radiation source is located outside the patient's body in this type of treatment. By using a machine such as a linear accelerator or a Gamma Knife we can focus the beam of radiation directly to the location of the cancer area of the patient [44].

2. **Brachytherapy (sealed source radiotherapy):** Brachytherapy is an advanced cancer treatment. In this case the radioactive seeds or sources are placed in or near the tumor for giving a high radiation dose to the tumor while reducing the radiation exposure in the surrounding healthy tissues. The term "brachy" is Greek for short distance. The brachytherapy radiation treatment is localized and precise [43].

3. **Systemic radioisotope therapy (unsealed source radiotherapy):** In this case we consume the radiotherapy orally (either liquid or pill) or infuse into a patient's body through an intravenous line or some other delivery process [44].

1.2 Biological effects of radiation

Radiation is a kind of energy which is carried by waves or a stream of particles. It can change the genes (DNA) and genes control how cells grow and divide. Radiation can damage the genes of a cancer cell so that it cannot grow and divide anymore. Therefore, for killing

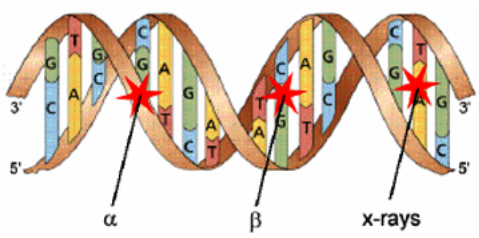

Figure 1.2: In direct effect the ionized particle interacts directly with the critical target in the cell.

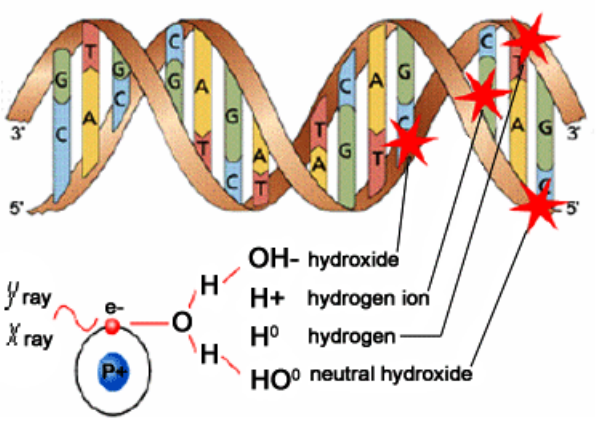

Figure 1.3: In indirect action the radiation interacts with other molecules and atoms (mainly water, since about 80 of a cell is composed of water) within the cell to produce free radicals, which can, through diffusion in the cell, damage the critical target within the cell.

cancer cells and shrink tumors we can use the radiotherapy but we have to think about the biological effect on the normal cells because in the same way the radiotherapy will destroy the healthy cells. Nowadays, ionizing radiation, by definition, interacts only with atoms by a process called ionization. There are two mechanisms by which radiation ultimately affects cells. These two mechanisms are commonly called direct and indirect effects.

1. **Direct effect:** In the direct effect the radiation interacts with the atoms of the DNA molecule, or some other cellular component troublesome to the survival of the cell (Figure 1.2). "If enough atoms are affected such that the chromosomes do not replicate properly, or if there is significant alteration in the information carried by the DNA molecule, then the cell may be destroyed by direct interference with its life-sustaining system", [45] .

2. **Indirect effect:** Since the troublesome component is a small part of the cell the probability of the radiation interacting with the DNA molecule is very small. However,

each cell of human body is mostly water and there is a much higher probability of radiation interacting with water than with air. Sometimes the bonds that hold the water molecule together are broken by the radiation when the radiation interacts with water. At that moment some fragments such as hydrogen (H) and hydroxyls (OH) will be produced. "These fragments may recombine or may interact with other fragments or ions to form compounds, such as water, which would not harm the cell. However, they could combine to form toxic substances, such as hydrogen peroxide (H_2O_2), which can contribute to the destruction of the cell" [45].

1.2.1 Cellular sensitivity to radiation

Not all living cells are equally sensitive to radiation. For instance reproducing cells are more sensitive than the cells which are not reproducing. By direct interaction an active cell will die or will suffer mutation but a direct interaction with the DNA of a dormant cell is much less effective.

Different cell systems have different sensitivities. The living cells can be classified according to their rate of reproduction, which also indicates their relative sensitivity to radiation. This classification is the following:

1. Lymphocytes and blood forming cells,
2. Reproductive and gastrointestinal (GI) cells,
3. Nerve and muscle cells.

Lymphocytes (white blood cells) and cells which produce blood are constantly regenerating, so they are sensitive. Reproductive and gastrointestinal cells are not regenerating as quickly, so they are less sensitive. The nerve and muscle cells are the slowest to regenerate and are the least sensitive cells [19].

The cells of human body have a tremendous ability to repair damage. So the damage is not always irreversible by all the radiation effect. In many cases, the cells are able to completely repair any damage and function normally.

If the damage is severe enough then the affected cell dies. In some instances maybe the cell is damaged but it is still able to reproduce. Sometimes the cell is still able to reproduce but the daughter cells die due to lacking in some critical life-sustaining component. The other possible result for radiation is that the affected cell will not die but it is simply mutated. The mutated cell reproduces and thus the mutation happens again and again. This may be the beginning time for making a malignant tumor [45].

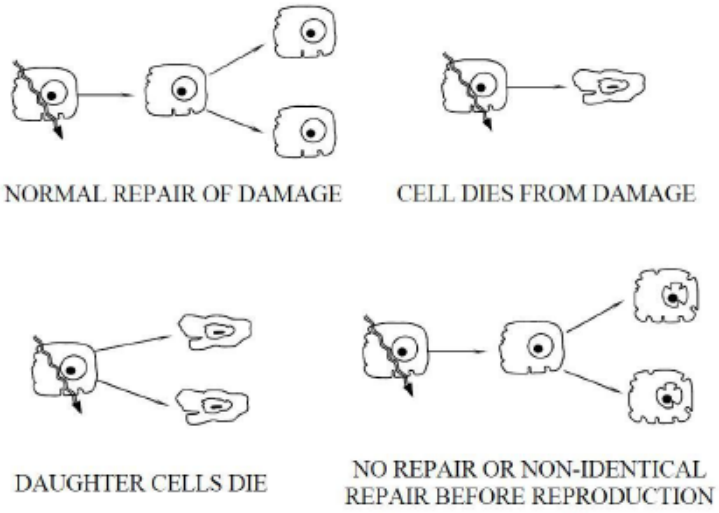

Figure 1.4: Process in cell damage.

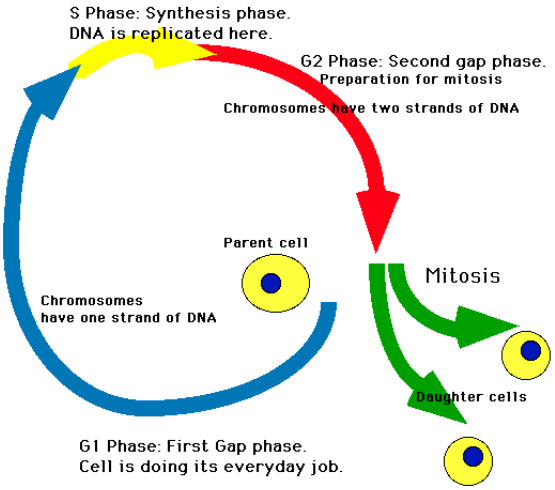

Figure 1.5: The cell life cycle. The parent cell is the resting stage, G1 = RNA and proteins are made, S = DNA is made, G2 = Apparatus for mitosis is built, M = Mitosis (the cell divides into 2 cells).

1.3 How does radiation work to treat cancer?

The waves or a stream of particles carry the radiation till the body. The genes (DNA) and some of the molecules of a cell are damaged by the radiation. Genes control how cells grow and divide. Since radiation damages the genes of a cancer cell so the cells cannot grow and divide any more. For this reason the radiation is used to kill cancer cells and shrink tumors [46].

1.3.1 Cell cycle

In order to understand the radiotherapy treatment work as a treatment, we need to know about the normal life cycle of a cell. The cell cycle goes through 5 phases. When a cell splits, or divides, into 2 cells, it is called mitosis. In Figure 1.5 we can observe the brief periods of the cycle of the cell with a nucleus [46], [19]:

1. **Resting stage**: In this step the cell doesn't divide and it spends much of its life. The duration of this stage depends on the type of cell. This step of a cell can last from a few hours to many years. The cell will go to the G1 phase when he gets the signal to reproduce (divide).

2. **G1 phase**: In this stage, the cell starts to make more proteins to get ready to divide. This phase lasts from 18 to 30 hours.

3. **S phase**: In this step, the chromosomes that contain the genetic code (DNA) are copied, and the new cells will have the same DNA. This phase lasts from 18 to 20 hours.

4. **G2 phase**: This stage takes place immediately before the division of the cell. This stage lasts from 2 to 10 hours.

5. **M phase (mitosis)**: In this phase, the cell actually splits into two new identical cells. This phase lasts only 30 to 60 minutes.

   (a) Cytoplasmic Division: It is a part of M phase. In this case the cytoplasm is often divided between the daughter cells being produced.

   (b) Daughter cells: "The result of mitosis plus division of the cytoplasm is typically two genetically identical daughter cells. Both daughter cells are each smaller than the original parent cell and have unduplicated chromosomes" [48].

1.3.2 Work of radiation

As said above, usually radiation works better on the cells that are actively or quickly dividing. So, the cell cycle is important for cancer treatment. It doesn't work as well on cells that are in the resting stage (G0) or are dividing slowly.
For the radiotherapy treatment it is good news that cancer cells tend to divide quickly and out of control. Radiation therapy kills cancer cells that are dividing, but it also affects dividing cells of normal tissues. The side effects of radiotherapy treatment happen because when the therapy kills the cancer cells simultaneously some normal cells are killed as well. Each time radiation therapy makes balance between destroying the cancer cells and sparing the normal cells.
Radiation cannot kill the cancer cells or normal cells right away, generally the radiotherapy takes many time to kill the cells. After some days or even weeks of treatment the cells will begin to die and they may continue to die off for months after treatment ends. So the radiation treatment has long-term side effects [46].

1.4 How does the doctor measure the dose of radiation?

The amount of energy absorbed by the tissues is called the radiation dose (or dosage). "Before 1985, dose was measured in a unit called a "rad" (radiation absorbed dose). Now the unit is called a "gray" (abbreviated as Gy). One Gy is equal to 100 rads; one centigray (abbreviated as cGy) is the same as 1 rad" [19].
Different tissues can absorb different types of radiation. "For example, the liver can receive a total dose of 3000 cGy, while the kidneys can tolerate only 1800 cGy" [47]. For the clinical use we divide the total dose into smaller doses (called fractions) which are given to the cancer cells daily over a specific time period. The doctor makes a ratio which compares the damage to the cancer cells with the damage to healthy cells. This ratio is called the therapeutic ratio. Doctor do apply technique for making the therapeutic ratio such that this therapeutic ratio will increase the number of damage of cancer cells but less increase as soon as possible the number of damage of normal cells [47].

Chapter 2

The interaction of radiation with matter

For well understanding the Boltzmann transport equations (BTE), we need to know the concept of photon and electron and their properties. Also cross section and various type of intersection of the particles with the matter are needed for the BTE. So in this chapter we discuss about the above mentioned subjects and also about some other things which are related with BTE. The contents of this chapter have been taken in their majority from [31] and [19].

2.1 Some basic concepts

2.1.1 Waves or particles

If we think about light without any prior knowledge, we would assume it to be composed of waves that are continuously emitted from a source (such as a light bulb). In fact, this was the dominant perception amongst scientists until the start of the 20th century. During those days a major problem of theoretical physics had started boggling the minds of the physicists. They had found it impossible to explain the dependence of energy radiated by a black body (a heated cavity) on the wavelength of emitted radiation if they considered light to have continuous wave characteristics. This mystery was solved by Max Planck who developed a theory in which light waves were not continuous but quantized and propagated in small wave packets. This wave packet was later called a photon. This theory and the corresponding mathematical model were extremely successful in explaining the black body

spectrum. The concept was further confirmed by Einstein when he explained the photoelectric effect, an effect in which a photon having the right amount of energy knocks off a bound electron from the atom.

Max Planck proposed that the electromagnetic energy is emitted and absorbed in the form of discrete bundles. The energy carried by such a bundle (that is, a photon) is proportional to the frequency of the radiation, i.e.,

$$E \propto v, \tag{2.1}$$

$$\Rightarrow E = hv. \tag{2.2}$$

Here $h = 6.626 \times 10^{-34}\text{Js} \cdot \text{s}$ is the Plank constant that was initially determined by Max Planck to solve the black body spectrum anomaly. It is now considered to be a universal constant. Planck's constant has a very important position in quantum mechanics. The frequency v and wavelength λ of electromagnetic radiation are related to its velocity of propagation in vacuum c by $c = v\lambda$. If radiation is travelling through another medium, its velocity should be calculated from

$$v = nv\lambda, \tag{2.3}$$

where n is the refractive index of the medium. The refractive index of most materials has a non-linear dependence on the radiation frequency.

These experiments and the consequent theoretical models confirmed that sometimes radiation behaves as particles and not as continuous waves. On the other hand, there were effects, like interference, which could only be explained if light was considered to have continuous wave characteristics.

To add to this confusion, de Broglie in 1920 introduced the idea that sometimes particles (such as electrons) behave like waves. He proposed that one could associate a wavelength to any particle having momentum p through the relation

$$\lambda = \frac{h}{p}. \tag{2.4}$$

For a particle moving close to the speed of light (the so called relativistic particle) and rest mass m_o (mass of the particle when it is not moving), the above equation can be written as

$$\lambda = \frac{h}{m_0 v}\sqrt{1 - \frac{v^2}{c^2}}. \tag{2.5}$$

For show moving particles with $v \ll c$, the de Broglie relation reduces to

$$\lambda = \frac{h}{mv}. \tag{2.6}$$

De Broglie's theory was experimentally confirmed at Bell Labs where electrons diffraction patterns consistent with the wave picture were observed. Based on these experiments and their theoretical explanations, it is now believed that all the entities in the Universe simultaneously possess localized (particle-like) and distributed (wave-like) properties. In simple terms, particles can behave as waves and waves can behave as particles. This principle, known as wave-particle duality, has played a central role in the development of quantum physics.

2.1.2 Photons

A photon represent one quantum of electromagnetic energy and it is treated as a fundamental particle in the standard model of particle physics. In this model the photon is assumed to have no rest mass. When the photon is travelling in the medium, it show down due to interaction with the medium and acquires an effect mass. In vacuum, however, it is considered to be massless. Photons do not correspond only to visible light. In fact, light spans a very narrow of their full energy spectrum.

Basic properties of photons: Rest mass = Zero, Electrical charge = Zero, Energy = $hv = \frac{hc}{\lambda}$ and Momentum = $\frac{h}{\lambda}$.

Examples: visible light, X-rays, γ-rays.

Sources of photons

Photons play very important roles not only in physics but also in engineering, medical diagnostics, and treatment. For example, laser light is used to correct vision, a process called laser surgery of the eye. In medical diagnostics, X-rays are used to make images of internal organs of the body. In the following we will look at some of the most important of sources of photons that have found wide applications in various fields.

X-ray machine

Since X-rays are high energy photons and can cause considerable damage to tissues, they are produced and employed in controlled laboratory environments. Production of X-rays is a relatively simple process in which a high Z target (i.e. an element having large number of protons, such as tungsten or molybdenum) is bombarded by high velocity electrons (see

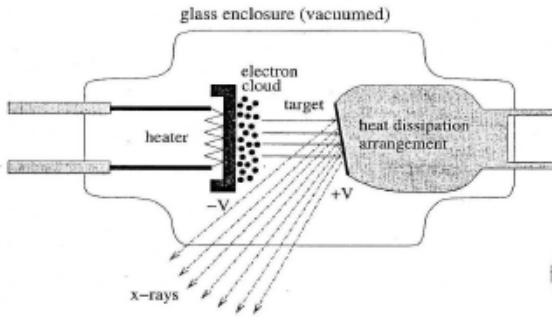

Figure 1.6.2: Sketch of a typical x-ray tube.

Figure 2.1: Sketch of a typical X-ray tube.

Figure 2.1). This results in the production of two types of X-rays: Bremsstrahlung and characteristic X-rays. Bremsstrahlung (a German word for braking radiation) refers to the radiation emitted by charged particles when they decelerate in a medium. In case of X-rays, the high energy electrons decelerate quickly in the target material and hence emit Bremsstrahlung. The emitted X-ray photons have continuous energy spectrum since there are no quantized energy transitions involved in this process. Bremsstrahlung are the X-rays that are usually employed to produce images of internal objects (such as internal body organs in medical diagnostics).

Radioactive sources of photons

There are a large number of radioactive elements that emit γ-rays. These γ-rays are often accompanied by α and β-particles. Besides naturally occurring sources it is possible to produce these isotopes in laboratory as well. This is normally done by bombarding a source material by neutrons. The nuclei, as a result, go into unstable states and try to get rid of these extra neutrons. In the process they also release energy in the form of γ-rays. The two most commonly used radioactive sources of γ-rays are iridium-192 ($^{192}_{17}$Ir) and cobalt-60 ($^{60}_{27}Co$) . The easiest way to produce cobalt-60 is by bombarding cobalt-59 with slow neutrons as represented by the following reaction

$$^{59}_{27}\mathrm{Co} + n \rightarrow ^{60}_{27}\mathrm{Co} + \gamma(7.492\mathrm{MeV}). \tag{2.7}$$

For this reaction we need slow neutrons. Californium-252 is an isotope that is commonly used as a source of neutrons. $^{252}_{98}$f is produced in nuclear reactors and has a half life of approximately 2.64 years. It can produce neutrons through a number of fission modes, such

Element	Isotope	Energy ($E_{\max}$)	$T_{1/2}$
Sodium	Na^{24}_{11}	1.368 MeV, 2.754 MeV	14.959 hours
Manganese	Mn^{54}_{25}	834.838 keV	312.3 days
Cobalt	Co^{60}_{27}	1.173 MeV, 1.332 MeV	5.271 years
Strontium	Sr^{85}_{38}	514.005 keV	64.84 days
Yttrium	Y^{88}_{39}	898.036 keV, 1.836 MeV	106.65 days
Niobium	Nb^{94}_{41}	765.803 keV	2.03 $\times 10^4$ years
Cadmium	Cd^{109}_{48}	88.034 keV	462.6 days
Cesium	Cd^{137}_{55}	661.657 keV	30.07 days
Lead	Ph^{210}_{82}	46.539 keV	22.3 years
Americium	Am^{241}_{95}	26.345keV, 59.541 keV	432.2 years

Table 2.1: Common γ emitters and their half lives.

Basic properties of electrons
Restmass $= 9.11 \times 10^{-31}$ kg $= 0.511$ Mev/c^2
Electricalcharge $= -1.602 \times 10^{-19}$ C
Internal structure : Believed to have internal structure.

as

$$^{252}_{98}\text{Cf} \rightarrow ^{94}_{38}\text{Sr} + ^{154}_{60}\text{Nd} + 4\text{n}. \tag{2.8}$$

However, the neutrons produced in this way have higher kinetic energies than needed for them to be optimally captured by cobalt-59. Therefore some kind of moderator, such as water, is used to slow down these neutrons before they reach the cobalt atoms. The resultant cobalt-60 isotope is radioactive and gives off 2 energetic γ-rays with a half life of around 5.27 years, as represented by the reaction below

$$^{60}_{27}\text{Co} \rightarrow ^{60}_{28}\text{Ni} + \beta + +2\gamma(1.17 \text{ MeV}, 1.33 \text{ MeV}). \tag{2.9}$$

2.1.3 Electrons

Electron is one of the fundamental particles of nature. It carries negative electrical charge and has very small mass and radius. Although we talk in terms of radius, none of the experiments so far has been able to associate any particular structure to it. Interestingly enough, even though it appears to have no structure, it seems to be spinning in well defined ways.

Element	Isotope	Energy ($E_{\max}$)	$T_{1/2}$
Sodium	$^{24}_{11}$P	1.393 MeV	14.959 hours
Phosphorus	$^{32}_{15}$P	1.71 MeV	14.262 days
Chromium	$^{51}_{24}$Cr	752.73 keV	27.702 years
Cobalt	$^{60}_{27}$Co	318.13 keV	5.271 days
Copper	$^{64}_{29}$Cu	578.7 keV	12.7 hours
Strontium	$^{90}_{38}$Sr	546.0 keV	28.79 years
Yttrium	$^{90}_{39}$Y	2.28 MeV	64.0 hours
Iodine	$^{125}_{53}$I	150.61 keV	59.408 hours
Cesium	$^{137}_{55}$Cs	513.97 keV	30.03 years
Thallium	$^{204}_{81}$Cu	763.4 keV	3.78 hours

Table 2.2: Common electrons emitters and their half lives.

Electron gun

These are used to produce intense beams of high energy electrons. Two types of electron guns are in common use: thermionic electron gun and field emission electron gun. A third type, photo emission electron gun, is now gaining popularity specially in high energy physics research.

The basic principle of an electron gun is the process in which an electron is provided enough kinetic energy by some external agent to break away from the overall electric field of the material. The three types mentioned above differ in the manner in which a material is stimulated for this ejection. The process is easier in metals in which almost free electrons are available in abundance. These electrons are so loosely bound that a simple heating of the metal can break them loose. Each metal has a different threshold energy needed to overcome the internal attractive force of the nuclei.

Radioactive sources of electrons

The cobalt-60 emits β-particles together with γ-rays. Although it can, in principle, be used as a source of electrons, it is not generally used for this purpose because of the associated high γ-rays background flux. There are a number of other elements as well whose unstable isotopes emit β-particles (see Table(2.2) with very low γ-rays backgrounds.

2.1.4 Inverse square law

The strength of radiation can be characterized by its flux, which is generally defined as the number of particles passing through a unit area, per unit time. Irrespective of the type of

source, this flux decreases as one moves away from the source. This decrease in flux depends on the type of source and the type of radiation. For example, laser light, which is highly collimated, does not suffer much degradation in flux with distance. On the other hand, the flux from radioactive sources decreases rapidly as the distance from it increases. The inverse square law, which is based on geometric considerations only, characterizes this change. It states that the radiation flux inversely proportional to the square of the distance from the point source, that is

$$\Phi \propto \frac{1}{r^2} \tag{2.10}$$

where r is the distance between the source and the point where flux is to be calculated.

2.1.5 Cross section

Cross section is the most quoted parameter in the fields of particle physics and radiation measurement because it gives a direct measure of what to expect from a certain beam of particles when it interacts with a material. Let us now see how this concept is defined mathematically.

Suppose we have a beam of particles with a flux Φ) (number of particles per unit area per unit time) incident on a target. After interacting with the target, some of the particles in the incident beam get scattered. Suppose that we have a detector, which is able to count the average number of particles per unit time (dN) that get scattered per unit solid angle ($d\Omega$). This average quantity divided by the flux of incident particles is defined as the differential cross section

$$\frac{d\sigma}{d\Omega}(E,\Omega) = \frac{1}{\Phi}\frac{dN}{d\Omega}. \tag{2.11}$$

It is apparent from this equation that the cross section σ has dimension of area. This fact has influenced some authors to define it as a quantity that represents the area to which the incident particle is exposed. The larger this area, the more probable it will be for the incident particle to interact with the target particle. However, it should be noted that this explanation of cross section is not based on any physical principle, rather devised artificially to explain a mathematical identity using its dimensions.

The differential cross section can be integrated to evaluate the total cross section at a certain energy (differential cross section is a function of energy of the incident particles), that is

$$\sigma(E) = \int \frac{d\sigma}{d\Omega} d\Omega. \tag{2.12}$$

The conventional unit of cross section is the barn (b), with $1\text{b} = 10^{-24}\text{cm}^2$.

2.1.6 Mean free path

As particles pass through material, they undergo collisions that may change their direction of motion. The average distance between these collisions is therefore a measure of the probability of a particular interaction. This distance, generally known as the mean free path, is i inversely proportional to the cross section and the density of the material, that is

$$\lambda_m \propto \frac{1}{\rho_n \sigma}, \tag{2.13}$$

where ρ_n and σ represent the number of density of the medium and cross section of the particle in that medium. Note that the definition of the mean free path depends on the type of cross section used in the calculation. For example, if scattering cross section is used then the mean free path would correspond to just the scattering process. However in most instances, such as when calculating the shielding required in a radiation environment, one uses total cross section, which gives the total mean free path.

The mean free path has a dependence on the energy distribution of the particles relative to the medium. For particles that can be described by the Maxwellian distribution, such as thermal neutrons in, a gas under standard conditions, the mean free path can be computed from

$$\lambda_m = \frac{1}{\sqrt{2}\rho_n \sigma}. \tag{2.14}$$

In all other cases, the mean free path should be estimated form

$$\lambda_m = \frac{1}{\rho_n \sigma}. \tag{2.15}$$

The number of density ρ_n in the above relation can be computed for any material from

$$\rho_n = \frac{N_A \rho}{A}, \tag{2.16}$$

where A is the atomic weight of the material, N_A is the Avogadro's number, and ρ is the weight density of the material. Mean free path is usually quoted in cm, for which we must take A in $g/mole$, N_A in $mole^{-1}$, ρ in g/cm^3, and σ in cm^2.

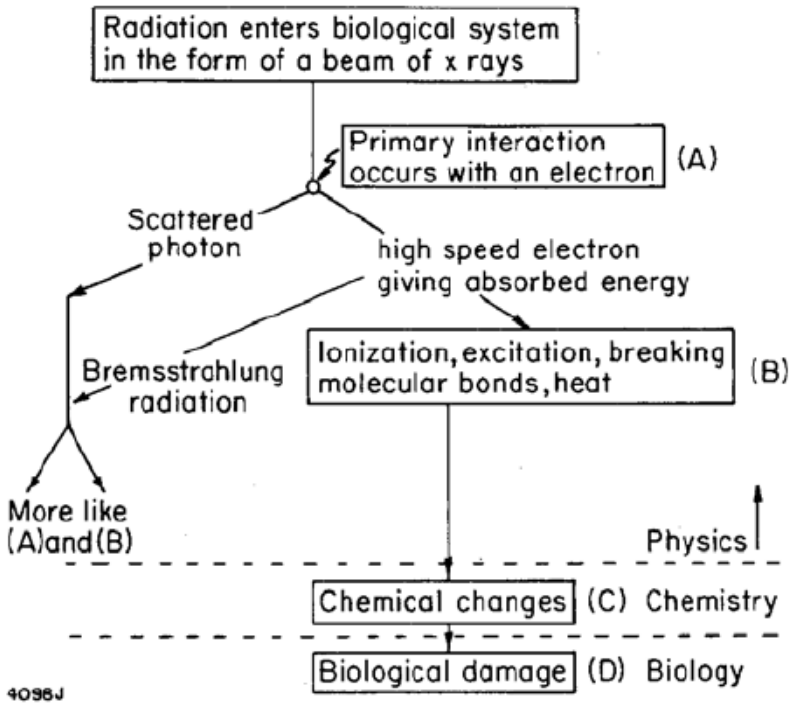

Figure 2.2: Schematic representation of the energy absorption due to radiation resulting in biological damage.

2.2 Absorption of energy

"When an X-ray beam (photon beam) passes through an absorbent medium, part of the energy which transports the beam is transferred to the medium where will produce the biological damage. The energy deposited per unit mass is called the absorbed dose, and is an amount used for the prediction of biological damage. The events that take place during the absorption of the dose and subsequent biological damage are quite complicated (see Figure 2.2). The initial step in the process generally takes into account the collision between a photon and some electron in the body, resulting in the dispersion of some radiation and the electrons start moving at high speed. On the journey through the fabric, the high speeds of the electrons leave a trail along which they occur ionizations, excitations of atoms and breaking of molecular bonds. All this leads to a biological damage.", [19].

2.3 Interaction of photons with matter

Since photons are not subject to Coulomb or nuclear forces, their interactions are localised at short distances. This means that although the intensity of a photon beam decreases as it passes through a material and photons are removed from the beam, the energy of individual photons that do not take part in any interaction is not affected.

2.3.1 Basic interaction mechanisms

Photons can primarily interact with material in three different ways: photoelectric effect, Compton scattering, and pair production. Other possible interaction mechanisms include Raleigh and Mie processes. These interaction mechanisms have different energy thresholds and regions of high cross-sections for different materials. Whenever a beam of photons of sufficient energy passes through a material, not all of the photons in the beam go through the same types of interaction.

Photoelectric effect

In the photoelectric effect, a photon incident with energy hv (where h is the Planck's constant and v the frequency) collides with an atom. As result of this collision, the photon is absorbed and an electron is ejected. Such electron is called a photoelectron. The photoelectron is ejected from the orbit of the atom with an energy $hv - E_s$. E_s is the energy of the electron in the orbit of atom from which it is expelled, leaving the atom in an excited state. The photoelectric effect can only occur when the kinetic energy of incident photon is greater than the electron binding energy. In materials with low atomic number, as the case of human tissue, the energy range in which it is a dominant effect is around 20 KeV. In addition, the photoelectric effect in human tissue is very simple. The value is very small, so the electron acquires essentially all the energy of the photon. Since the photoelectric effect is produced at very low energies, electrons begin to move producing negligible bremsstrahlung. This effect is depends on the atomic number of the material.

Photoelectric effect is one of the process that confirm the idea of the concept of wave particle duality. It was originally explained by Einstein and earned him a Nobel Prize. The effect is rather simple: when light shines on a material, electrons can be emitted. The emission of electrons, however, does not depend on the intensity of light, but rather on its frequency. If its frequency is lower than a certain value, that depends on the target material,

no electrons are emitted. Certainly this cannot be explained on the basis of classical wave-like picture of light. Einstein explained this effect by arguing that light is transferred to the material in packets called quanta, each of which carries an energy equal to

$$E_\gamma = hv = \frac{hc}{\lambda}. \tag{2.17}$$

where v and λ are the frequency and wavelength of light, respectively, and c is the velocity of light in vacuum. Now, since electrons in the materiel are bonded therefore to set them free the energy delivered must be greater than their binding energy. For metals, this energy is called work function and generally represented by the symbol ϕ. Hence, in order an electron to be emitted from a metal surface, we must have

$$E_\gamma \geq \phi, \tag{2.18}$$

$$v \geq \frac{\phi}{h}, \tag{2.19}$$

$$\lambda \leq \frac{hc}{\phi}. \tag{2.20}$$

If the photon energy is larger than the work function, the rest of the energy is carried away by the emitted electron, that is

$$E_c = E_\gamma - \phi. \tag{2.21}$$

Proving this theory is quite simple as one can design an experiment that measures the electron energy as function of the incident light frequency or wave length and see if it follows the above relation.

Since most metals have very low work function, of the order of a few electron volts, therefore even very low energy light can let them free. The work function of metals is approximately half of the binding energy of free metallic atoms.

The photoelectric effect can also occur in free atoms. During this process, a photon is completely absorbed by an atom making it unstable. To return to the stable state, the atom emits an electron from one of its bound atomic shells. Naturally the process requires that the incident photon has energy greater than or equal to the binding energy of the most loosely bound electron in the atom. The energy carried away by the emitted electron can be found by subtracting the binding energy from the incident photon energy, that is

$$E_\mathsf{e} = E_\gamma - E_b, \tag{2.22}$$

where E_b is the binding energy of the atom.

Compton scattering

Compton scattering refers to the inelastic scattering of photons from free and loosely bound electrons which are at rest. Since the electron are almost free, it may also get scattered as a result of the collision.

Compton scattering was first discovered and studied by Compton in 1923. During an scattering experiment he found out that the wave length of the scattered light was different from that of the incident light. He successfully explained this phenomenon by considering light to consist of quantized wave packets or photons.

Figure 2.3 shows this process for a bound electron. The reader may recall that the binding energies of low Z elements are of the order of a few hundreds eV, while the γ-ray sources used in laboratories have energies in the range of hundred of keV. Therefore, the bound electrons can be considered almost free and at rest with respect to incident photons. In general, for orbital electrons, the Compton effect is more probable than photoelectric effect if the energy of the incident is higher than the binding energy of innermost electrons in the target atom.

Simple energy and linear momentum conservation laws can be used to derive the relation between wavelength of incident and scattered photons,

$$\lambda = \lambda_0 + \frac{h}{m_0 c}[1 - \cos\theta]. \tag{2.23}$$

Here λ_0 and λ represent wavelength of incident and scattered photons respectively, m_0 is the rest energy of electrons and θ is the angle between incident and scattered photons.

Thompson scattering

Thompson scattering is an elastic scattering process between a free electron and a photon of low energy. By low energy we mean the energy at which the quantum effects are not significant. Therefore in order to drive kinematic quantities related to Thompson scattering, the concept of classical electromagnetic theory suffices.

The differential and total cross sections for Thompson scattering are given by

$$\frac{d\sigma_{th}}{d\Omega} = r_{\mathrm{e}}^2 \sin^2\theta \tag{2.24}$$

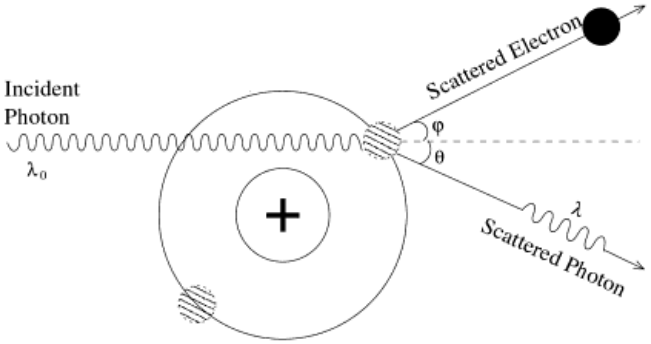

Figure 2.3: Compton scattering of a photon having energy $E_{\gamma 0} = \dfrac{hc}{\lambda_0}$ from a bound electron. Some of the energy of the incident photon goes into knocking the orbital electron out of its orbit.

and

$$\sigma_{th} = \frac{8\pi}{3} r_{\mathsf{e}}^2 = 6.25 \times 10^{-29} \mathrm{m}^2 \tag{2.25}$$

where θ is the photon scattering angle with respect to its original direction of motion and r_{e} is the classical electrons radius.

Rayleigh scattering

In this elastic scattering process there is very minimal coupling of photons to the internal structure of the target atom. The theory of Rayleigh scattering was first proposed by Lord Rayleigh in 1871, and it is applicable when the radius of the target is much smaller was the wavelength of the incident photon. A Rayleigh scattered photon has almost then the same wavelength as the incident photon, which implies that the energy transfer during the process is extremely small. For most of the X-ray and low energy γ-ray, the Rayleigh process is the predominant mode of elastic scattering.

The cross section for this process is inversely proportional to the fourth power of the wavelength of the incident radiation and can be written as

$$\sigma_{ry} = \frac{8\pi a^6}{3} \left[\frac{2\pi n_m}{\lambda_0}\right]^4 \left[\frac{m^2 - 1}{m^2 + 1}\right]^2 . \tag{2.26}$$

Here λ_0 is the wavelength of the incident photon, a is the radius of the target particle, and $m = n_s/n_m$ is the ratio of the index of refraction of the target particle to that of the surrounding medium.

Pair production

Pair production is the process that results in the conversion of a photon into an election-positron pair. Since photon has no rest mass, while both the electron and the positron do, therefore we can say that this process converts energy into mass according: to Einstein's mass energy relation $E = mc^2$. Earlier in the chapter we discussed the process of electron-positron annihilation, in which mass converts into energy. Hence we can think of pair production as the inverse process of the electron-positron annihilation. However there is one operational difference between the two processes: the pair production always takes part in a material while the electron positron annihilation does not have any such requirement. To be more specific for the pair production to take place, there must be another particle in the vicinity of the photon to ensure momentum conservation. The process in the vicinity of a heavy nucleus can be represented as

$$\gamma + X \rightarrow e + e^{+} + X^{\star}, \tag{2.27}$$

where X and $X^{\star}$ represent the ground and excited states of a heavy nucleus.

2.4 Interaction of electrons with matter

The way an electron beam would behave when passing through matter depends, to a large extent, on its energy. At low to moderate energies, the primary modes of interaction are the following:

1. Ionization,
2. Møller scattering,
3. Mott scattering,
4. Bhabha scattering, and
5. Electron-positron annihilation.

At higher energies the emission of bremsstrahlung dominates as shown in Figure 2.4.

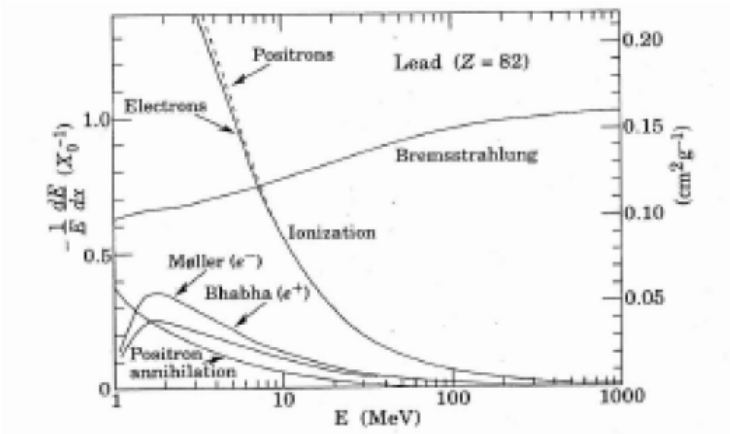

Figure 2.4: Fractional energy loss of electrons and positrons per radiation length as a function of energy 19 MeV.

2.4.1 Interaction modes

A. Elastic scattering

Elastic scattering to a process in which an incident particle scatters off a target in such a way that the total kinetic energy of the system remains constant. It should be noted that elastic scattering elastically does not imply that there is no energy transfer between incident and target particles. The incident particle can, and in most cases does, loose some of its energy to the target particle. However this energy does not go into any target excitation process, and the electronic and nuclear states of the target are not affected.

The best way to mathematically model the elastic scattering process is by considering both the incident and target particles to have no internal structure. Such particles are generally referred to as point-like particles.

There are also special types of elastic scattering processes in which the incident particle transfers none or very minimal energy to the target. A common example is the Rayleigh scattering of photons.

B. Inelastic scattering

In inelastic scattering process the incident particle excites the atom to a higher electronic or nuclear state, which usually comes back to the ground state by emitting one or more particles. In this type of reaction the kinetic energy is not conserved because some of it goes into the excitation process. However the total energy of the system remains constant.

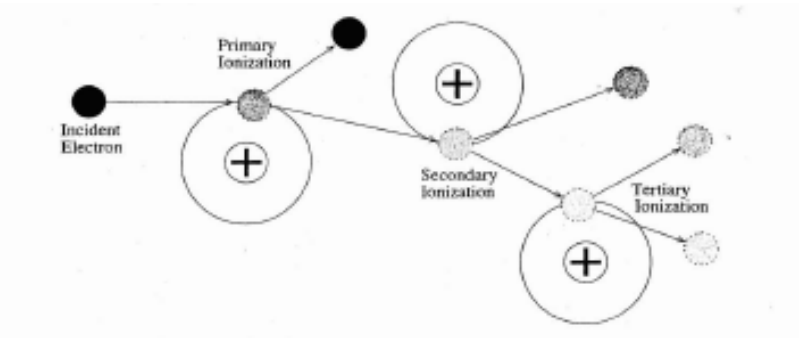

Figure 2.5: Depiction of electron-induced ionization processes. At each stage of ionization, if the ejected electron has an energy greater than the binding energy of the atom, it can cause another ionization.

C. Ionization

If an incident electron guts enough energy from the atom, it may eject one of its loosely bound electrons', resulting in the ionization of the atom. The energy of the ejected electron depends on the incident electron energy as well as on its binding energy. If the energy carried away by the ejected electron is high enough it can produce secondary ionization in the same manner as the primary ionization took place. The process can continue until the energy of the ejected electron is less than the ionization potential of the atom. This process is graphically depicted in Figure 2.5. It should, however, be noted that not all electrons that have energy higher than the ionization potential of the atom produce subsequent ionization. The probability with which an electron can cause ionization depends on its cross section, which to a large extent depends on its energy and the type of target atom. It has been seen that, at each step of this ionization, only about one third of the electrons cause subsequent ionizations.

The ionization of atoms or molecules is a highly researched area due to its utility in material and physics research. Electrons have be ability to penetrate deep into the materials and can therefore be used to extract information about the. structure of the material.

As it can be seen from Figure 2.4, the ionization with electrons dominates at low to moderate energies. Electron impact ionization is a term that is extensively used in literature to characterize the process of ionization with electrons at relatively high energies. This useful process is routinely employed in spectroscopy of materials in gaseous state.

Symbolically, for an atom or a molecule X_q, with total positive charge q, the electron

ionization process can be written as

$$e + X_q \rightarrow X_{q+1} + 2e. \tag{2.28}$$

D. Møller scattering

This refers to the elastic scattering of an electron from another electron (or a positron from another positron). The interaction can be symbolically described by

$$e + e \rightarrow e + e. \tag{2.29}$$

In quantum electrodynamics, Møller scattering is said to occur due to exchange of virtual photons between the electrons. In classical electrodynamic terms one can simply call it a consequence of Coulomb repulsion between the two electrons.

E. Mott scattering

Mott scattering is the scattering of a relativistic electron by a Coulomb field. It is an elastic scattering, hence there is no net energy variation within the medium due to Mott scattering, but it is an important mechanism in the sense that it changes the trajectories of electrons.

F. Bhabha scattering

It is a scattering of an electron from a positron. This interaction can be written as

$$e + e^+ \rightarrow e + e^+. \tag{2.30}$$

In terms of quantum electrodynamics, as with Møller scattering, Bhabha scattering is also considered to be due to exchange of virtual photons between the electron and the positron. Classically, it can be thought to occur because of the Coulomb attraction between the two particles.

G. Electron-positron annihilation

The process of electron-positron annihilation has already been explained earlier in this chapter. In this process an electron and a positron annihilate each other and produce at least two photons. It is a perfect example of the notion that mass can be converted into energy. We saw earlier that during this process, to conserve energy and momentum, at least two

photons, each having 511 keV, are produced. However, more than two electrons can be and in fact are produced. The cross section for this process at low electron energies in a material is not very high and decreases to almost zero at high energies. This low cross section is due to the very low abundance of positrons in materials. Figure 2.4 shows this behaviour for electrons of energy from 1 MeV to 100 MeV. Due to its lower cross section, this process does not contribute significantly to the total energy loss specially at moderate to high energies.

A point that is worth mentioning here is that the electron-positron annihilation process can also produce particles other than photons provided their center-of-mass energy before collision is high enough. For example, at very high energies (several GeV), the annihilation process produces quarks, which form mesons. Since discussion of such interactions is out of the scope of this memory, the interested reader is referred to standard texts of particle physics and high energy physics.

H. Bremsstrahlung

The process of bremsstrahlung refers to the emission of radiation when a charged particle accelerates in a material. For electrons we came up with a critical or cut-off wavelength below which no bremsstrahlung photons can be emitted. This wavelength is given

$$\lambda_{\min} = \frac{hc}{eV}, \tag{2.31}$$

where e is the unit electronic charge, $h = 6.626 \times 10^{-34}$ is the Planck's constant, c is the velocity of light in vacuum and V is the potential experienced by the electron. For high Z materials, the process of bremsstrahlung dominates other types of interactions above about 10 MeV.

As it can be seen from Figure 2.4, the bremsstrahlung process is the dominant mode through which the moderate to high energy electrons loose energy in high Z materials.

H. Cherenkov radiation

We saw that an electron, being a very light particle, can emit Cherenkov radiation when accelerated to high energies in a medium. Its energy should be so high that its velocity becomes higher than the velocity of light in that medium. The velocity of light in a medium of refractive index n is given by c/n, where c is the velocity of light in vacuum. For Cherenkov

radiation to be emitted, the velocity of the charged particle traversing the medium must be greater than this velocity, that is to say,

$$v_{\mathrm{th}} \geq \frac{c}{n}. \tag{2.32}$$

Similarly, the threshold energy is given by

$$E_{th} = \gamma_{\mathrm{th}} m_0 c^2, \tag{2.33}$$

where m_0 is the electron rest mass, c is the velocity of light in vacuum, and γ_{th} is the relativistic factor defined as

$$\gamma_{th} = \left[1 - \frac{v_{th}^2}{c^2}\right]^{-1/2} = \left[1 - \beta_{th}^2\right]^{-1/2}. \tag{2.34}$$

Here the term $\beta_{th} = v_{th}/c$ is the oft-quoted condition for Cherenkov emission. From the above equations we can also deduce that

$$\gamma_{th} = \frac{n}{\sqrt{n^2 - 1}}. \tag{2.35}$$

An important factor is the direction of emission of Cherenkov light. As the light is emitted in the form of a cone, we can define an angle of emission as the direction of the cone. This angle Θ_c of the Cherenkov for a particle moving in a medium of refractive index n is given by

$$\Theta_c = \arccos\left(\frac{1}{\beta n}\right). \tag{2.36}$$

This equation can be used to define the maximum angle $\Theta_c^{\max}$ that one should expect to see in a medium. The maximum will occur when $\beta = 1$, that is, when the particle's velocity is approximately equal to the velocity of light in vacuum. Hence

$$\Theta_c^{\max} = \arccos\left(\frac{1}{n}\right). \tag{2.37}$$

2.4.2 Range of electrons

As opposed to heavy charged particles, the range of electrons is very difficult to treat mathematically. The primary reason for the difficulty lies in the higher large-angle scattering probability of electrons due to their extremely low mass as compared to the heavy charged particles. However, it has been found that the bulk properties of an electron beam can

be characterized by relatively simple relations. The attenuation of an electron beam, for example, has been seen to follow an approximately exponential curve given by

$$N = N_0 \mathrm{e}^{-\mu x}. \tag{2.38}$$

Here, N represents the number of electrons transmitted through a thickness x of the material. N_0 is the absorption coefficient of the material for the electrons and it is also a function of the electron energy. For electrons having a continuous energy spectrum, it depends on their endpoint energy. Following the analogy of attenuation of photons in matter, here we can define also a path length or absorber thickness as

$$t = \frac{1}{\mu}, \tag{2.39}$$

the interpretation of which can be understood by substituting $x = t$ in the exponential relation above.

$$\begin{aligned} N &= N_0 \mathrm{e}^{-1} \\ \Rightarrow \text{No. of electrons absorbed} &= N_0 - N = N_0(1 - \mathrm{e}^{-1}) \\ &= 0.63 N_0. \end{aligned} \tag{2.40}$$

This implies that t is the thickness of the material which absorbs about 63% of the electrons of a certain energy. In Figure 2.6 we have plotted N versus x on both linear and semilogarithmic scales. Since the behaviour of electrons is not perfectly logarithmic, if one performs an experiment to measure the variation of electron intensity with respect to the thickness of the material, a perfect straight line on the semilogarithmic scale is not obtained. Such a curve is known as absorption curve. Absorption curves for specific materials are routinely obtained to determine the range of electrons in the material.

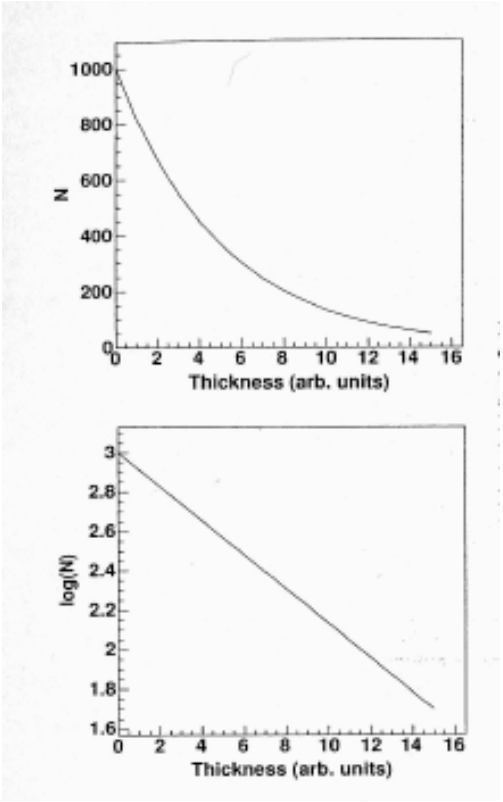

Figure 2.6: Plot of number of electrons transmitted per unit thickness of an arbitrary material. For this plot we have arbitrarily taken the initial number of electrons to be 10^3 and $\mu = 1/5$. The plot is shown on both linear (upper) and semilogarithmic (lower) scales.

Chapter 3

Transport equations. Energy deposition and absorbed dose

3.1 Transport equations

As mentioned before, this work is based on the mathematical model presented by Hensel, Iza-Teran and Siedow in [15].

The scheme for the computation of the absorbed dose, according to the model described in [15], is as follows:

1. First, solve the Boltzmann transport equation for photons. The output is ψ_γ, the density of photons inside the given spatial domain.

2. Second,

   (a) Solve the Boltzmann transport equation for electrons

   or, taking profit of the Physics behind,

   (b) Solve the Fokker-Planck approximation of the Boltzmann transport equation for electrons. This approximation is useful because solving the Boltzmann transport equation for electrons is more challenging than solving the one for photons.

   The output of Step 1, ψ_γ, enters as a source term in Step 2. Thus, this is a sequential plan; one needs to complete Step 1 before carrying on Step 2.

   The output of Step 2 is ψ_e, the density of electrons inside the given spatial domain.

3. Third, use ψ_{e} to compute the absorbed dose via a given explicit formula which takes into account the radiation exposure time.

Chapter 4 of this memory contains the resolution of Step 1.

Now we will show the transport equations, together with the associated boundary conditions.

The Boltzmann transport equation for photons is

$$\begin{aligned}\boldsymbol{\Omega}_\gamma \cdot \nabla\psi_\gamma(\mathbf{r},\boldsymbol{\Omega}_\gamma,\epsilon_\gamma) =&\rho_{\mathsf{e}}(\mathbf{r})\int_0^\infty\int_{S^2}\tilde{\sigma}_{C,\gamma}(\epsilon'_\gamma,\epsilon_\gamma,\boldsymbol{\Omega}'_\gamma.\boldsymbol{\Omega}_\gamma)\psi_\gamma(\mathbf{r},\boldsymbol{\Omega}'_\gamma,\epsilon'_\gamma)\ \mathrm{d}\boldsymbol{\Omega}'_\gamma\ \mathrm{d}\epsilon'_\gamma\\ &-\rho_{\mathsf{e}}(\mathbf{r})\sigma^{\mathrm{tot}}_{C,\gamma}(\epsilon_\gamma)\psi_\gamma(\mathbf{r},\boldsymbol{\Omega}_\gamma,\epsilon_\gamma),\end{aligned}\tag{3.1}$$

where ρ_{e} is the electron density of the medium and $\tilde{\sigma}_{c,\gamma}$ is the scattering cross section of the photons, differential in angle and energy for Compton scattering of photons and $\sigma^{\mathrm{tot}}_{C,\gamma}(\epsilon_\gamma)$ is the total Compton scattering cross section of photons.

According to [15], $\psi_\gamma(\mathbf{r},\boldsymbol{\Omega}_\gamma,\epsilon_\gamma)\cos\Theta\ \mathrm{d}A\ \mathrm{d}\boldsymbol{\Omega}_\gamma\ \mathrm{d}\epsilon_\gamma\ \mathrm{d}t$ is the number of photons that move in time dt through area dA into the element of solid angle $d\boldsymbol{\Omega}_\gamma$ around $\boldsymbol{\Omega}_\gamma$ with an energy in the interval $(\epsilon_\gamma,\epsilon_\gamma+d\epsilon_\gamma)$, Θ is the angle between direction $\boldsymbol{\Omega}_\gamma$ and outer normal of dA and $\boldsymbol{\Omega}_\gamma=(\sin\varphi_\gamma\cos\vartheta_\gamma,\sin\varphi_\gamma\sin\vartheta_\gamma,\cos\varphi_\gamma)^{\mathrm{T}}$ where φ_γ is the zenith angle and $\vartheta_\gamma$is the polar angle in a Cartesian coordinate system respectively.

A similar definition holds for $\psi_{\mathsf{e}}(\mathbf{r},\boldsymbol{\Omega}_{\mathsf{e}},\epsilon_{\mathsf{e}})\cos\Theta\ \mathrm{d}A\ \mathrm{d}\boldsymbol{\Omega}_{\mathsf{e}}\ \mathrm{d}\epsilon_{\mathsf{e}}\ \mathrm{d}t$ being the respective phase space fluency of electrons, ϵ_{e} their kinetic energy and $\boldsymbol{\Omega}_{\mathsf{e}}$ their direction of flight.

The Boltzmann transport equation for electrons is

$$\begin{aligned}\boldsymbol{\Omega}_{\mathsf{e}} \cdot \nabla\psi_{\mathsf{e}}(\mathbf{r},\boldsymbol{\Omega}_{\mathsf{e}},\epsilon_{\mathsf{e}}) =&\rho_{\mathsf{e}}(\mathbf{r})\int_0^\infty\int_{S^2_{1/2}}\tilde{\sigma}_{C,\mathsf{e}}(\epsilon'_\gamma,\epsilon_{\mathsf{e}},\boldsymbol{\Omega}'_\gamma\cdot\boldsymbol{\Omega}_{\mathsf{e}})\psi_\gamma(\mathbf{r},\boldsymbol{\Omega}'_\gamma,\epsilon'_\gamma)\ \mathrm{d}\boldsymbol{\Omega}'_\gamma\ \mathrm{d}\epsilon'_\gamma\\ &+\rho_{\mathsf{e}}(\mathbf{r})\int_{\epsilon_s}^\infty\int_{S^2_{1/4}}\tilde{\sigma}_{\mathrm{M}}(\epsilon'_{\mathsf{e}},\epsilon_{\mathsf{e}},\boldsymbol{\Omega}'_{\mathsf{e}}\cdot\boldsymbol{\Omega}_{\mathsf{e}})\psi_{\mathsf{e}}(\mathbf{r},\boldsymbol{\Omega}'_{\mathsf{e}},\epsilon'_{\mathsf{e}})\ \mathrm{d}\boldsymbol{\Omega}'_{\mathsf{e}}\ \mathrm{d}\epsilon'_{\mathsf{e}}\\ &+\rho_{\mathsf{e}}(\mathbf{r})\int_{\epsilon_s}^\infty\int_{S^2_{2/4}}\tilde{\sigma}_{\mathrm{M},\delta}(\epsilon'_{\mathsf{e}},\epsilon_{\mathsf{e}},\boldsymbol{\Omega}'_{\mathsf{e}}\cdot\boldsymbol{\Omega}_{\mathsf{e}})\psi_{\mathsf{e}}(\mathbf{r},\boldsymbol{\Omega}'_{\mathsf{e}},\epsilon'_{\mathsf{e}})\ \mathrm{d}\boldsymbol{\Omega}'_{\mathsf{e}}\ \mathrm{d}\epsilon'_{\mathsf{e}}\\ &+\rho_{\mathsf{c}}(\mathbf{r})\int_{S^2}\sigma_{\mathrm{Mott}}(\mathbf{r},\epsilon_{\mathsf{e}},\boldsymbol{\Omega}'_{\mathsf{e}}\cdot\boldsymbol{\Omega}_{\mathsf{e}})\psi_{\mathsf{e}}(\mathbf{r},\boldsymbol{\Omega}'_{\mathsf{e}},\epsilon_{\mathsf{e}})\ \mathrm{d}\boldsymbol{\Omega}'_{\mathsf{e}}\\ &-\rho_{\mathsf{e}}(\mathbf{r})\sigma^{\mathrm{tot}}_{\mathrm{M}}(\epsilon_{\mathsf{e}})\psi_{\mathsf{e}}(\mathbf{r},\boldsymbol{\Omega}_{\mathsf{e}},\epsilon_{\mathsf{e}})\\ &-\rho_{\mathsf{c}}(\mathbf{r})\sigma^{\mathrm{tot}}_{\mathrm{Mott}}(\mathbf{r},\epsilon_{\mathsf{e}})\psi_{\mathsf{e}}(\mathbf{r},\boldsymbol{\Omega}_{\mathsf{e}},\epsilon_{\mathsf{e}}),\end{aligned}\tag{3.2}$$

where ρ_{c} is the density of atomic cores in the medium and $\tilde{\sigma}_{C,\mathsf{e}}$ is the scattering cross section of electrons differential in angle and energy for Compton scattering of electrons. $\tilde{\sigma}_{\mathrm{M}}$ is the scattering cross section for primary electrons differential in angle and energy for Møller scattering and $\tilde{\sigma}_{\mathrm{M},\delta}$ is the cross section for secondary electrons ('delta-rays') . The scattering cross section for Mott scattering σ_{Mott} is only differential in angle, because Mott scattering is an elastic scattering. The total cross section for Møller and Mott scattering are $\sigma_{\mathrm{M}}^{\mathrm{tot}}$and $\sigma_{\mathrm{Mott}}^{\mathrm{tot}}$ respectively.
The angular integration in the electron equation are restricted by the kinematics of the scattering events. We define

$$\int_{S^2_{1/2}} f(\varphi,\vartheta)\mathrm{d}\Omega := \int_0^{2\pi}\int_0^{\frac{\pi}{2}} f(\varphi,\vartheta)\sin\vartheta\,\mathrm{d}\vartheta\;\mathrm{d}\varphi,$$

$$\int_{S^2_{1/4}} f(\varphi,\vartheta)\mathrm{d}\Omega := \int_0^{2\pi}\int_0^{\frac{\pi}{4}} f(\varphi,\vartheta)\sin\vartheta\,\mathrm{d}\vartheta\;\mathrm{d}\varphi \qquad \text{and}$$

$$\int_{S^2_{2/4}} f(\varphi,\vartheta)\mathrm{d}\Omega := \int_0^{2\pi}\int_{\frac{\pi}{4}}^{\frac{\pi}{2}} f(\varphi,\vartheta)\sin\vartheta\,\mathrm{d}\vartheta\;\mathrm{d}\varphi$$

where the axes of reference are defined by $\mathbf{\Omega}_\gamma$ and $\mathbf{\Omega}_{\mathsf{e}}$ in (5.29) and (3.2) respectively.
Let $Q \subset \mathbb{R}^3$ be the domain such that Q will be non empty, open, bounded and convex. Again let ∂Q be the boundary of the domain Q and $\bar{Q}$ be the closure of the domain. So, $\bar{Q} = Q \cup \partial Q$. Let Γ is the irradiated part and Λ is the non irradiated part of the total surface ∂Q i.e., $\partial Q = \Gamma \cup \Lambda$. Here $\boldsymbol{n}(\mathbf{r})$ is the outward unit normal at $\mathbf{r} \in \partial Q$.

$$\left.\begin{array}{ccc}
\psi_\gamma(\mathbf{r},\mathbf{\Omega}_\gamma,\epsilon_\gamma)\mid_{\mathrm{r}\in\Gamma} = \psi_\gamma^{(0)}(\mathbf{r},\mathbf{\Omega}_\gamma,\epsilon_\gamma), & \text{for} & \boldsymbol{n}(\mathbf{r})\cdot\mathbf{\Omega}_\gamma < 0 \\
\psi_\gamma(\mathbf{r},\mathbf{\Omega}_\gamma,\epsilon_\gamma)\mid_{\mathrm{r}\in\Lambda} = 0; & \text{for,} & \boldsymbol{n}(\mathbf{r})\cdot\mathbf{\Omega}_\gamma < 0 \\
\psi_{\mathsf{e}}(\mathbf{r},\mathbf{\Omega}_{\mathsf{e}},\epsilon_{\mathsf{e}})\mid_{\mathrm{r}\in\Gamma} = \psi_{\mathsf{e}}^{(0)}(\mathbf{r},\mathbf{\Omega}_{\mathsf{e}},\epsilon_{\mathsf{e}}), & \text{for} & \boldsymbol{n}(\mathbf{r})\cdot\mathbf{\Omega}_{\mathsf{e}} < 0 \\
\psi_{\mathsf{e}}(\mathbf{r},\mathbf{\Omega}_{\mathsf{e}},\epsilon_{\mathsf{e}})\mid_{\mathrm{r}\in\Lambda} = 0, & \text{for} & \boldsymbol{n}(\mathbf{r})\cdot\mathbf{\Omega}_{\mathsf{e}} < 0
\end{array}\right\}. \tag{3.3}$$

"Boundary conditions are only formulated for fluences that are going into the patient's body, because multiple scattering inside the body can lead to outward fluences.

The transport equations (5.29),(3.2) together with the boundary conditions (3.3) model the transport of photons and electrons in heterogeneous biological tissue. Different media like muscle and bone are modelled by different densities of electrons ρ_{e}, atomic cores ρ_{c} and Mott cross sections (which depend on the atomic number Z=Z(r) of the irradiated media). So heterogeneous media are included into the model from beginning [...]" [15].

3.2 Energy deposition and absorbed dose

In this section we discuss about the energy deposition in the molecule which is needed for the dose calculation. Also we talk about the formulation of the dose calculation in here. Most of the content of this section has been extracted from reference [15].

From [15] we know that regarding scattering "only one type leads to energy deposition in the irradiated medium namely Møller scattering. We see that by a Møller scattering event a free electron transfers energy and momentum to a bound electron, so that the latter can leave the molecule and then the binding energy of the electron has been transferred to the molecule". Indeed, let us recall that we consider only Møller and Mott scattering in the model, and we know that Mott scattering does not cause energy changes in the system, because it is an elastic event.

We see the energy balance in below.

Let us consider two electrons; one is moving with kinetic energy ϵ'_{e}, and the other one is at rest, hence its kinetic energy is zero, inside a molecule. We call primary electron the one which is moving and secondary electron the one which is at rest. When the primary electron impacts against the secondary electron then the secondary electron will be able to leave the bounded molecule or not, depending on the kinetic energy of the primary electron. If the primary electron impacts with high kinetic energy then the kinetic energy of the secondary electron may become larger than the binding energy of the molecule, in this case the secondary electron will leave the atom and this atom will become ionized. After that the adjectives "primary" and "secondary" may refer to a different electron, by definition we call primary electron the one with larger kinetic energy.
Let ϵ_{e}, ϵ_δ, and ϵ_{B} be, respectively, the kinetic energy of primary electron, secondary electron, and the energy of the ionized molecule. The energy before the impact must be equal to the energy after impact. Therefore the energy balance will be the following:

$$\epsilon'_{\mathsf{e}} = \epsilon_{\mathsf{e}} + \epsilon_\delta + \epsilon_{\mathsf{B}}. \tag{3.4}$$

Note that $\epsilon_{\mathsf{B}} = \epsilon_{\mathsf{B}}(\mathbf{r})$ because the medium can be heterogeneous. Since $\epsilon_{\mathsf{e}} \geq \epsilon_\delta$ so we get

$$\epsilon_{\mathsf{e}} \geq \frac{\epsilon'_{\mathsf{e}} - \epsilon_{\mathsf{B}}}{2} \tag{3.5}$$

and

$$\epsilon_\delta \leq \frac{\epsilon'_{\mathsf{e}} - \epsilon_{\mathsf{B}}}{2}. \tag{3.6}$$

We consider that the upper limit of the range of binding energy of the electron in tissue is ϵ_{s}. Also we need some knowledge about the energy transfer process in a Møller scattering event and to sum over all possible combinations of outgoing and incoming energies and direction of electrons in Møller scattering for calculating the absorbed dose.

"The electrons of different types of atoms have different degrees of freedom to move around. With some types of materials, such as metals, the outermost electrons in the atoms are so loosely bound that they chaotically move in the space between the atoms of that material by nothing more than the influence of room-temperature heat energy. Because these virtually unbound electrons are free to leave their respective atoms and float around in the space between adjacent atoms, they are often called free electrons", [49]. But the electrons of some other types of materials such as glass, have very little freedom to move around. Some of these electrons can leave their respective atoms by the external force such as physical rubbing and transfer to the atoms of another material. These electrons cannot move easily between atoms within that material [49].

From the above discussion, we can arrive at the following three conclusions about the energy changes after impact between the incoming electron and resting electron in molecule:

1. When the incoming electron (free electron) impacts to the resting electron in the atom then one of them will leave the atom, the one which energy is greater than the upper limit of the binding energy of the electron (ϵ_{s}) and the other one will stay in the atom. In this situation the atom will not be ionized.

2. After impact, if the energy both of them are greater than the binding energy then the two electrons will leave the atom. So, the atom will loss one electron and it will be ionized here.

3. After impact, if the energy of both of them is less or equal than the binding energy then the resting electron in the atom will not leave its respective atom and the incoming electron will stay freely between the atoms without any influence. Here, also the atom will not be ionized like in the first case.

Therefore we get two different contributions for the absorbed dose:

1. If $\epsilon_\delta \leq \epsilon_\mathsf{s}$ (or $\epsilon_\delta \in [0, \epsilon_\mathsf{s}]$), then delta electron (secondary electron) will not leave the atom and its energy ϵ_δ which got from the primary electron is absorbed locally by the atom. So, we see that the ionization energy of the molecule ϵ_B and the kinetic energy ϵ_δ of the secondary electron contributes to the absorbed dose. Therefore, the energy loss $(\epsilon'_\mathsf{e} - \epsilon_\mathsf{e})$ of the primary electron enters into the dose formula.
   The limits of energy integration are, for the incoming primary electron, $\epsilon'_\mathsf{e} \in [\epsilon_\mathsf{s},\ \infty)$, and for the scattered primary electron, $\epsilon_\mathsf{e} \in [\epsilon'_\mathsf{e} - \epsilon_\mathsf{s} - \epsilon_\mathsf{B},\ \epsilon'_\mathsf{e} - \epsilon_\mathsf{B}]$, because we know $\epsilon_\mathsf{e} = \epsilon'_\mathsf{e} - \epsilon_\delta - \epsilon_\mathsf{B}$, where $\epsilon_\delta \in [0,\ \epsilon_\mathsf{s}]$.

2. If $\epsilon_\delta \geq \epsilon_\mathsf{s}$ $\left(\text{or } \epsilon_\delta \in \left[\epsilon_\mathsf{s},\ \dfrac{\epsilon'_\mathsf{e} - \epsilon_\mathsf{B}}{2}\right]\right)$, i.e., delta electrons are transported, so in this case only the ionization energy ϵ_B of the molecule contributes to the absorbed dose, i.e., $\epsilon_\mathsf{B} = [\epsilon'_\mathsf{e} - \epsilon_\mathsf{e} - \epsilon_\delta]$ enters into the dose formula.
   The limits of the energy of the incoming electron come from, $\epsilon'_\mathsf{e} \in [\epsilon_\mathsf{s},\ \infty)$. We get from (3.4) that $\epsilon_\mathsf{e} = \epsilon'_\mathsf{e} - \epsilon_\delta - \epsilon_\mathsf{B}$. Here, $\epsilon_\delta \in \left[\epsilon_\mathsf{s},\ \dfrac{\epsilon'_\mathsf{e} - \epsilon_\mathsf{B}}{2}\right]$. So we get the limit of the energy for the scattered primary electron, $\epsilon_\mathsf{e} \in \left[\dfrac{\epsilon'_\mathsf{e} - \epsilon_\mathsf{B}}{2},\ \epsilon'_\mathsf{e} - \epsilon_\mathsf{s} - \epsilon_\mathsf{B}\right]$.

Therefore the exact formula for the absorbed dose is the following:

$$\begin{aligned} D(r) = \frac{mc^2\rho_\mathsf{e}(\mathbf{r})}{\rho(\mathbf{r})} T \int_{S^2}\int_{S^2_{1/4}}\int_{\epsilon_\mathsf{s}}^{\infty}\int_{\epsilon'_\mathsf{e}-\epsilon_\mathsf{s}-\epsilon_\mathsf{B}}^{\epsilon'_\mathsf{e}-\epsilon_\mathsf{B}} [\epsilon'_\mathsf{e} - \epsilon_\mathsf{e}]\tilde{\sigma}_\mathrm{M}(\epsilon'_\mathsf{e}, \epsilon_\mathsf{e}, \mathbf{\Omega}'_\mathsf{e}\cdot\mathbf{\Omega}_\mathsf{e})\psi_\mathsf{e}(\mathbf{r}, \mathbf{\Omega}'_\mathsf{e}, \epsilon'_\mathsf{e})\ \mathrm{d}\epsilon_\mathsf{e}\ \mathrm{d}\epsilon'_\mathsf{e}\ \mathrm{d}\mathbf{\Omega}'_\mathsf{e}\ \mathrm{d}\mathbf{\Omega}_\mathsf{e} \\ + \frac{mc^2\rho_\mathsf{e}(\mathbf{r})}{\rho(\mathbf{r})} T \int_{S^2}\int_{S^2_{1/4}}\int_{\epsilon_\mathsf{s}}^{\infty}\int_{\frac{\epsilon'_\mathsf{e}-\epsilon_\mathsf{B}}{2}}^{\epsilon'_\mathsf{e}-\epsilon_\mathsf{s}-\epsilon_\mathsf{B}} [\epsilon'_\mathsf{e} - \epsilon_\mathsf{e} - \epsilon_\delta]\tilde{\sigma}_\mathrm{M}(\epsilon'_\mathsf{e}, \epsilon_\mathsf{e}, \mathbf{\Omega}'_\mathsf{e}\cdot\mathbf{\Omega}_\mathsf{e}) \\ \times \psi_\mathsf{e}(\mathbf{r}, \mathbf{\Omega}'_\mathsf{e}, \epsilon'_\mathsf{e})\ \mathrm{d}\epsilon_\mathsf{e}\ \mathrm{d}\epsilon'_\mathsf{e}\ \mathrm{d}\mathbf{\Omega}'_\mathsf{e}\ \mathrm{d}\mathbf{\Omega}_\mathsf{e}, \end{aligned} \tag{3.7}$$

where mc^2 is being the rest energy of the electron to rescale energy, ρ the local density of the medium and T is the duration of the irradiation. If all quantities are calculated in SI units this formula leads to SI unit $\mathrm{J\,kg^{-1}}$ or Gray (Gy) for the dose.
From the reference [15], we get $\epsilon_\delta = 0$ hence the integral kernels of both contribution to the dose (3.7) become identical. Therefore by adding the two parts of (3.7) we get the following formula for the absorbed dose

$$D(r) = \frac{mc^2\rho_\mathsf{e}(\mathbf{r})}{\rho(\mathbf{r})} T \int_{S^2}\int_{S^2_{1/4}}\int_{\epsilon_\mathsf{s}}^{\infty}\int_{\frac{\epsilon'_\mathsf{e}-\epsilon_\mathsf{B}}{2}}^{\epsilon'_\mathsf{e}-\epsilon_\mathsf{B}} [\epsilon'_\mathsf{e} - \epsilon_\mathsf{e}]\tilde{\sigma}_\mathrm{M}(\epsilon'_\mathsf{e}, \epsilon_\mathsf{e}, \mathbf{\Omega}'_\mathsf{e}\cdot\mathbf{\Omega}_\mathsf{e})\psi_\mathsf{e}(\mathbf{r}, \mathbf{\Omega}'_\mathsf{e}, \epsilon'_\mathsf{e})\ \mathrm{d}\epsilon_\mathsf{e}\ \mathrm{d}\epsilon'_\mathsf{e}\ \mathrm{d}\mathbf{\Omega}'_\mathsf{e}\ \mathrm{d}\mathbf{\Omega}_\mathsf{e}. \tag{3.8}$$

Now we use the Fokker-Planck asymptotic which was done for the BTE for electron for this dose formula. “This can again be done in a standard way, leading to the final result for the

asymptotically developed absorbed dose", [15]

$$D(r) = \frac{mc^2}{\rho(\mathbf{r})} T \int_{\epsilon_{\mathsf{s}}}^{\infty} S_{\mathrm{M}}(\mathbf{r}, \epsilon'_{\mathsf{e}}) \Phi(\mathbf{r}, \epsilon'_{\mathsf{e}}) \, \mathrm{d}\epsilon'_{\mathsf{e}}, \tag{3.9}$$

with $\Phi(\mathbf{r}, \epsilon_{\mathsf{e}}) := \int_{S^2} \psi_{\mathsf{e}}(\mathbf{r}, \mathbf{\Omega}'_{\mathsf{e}}, \epsilon_{\mathsf{e}}) \, \mathrm{d}\mathbf{\Omega}'_{\mathsf{e}}$.

Here S_{M} is the stopping power. The average energy loss of the particle per unit path length is called the stopping power, measured for example in MeV/cm.

Chapter 4

Numerical solution of the Boltzmann transport equation for photons

This chapter in devoted to the numerical resolution of the Boltzmann transport equation for photons. We solve the problem in a rectangular parallelepiped Q, full of water till a height H_W and with air in the rest. Considering water is typical in radiotherapy because its radiative properties are similar to those of human body. Besides, we will suppose that the irradiated area is rectangular and it is located on the upper face of Q. We should mention, however, that the method employed can be adapted to other geometries. In Figure 4.8, $\mathbf{R}(t)$ is a point where we would like to find the number of photons travelling in the direction $\mathbf{\Omega}_\gamma$. Here $\mathbf{r}^\star$ is the boundary point and ABDG is the area which is being irradiated by photons. In order to solve the BTE, we need an algorithm for computing $\mathbf{r}^\star$ for a given choice of $\mathbf{R}(t)$ and $\mathbf{\Omega}_\gamma$. In the above mentioned figure we see a unit sphere centered at $\mathbf{R}(t)$. In the mathematical model of Boltzmann photon transport equation we observe that for calculating the number of photons we need to calculate some integrals (in Equations (4.18), (4.19)) and the integrating area is the total or a part of the surface of the unit sphere. The total area will be needed when the energy is less or equal than $\frac{0.511}{2}$ MeV. But we like to solve the Boltzmann photon transport equation for the dose calculation of cancer treatment and for this treatment we use energies in practice greater than $\frac{0.511}{2}$ MeV. For this reason we will only show numerical results for energies greater than $\frac{0.511}{2}$ MeV, although our MATLAB

code is able to solve for smaller energies as well.

Since we know the boundary value of the number of photons, we can find the number of noninteracting photons at $\mathbf{R}(t)$ in the direction $\mathbf{\Omega}_\gamma$ for any energy by the formula (4.12) directly. If the boundary point of $\mathbf{\Omega}_\gamma$ is outside of the radiative area ABDG then the number of noninteracting photons is zero at $\mathbf{R}(t)$ because the boundary value is zero in the direction $\mathbf{\Omega}_\gamma$.

Let us consider a photon which is located at $\mathbf{R}(t)$ and travels with direction $\mathbf{\Omega}_\gamma$. The condition for that photon to have been scattered only once (and thus to be considered in $\psi_\gamma^{(1)}$) is that it comes from the radiative area ABDG and it has suffered only one scattering event at any point of the segment joining $\mathbf{r}^\star$ and $\mathbf{R}(t)$. The boundary point $\mathbf{r}^\star$ is the intersection of ∂Q with the line passing through R(t) and parallel to $\mathbf{\Omega}_\gamma$ when we travel in the direction $-\mathbf{\Omega}_\gamma$. Notice that, for fixed $\mathbf{R}(t)$, the boundary point $\mathbf{r}^\star$ changes if $\mathbf{\Omega}_\gamma$ changes.

The noninteracting photons come at $\mathbf{R}(t)$ only from the radiative area and then those photons interact at the point $\mathbf{R}(t)$ and go into direction $\mathbf{\Omega}_\gamma$. Therefore, one time interacting photons which are going in the direction $\mathbf{\Omega}_\gamma$ from $\mathbf{R}(t)$ come only from the radiative area ABDG. So, when the boundary point $\mathbf{r}^\star$ is inside the radiative area then the value of the number of one time interacting photon is nonzero, otherwise this value will be zero at $\mathbf{R}(t)$. We see from the above discussion that only a small part of the total surface of the unit sphere provides the nonzero value of the integrand. On the other hand, we see from the equation (4.34) that for a fixed $\mathbf{\Omega}_\gamma$ and for a fixed energy ϵ_γ there is an integrating area that comes from the transport equation of photons. So if this integration area does not intersect with the mentioned small part of the surface then obviously the value of the integration will be zero but, if they are intersecting then this intersecting part will provide the nonzero value for the integration and this intersecting part is the support of the integrand. So, for finding the number of one time interacting photons at $\mathbf{R}(t)$ we will take this intersecting area for integrating. But the shape of this intersecting area may be peculiar, so it is difficult to integrate in this area. On account of this, we take the minimum rectangle containing this intersecting area as domain of integration.

The one time scattered photons arrive at $\mathbf{R}(t)$ and interact at this point. Then, with a certain probability, they go in the direction $\mathbf{\Omega}_\gamma$. That means that one time interacting photons are the source of two times interacting photons. This one time interacting photons

may come from any position of the surface of the unit sphere. So, for finding the two times interacting photons at $\mathbf{R}(t)$ in the direction $\mathbf{\Omega}_\gamma$, only the limit of the integration which come from the formula of BTE in the mathematical model will be the support of this integrand. We take the minimum rectangle containing the support for the integration.

Similarly the two times interacting photons are the source of three times interacting photons and this two times interacting photons come in any direction. Therefore, for finding three times interacting photons the support of the integration will be same as the support that has used for finding the two times interacting photons. And for finding the more times interacting photons the support is the same. But we see the number of three time interacting photons is very small than the number of noninteracting, one time interacting and two times interacting photons. So for time minimizing and the value accuracy we take the number of noninteracting, one time interacting and two times interacting photons for the total number of photons at that point in the direction $\mathbf{\Omega}_\gamma$ only.

When the energy increases the domain of integration over the surface become smaller. We observed that if the energy is 20-30 MeV then the limiting area in the integration (4.34) is very small. In that case if we don't into consideration the support for the integration then maybe the nodes of the quadrature mesh will not touch the support, then the value of the integral will be badly approximated by zero. So, for minimizing the time and for value accuracy we must use the support of the integrand for the integrating area. In this chapter we discuss the process for finding the support in detail.

We show the support with the full surface area of the unit sphere in the Figure 4.12. Also we separate this support that has been shown in this figure. We mentioned previously only the noninteracting photons come from the radiative area and interact at $\mathbf{R}(t)$ then go in the direction $\mathbf{\Omega}_\gamma$. Those photons are called the one time interacting photons. But some photons come from the radiated area at the previous point of $\mathbf{R}(t)$ on the direction $\mathbf{\Omega}_\gamma$ and interact at that point then go in the direction of $\mathbf{\Omega}_\gamma$. These one time interacting photons (see Figure 4.1) also go to the point $\mathbf{R}(t)$. Therefore we will have to consider these number of photons because these also the one time interacting photon going from the point $\mathbf{R}(t)$. There are an infinite number of points before $\mathbf{R}(t)$ on the $\mathbf{\Omega}_\gamma$ direction, but the formula for finding the number of one time interacting photon contains this idea. So it is good news that we don't need to calculate the number of one time interacting photons separately at each point before $\mathbf{R}(t)$ on the direction line of Ω_γ. For two times or more times interacting photons this process will be the same.

We have made a MATLAB code for solving the photon transport equation that is described

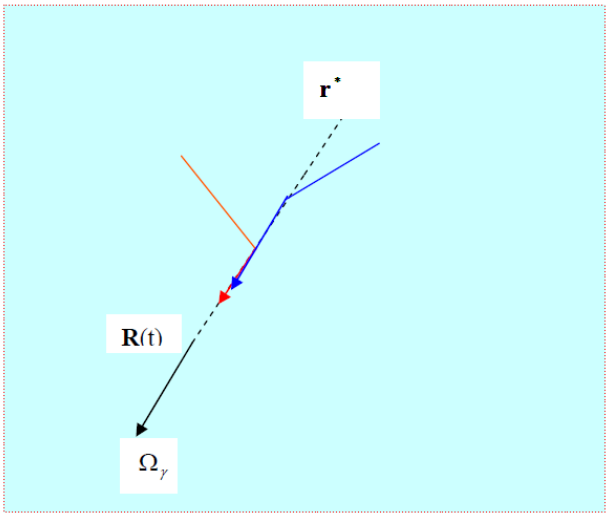

Figure 4.1

in this chapter. In the energy range studied we see photon has large mean free path in air and tissue. So the approximate development of the Boltzmann photon transport equation is based on the observation of photons ([18], table A3). The mean free path of photons are in the range of about 10 to 50 centimetres. Therefore the photon which enters a patient's body is only subject only to a few Compton scattering events, say 1 to 3 or even none, before it leaves the body.

"To calculate the absorbed dose in the patients body it is not of interest to calculate the complete history of the photons, but suffices to consider only those that made M interaction in the body, M being 2 or 3", [15].

Since the mean free path of photon is large so we find the number of noninteracting photos, one time interacting photons and two times interacting photons. But for experiment, we also calculate three times interacting photons and observed that this number is very small and the time is very high, so we don't consider the three times interacting photons only we count for the total number of photos which are noninteracting photons , one time and two times interacting photons that has described in this chapter. We give the results of the Boltzmann photon transport equation for some example and discuss. We represent the combination of the number of photons on the some individual plane and discuss graphically in here. A two-dimensional composite trapezoidal formula has been used for calculating the integral involved in the mathematical model. For our confidence we check this methods in this chapter also.

4.1 Resolution of the BTE of photons

To find an approximate solution for the photons we decompose the photon fluency ψ_γ formally into a series of 0-times, 1-times, ..., i-times, ..., at least N-times scattered photons [11]. Then

$$\psi_\gamma(\mathbf{r}, \mathbf{\Omega}_\gamma, \epsilon_\gamma) = \sum_{i=1}^{N} \psi_\gamma^{(i)}(\mathbf{r}, \mathbf{\Omega}_\gamma, \epsilon_\gamma). \tag{4.1}$$

where for $i = 0,\ 1,\ \cdots,\ N-1$, $\psi_\gamma^{(i)}$ is the number of photons that are scattered i-times and $\psi_\gamma^{(N)}$ is the number of photons that are scattered N or more times. This is only a formal decomposition, physically all photons are indistinguishable. Using this approach in the photon transport equation (5.29) one gets

$$\mathbf{\Omega}_\gamma \cdot \nabla \sum_{i=0}^{N} \psi_\gamma^{(i)} + \rho_\mathsf{e} \sigma_{C,\gamma}^{\mathrm{tot}} \sum_{i=0}^{N} \psi_\gamma^{(i)} = \rho_\mathsf{e} \int\int \tilde{\sigma}_{C,\gamma}(\epsilon'_\gamma, \epsilon_\gamma, \mathbf{\Omega'}_\gamma \cdot \mathbf{\Omega}_\gamma) \sum_{i=0}^{N} \psi_\gamma^{(i)}(\mathbf{\Omega'}_\gamma, \epsilon'_\gamma)\ \mathrm{d}\mathbf{\Omega'}_\gamma\ \mathrm{d}\epsilon'_\gamma. \tag{4.2}$$

As it is explained in [15],interchanging the order of integration and summation and using the fact that photons are scattered $(i-1)$-times can only act as a source for photons that are scattered i-times, one can uniquely decompose the integrodifferential equation into a system of differential equations and one integrodifferential equation:

$$\mathbf{\Omega}_\gamma \cdot \nabla \psi_\gamma^{(0)} + \rho_\mathsf{e} \sigma_{C,\gamma}^{\mathrm{tot}} \psi_\gamma^{(0)} = 0$$

$$\mathbf{\Omega}_\gamma \cdot \nabla \psi_\gamma^{(1)} + \rho_\mathsf{e} \sigma_{C,\gamma}^{\mathrm{tot}} \psi_\gamma^{(1)} = \rho_\mathsf{e} \int\int \tilde{\sigma}_{C,\gamma}(\epsilon'_\gamma, \epsilon_\gamma, \mathbf{\Omega'}_\gamma \cdot \mathbf{\Omega}_\gamma) \psi_\gamma^{(0)}(\mathbf{\Omega'}_\gamma, \epsilon'_\gamma)\ \mathrm{d}\mathbf{\Omega'}_\gamma\ \mathrm{d}\epsilon'_\gamma$$

$$\vdots$$

$$\mathbf{\Omega}_\gamma \cdot \nabla \psi_\gamma^{(i)} + \rho_\mathsf{e} \sigma_{C,\gamma}^{\mathrm{tot}} \psi_\gamma^{(i)} = \rho_\mathsf{e} \int\int \tilde{\sigma}_{C,\gamma}(\epsilon'_\gamma, \epsilon_\gamma, \mathbf{\Omega'}_\gamma \cdot \mathbf{\Omega}_\gamma) \psi_\gamma^{(i-1)}(\mathbf{\Omega'}_\gamma, \epsilon'_\gamma)\ \mathrm{d}\mathbf{\Omega'}_\gamma\ \mathrm{d}\epsilon'_\gamma$$

$$\vdots$$

$$\begin{aligned} \mathbf{\Omega}_\gamma \cdot \nabla \psi_\gamma^{(N)} + \rho_\mathsf{e} \sigma_{C,\gamma}^{\mathrm{tot}} \psi_\gamma^{(N)} =& \rho_\mathsf{e} \int\int \tilde{\sigma}_{C,\gamma}(\epsilon'_\gamma, \epsilon_\gamma, \mathbf{\Omega'}_\gamma \cdot \mathbf{\Omega}_\gamma) \psi_\gamma^{(N-1)}(\mathbf{\Omega'}_\gamma, \epsilon'_\gamma)\ \mathrm{d}\mathbf{\Omega'}_\gamma\ \mathrm{d}\epsilon'_\gamma \\ &+ \rho_\mathsf{e} \int\int \tilde{\sigma}_{C,\gamma}(\epsilon'_\gamma, \epsilon_\gamma, \mathbf{\Omega'}_\gamma \cdot \mathbf{\Omega}_\gamma) \psi_\gamma^{(N)}(\mathbf{\Omega'}_\gamma, \epsilon'_\gamma)\ \mathrm{d}\mathbf{\Omega'}_\gamma\ \mathrm{d}\epsilon'_\gamma. \end{aligned} \tag{4.3}$$

If we restrict the system of photons that are scattered at most M times we get the following set of M coupled partial differential equations with $M < N$

$$\mathbf{\Omega}_\gamma \cdot \nabla \psi_\gamma^{(0)} + \rho \sigma_{C,\gamma}^{\mathrm{tot}} \psi_\gamma^{(0)} = 0$$

$$\boldsymbol{\Omega}_\gamma \cdot \nabla \psi_\gamma^{(1)} + \rho_{\mathsf{e}} \sigma_{C,\gamma}^{\mathrm{tot}} \psi_\gamma^{(1)} = \rho_{\mathsf{e}} \int \int \tilde{\sigma}_{C,\gamma}(\epsilon'_\gamma, \epsilon_\gamma, \boldsymbol{\Omega}'_\gamma \cdot \boldsymbol{\Omega}_\gamma) \psi_\gamma^{(0)}(\boldsymbol{\Omega}'_\gamma, \epsilon'_\gamma) \, \mathrm{d}\boldsymbol{\Omega}'_\gamma \, \mathrm{d}\epsilon'_\gamma$$

.

.

.

$$\boldsymbol{\Omega}_\gamma \cdot \nabla \psi_\gamma^{(M)} + \rho_{\mathsf{e}} \sigma_{C,\gamma}^{\mathrm{tot}} \psi_\gamma^{(M)} = \rho_{\mathsf{e}} \int \int \tilde{\sigma}_{C,\gamma}(\epsilon'_\gamma, \epsilon_\gamma, \boldsymbol{\Omega}'_\gamma \cdot \boldsymbol{\Omega}_\gamma) \psi_\gamma^{(M-1)}(\boldsymbol{\Omega}'_\gamma, \epsilon'_\gamma) \, \mathrm{d}\boldsymbol{\Omega}'_\gamma \, \mathrm{d}\epsilon'_\gamma. \quad (4.4)$$

This set of differential equations can be solved with less effort than the exact original integrodifferential equation. The idea is to solve the above equations for $\psi_\gamma^{(0)}, ..., \psi_\gamma^{(M)}$ and compute ψ_γ via the approximation

$$\psi_\gamma(\mathbf{r}, \boldsymbol{\Omega}_\gamma, \epsilon_\gamma) \approx \sum_{i=0}^{M} \psi_\gamma^{(i)}(\mathbf{r}, \boldsymbol{\Omega}_\gamma, \epsilon_\gamma). \quad (4.5)$$

Let $Q \subset \mathbb{R}^3$ be the spatial domain, Q is assumed to be non empty, open, bounded and convex. Again let ∂Q be the boundary of the domain Q and $\bar{Q}$ be the closure of the domain. So, $\bar{Q} = Q \cup \partial Q$. Let $\Gamma \subset \partial Q$ be the irradiated part and let $\Lambda = \partial Q \setminus \Gamma$ be the non irradiated part. Here $\boldsymbol{n}(\mathbf{r})$ is the outward unit normal at $\mathbf{r} \in \partial Q$.
The following are the boundary conditions needed for computing $\psi_\gamma^{(0)}, ..., \psi_\gamma^{(M)}$.

$$\left.\begin{array}{rll} \psi_\gamma^{(0)}(\mathbf{r}, \boldsymbol{\Omega}_\gamma, \epsilon_\gamma) \mid_{\mathrm{r}\in\Gamma} = \psi_\gamma^{(0)}(\mathbf{r}, \boldsymbol{\Omega}_\gamma, \epsilon_\gamma); & \text{for} & \boldsymbol{n}(\mathbf{r}) \cdot \boldsymbol{\Omega}_\gamma < 0 \\ \psi_\gamma^{(0)}(\mathbf{r}, \boldsymbol{\Omega}_\gamma, \epsilon_\gamma) \mid_{\mathrm{r}\in\Lambda} = 0; & \text{for} & \boldsymbol{n}(\mathbf{r}) \cdot \boldsymbol{\Omega}_\gamma < 0 \\ \psi_\gamma^{(i)}(\mathbf{r}, \boldsymbol{\Omega}_\gamma, \epsilon_\gamma) \mid_{\mathrm{r}\in\partial Q} = 0; & \text{for} & \boldsymbol{n}(\mathbf{r}) \cdot \boldsymbol{\Omega}_\gamma < 0, \ 1 \le i \le M. \end{array}\right\} \quad (4.6)$$

4.1.1 Obtaining $\psi_\gamma^{(i)}$ for $i = 0, ..., M$

We get from the previous discussion

$$\sum_{i=0}^{M} \psi_\gamma^{(i)}(\mathbf{r}, \boldsymbol{\Omega}_\gamma, \epsilon_\gamma) \approx \psi_\gamma(\mathbf{r}, \boldsymbol{\Omega}_\gamma, \epsilon_\gamma).$$

Now our objective is to obtain $\psi_\gamma^{(i)}$ for $i = 0, ..., M$.

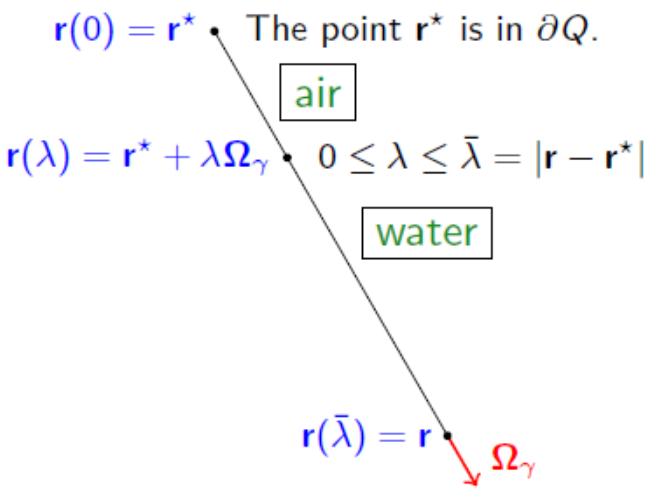

Figure 4.2

4.1.2 Obtaining $\psi_\gamma^{(0)}$

We begin to solve the first equation of (4.4) to get $\psi_\gamma^{(0)}$.
In particular given $\mathbf{r}^\star \in \partial Q$ and $\mathbf{\Omega}_\gamma \in S^2$ (photon direction) such that $\mathbf{\Omega}_\gamma \cdot \boldsymbol{n}(\mathbf{r}^\star) < 0$, we get an analytical expression for the value of $\psi_\gamma^{(0)}$ on the line passing from $\mathbf{r}^\star$ in the direction $\mathbf{\Omega}_\gamma$. Naturally it is the part of the line which is contained in the domain Q (see Figure 4.2). The equation of the segment is

$$\mathbf{r}(\lambda) = \mathbf{r}^\star + \lambda \mathbf{\Omega}_\gamma, \tag{4.7}$$

with $\lambda \in [0,\ L]$ for some positive value of L. Here $\lambda \geq 0$ such that $\mathbf{r}(\lambda) \in Q$. This Figure 4.2 represents the path of the photon.
Thus the first equation of (4.4)

$$\mathbf{\Omega}_\gamma \cdot \nabla \psi_\gamma^{(0)}(\mathbf{r}, \mathbf{\Omega}_\gamma, \epsilon_\gamma) + \rho_{\mathsf{e}}(\mathbf{r}) \sigma_{C,\gamma}^{\mathrm{tot}}(\epsilon_\gamma) \psi_\gamma^{(0)}(\mathbf{r}, \mathbf{\Omega}_\gamma, \epsilon_\gamma) = 0 \tag{4.8}$$

implies

$$\frac{\mathrm{d}\psi_\gamma^{(0)}(\mathbf{r}(\lambda), \mathbf{\Omega}_\gamma, \epsilon_\gamma)}{\mathrm{d}\lambda} + \rho_{\mathsf{e}}(\mathbf{r}(\lambda)) \sigma_{C,\gamma}^{\mathrm{tot}}(\epsilon_\gamma) \psi_\gamma^{(0)}(\mathbf{r}(\lambda), \mathbf{\Omega}_\gamma, \epsilon_\gamma) = 0. \tag{4.9}$$

If we define

$$y(\lambda) = \psi_\gamma^{(0)}(\mathbf{r}(\lambda), \mathbf{\Omega}_\gamma, \epsilon_\gamma),$$

$$f(\lambda) = -\rho_{\mathsf{e}}(\mathbf{r}(\lambda)) \sigma_{C,\gamma}^{\mathrm{tot}}(\epsilon_\gamma)$$

and

$$y_0 = \psi_\gamma^{(0)}(\mathbf{r}^\star, \mathbf{\Omega}_\gamma, \epsilon_\gamma)$$

then our problem (4.9) is formulated as follows

$$\left.\begin{array}{c} y'(\lambda) = f(\lambda)y(\lambda) \\ y(0) = y_0 \end{array}\right\}. \tag{4.10}$$

The solution of equation (4.10) is clearly

$$y(\lambda) = y_0 \mathrm{e}^{\int_0^\lambda f(s)\ \mathrm{d}s}. \tag{4.11}$$

Hence the solution of the first equation of (4.4) is

$$\psi_\gamma^{(0)}(\mathbf{r}(\lambda), \mathbf{\Omega}_\gamma, \epsilon_\gamma) = \psi_\gamma^{(0)}(\mathbf{r}^\star, \mathbf{\Omega}_\gamma, \epsilon_\gamma)\mathrm{e}^{-\rho_\mathsf{e}(r(s))\int_0^\lambda \sigma_{C,\gamma}^{\mathrm{tot}}(\epsilon_\gamma)\ \mathrm{d}s} \tag{4.12}$$

which takes the value 0 if $\mathbf{r}^\star \in \Lambda$. This process can be performed for each value of $\epsilon_\gamma > 0$ (energy of photon) according to (4.6).

4.1.3 Obtaining $\psi_\gamma^{(i)}$ for $i = 1, ..., M$

For known $\psi_\gamma^{(0)}$ we will have to find $\psi_\gamma^{(i)}$, $i = 1, ..., M$ given the similarity to the equation for $\psi_\gamma^{(0)}$, proceed in a similar way.
For $i \geq 1$ the i^{th} equation of (4.4) is

$$\mathbf{\Omega}_\gamma \cdot \nabla\psi_\gamma^{(i)} + \rho_\mathsf{e}\sigma_{C,\gamma}^{\mathrm{tot}}\psi_\gamma^{(i)} = \rho_\mathsf{e}\int\int \tilde{\sigma}_{C,\lambda}(\epsilon'_\gamma, \epsilon_\gamma, \mathbf{\Omega'}_\gamma \cdot \mathbf{\Omega}_\gamma)\psi_\gamma^{(i-1)}(\mathbf{r}(\lambda), \mathbf{\Omega'}_\gamma, \epsilon'_\gamma)\ \mathrm{d}\mathbf{\Omega'}_\gamma\ \mathrm{d}\epsilon'_\gamma. \tag{4.13}$$

If we write on the line $\mathbf{r}(\lambda)$ for fixed $\mathbf{\Omega}_\gamma$ and ϵ_γ then the equation becomes the following:

$$\begin{aligned}\frac{\mathrm{d}\psi_\gamma^{(i)}(\mathbf{r}(\lambda), \mathbf{\Omega}_\gamma, \epsilon_\gamma)}{\mathrm{d}\lambda} &+ \rho_\mathsf{e}(\mathbf{r}(\lambda))\sigma_{C,\gamma}^{\mathrm{tot}}(\epsilon_\gamma)\psi_\gamma^{(i)}(\mathbf{r}(\lambda), \mathbf{\Omega}_\epsilon) \\ &= \rho_\mathsf{e}(\mathbf{r}(\lambda))\int_0^\infty \int_{S^2} \tilde{\sigma}_{C,\gamma}(\epsilon'_\gamma, \epsilon_\gamma, \mathbf{\Omega'}_\gamma \cdot \mathbf{\Omega}_\gamma)\psi_\gamma^{(i-1)}(\mathbf{r}(\lambda), \mathbf{\Omega'}_\gamma, \epsilon'_\gamma)\ \mathrm{d}\mathbf{\Omega'}_\gamma\ \mathrm{d}\epsilon'_\gamma.\end{aligned} \tag{4.14}$$

As we did in the homogeneous case, we write our problem by using more simple notation:

$$y(\lambda) = \psi_\gamma^{(i)}(\mathbf{r}(\lambda), \mathbf{\Omega}_\gamma, \epsilon_\gamma)$$

$$f(\lambda) = -\rho_{\mathsf{e}}(\mathbf{r}(\lambda))\sigma^{\mathrm{tot}}_{C,\gamma}(\epsilon_\gamma)$$

$$g(\lambda) = \rho_{\mathsf{e}}(\mathbf{r}(\lambda)) \int_0^\infty \int_{S^2} \tilde{\sigma}_{C,\gamma}(\epsilon'_\gamma, \epsilon_\gamma, \mathbf{\Omega'}_\gamma \cdot \mathbf{\Omega}_\gamma)\psi^{(i-1)}_\gamma(\mathbf{r}(\lambda), \mathbf{\Omega'}_\gamma, \epsilon'_\gamma)\ \mathrm{d}\mathbf{\Omega}'_\gamma\ \mathrm{d}\epsilon'_\gamma. \tag{4.15}$$

Thus equation (4.14) is written

$$\left.\begin{array}{c} y'(\lambda) = f(\lambda)y(\lambda) + g(\lambda) \\ y(0) = y_0 \end{array}\right\} \tag{4.16}$$

and therefore

$$\begin{aligned} y(\lambda) &= \left\{ \int_0^\lambda g(t)\mathrm{e}^{-\int_0^t f(s)\ \mathrm{d}s}\mathrm{d}t \right\} \mathrm{e}^{\int_0^\lambda f(s)\ \mathrm{d}s} \\ &= \int_0^\lambda \left\{ g(t)\mathrm{e}^{\int_t^\lambda f(s)\ \mathrm{d}s} \right\} \mathrm{d}t. \end{aligned} \tag{4.17}$$

Then the solution of (4.16)is;

$$\psi^{(i)}_\gamma(\mathbf{r}(\lambda), \mathbf{\Omega}_\gamma, \epsilon_\gamma) = \int_0^\lambda g^{(i-1)}_{\epsilon_\gamma, \mathbf{\Omega}_\gamma}(t)\mathrm{e}^{-(\int_t^\lambda \rho_{\mathsf{e}}(r(s))\ \mathrm{d}s)\sigma^{\mathrm{tot}}_{C,\gamma}(\epsilon_\gamma)}\ \mathrm{d}t, \tag{4.18}$$

where we use the notation

$$g^{(i-1)}_{\epsilon_\gamma, \mathbf{\Omega}_\gamma}(\lambda) = \rho_{\mathsf{e}}(\mathbf{r}(\lambda)) \int_0^\infty \int_{S^2} \tilde{\sigma}_{C,\gamma}(\epsilon'_\gamma, \epsilon_\gamma, \mathbf{\Omega'}_\gamma \cdot \mathbf{\Omega}_\gamma)\psi^{(i-1)}_\gamma(\mathbf{r}(\lambda), \mathbf{\Omega}'_\gamma, \epsilon'_\gamma)\ \mathrm{d}\mathbf{\Omega}'_\gamma\ \mathrm{d}\epsilon'_\gamma. \tag{4.19}$$

4.1.4 Resolution of the improper integral in the interval $[0, \infty)$.

In the formula of $\psi^{(i)}_\gamma$, for $i \geq 1$, we see that $g^{(i-1)}_{\epsilon\gamma, \mathbf{\Omega}_\gamma}$ contains the integral

$$\int_0^\infty \int_{S^2} \tilde{\sigma}_{C,\gamma}(\epsilon'_\gamma, \epsilon_\gamma, \mathbf{\Omega}'_\gamma \cdot \mathbf{\Omega}_\gamma)\psi^{(i-1)}_\gamma(\mathbf{r}(\lambda), \mathbf{\Omega}'_\gamma, \epsilon'_\gamma)\ \mathrm{d}\mathbf{\Omega}'_\gamma\ \mathrm{d}\epsilon'_\gamma, \tag{4.20}$$

where

$$\tilde{\sigma}_{C,\gamma}(\epsilon'_\gamma, \epsilon_\gamma, \mathbf{\Omega}'_\gamma \cdot \mathbf{\Omega}_\gamma) = \sigma_{C,\gamma}(\epsilon'_\gamma, \mathbf{\Omega}'_\gamma \cdot \mathbf{\Omega}_\gamma)\delta_{C,\gamma}(\epsilon'_\gamma, \epsilon_\gamma, \mathbf{\Omega}'_\gamma \cdot \mathbf{\Omega}_\gamma) \tag{4.21}$$

with

$$\sigma_{C,\gamma}(\epsilon'_\gamma, \mathbf{\Omega}'_\gamma \cdot \mathbf{\Omega}_\gamma) = \frac{r^2_{\mathsf{e}}}{2}\left[\frac{1}{1+\epsilon'_\gamma(1-\cos\theta)}\right]^3 + \left[1 + \cos^2\theta + \frac{\epsilon'^2_\gamma(1-\cos\theta)^2}{1+\epsilon'_\gamma(1-\cos\theta)}\right] \tag{4.22}$$

and

$$\delta_{C,\gamma}(\epsilon'_\gamma, \epsilon_\gamma, \mathbf{\Omega'}_\gamma \cdot \mathbf{\Omega}_\gamma) = \delta\left[\epsilon_\gamma - \frac{\epsilon'_\gamma}{1+\epsilon'_\gamma(1-\cos\theta)}\right]. \tag{4.23}$$

In the expressions above, $\cos\theta = \mathbf{\Omega}'_\gamma \cdot \mathbf{\Omega}_\gamma$.

We know from [12] that

$$\int_0^\infty G(\epsilon'_\gamma)\delta(h(\epsilon'_\gamma, \epsilon_\gamma))\ \mathrm{d}\epsilon'_\gamma = \sum \frac{G(E'_\gamma)}{|\frac{\partial h}{\partial \epsilon'_\gamma}(E'_\gamma, \epsilon_\gamma)|}, \tag{4.24}$$

where the sum is taken over all those $E'_\gamma \in (0,\infty)$ such that $h(E'_\gamma, \epsilon_\gamma) = 0$. In case there exist no E'_γ in $(0,\infty)$ such that $h(E'_\gamma, \epsilon_\gamma) = 0$ then

$$\int_0^\infty G(\epsilon')\delta(h(\epsilon'_\gamma, \epsilon_\gamma))\ \mathrm{d}\epsilon'_\gamma = 0.$$

Here

$$h(\epsilon'_\gamma, \epsilon_\gamma, \mathbf{\Omega}'_\gamma \cdot \mathbf{\Omega}_\gamma) = \epsilon_\gamma - \frac{\epsilon'_\gamma}{1 + \epsilon'_\gamma(1-\cos\theta)}.$$

Now we will find the value of incoming energy ϵ'_γ for given ϵ_γ and $\mathbf{\Omega'}_\gamma \cdot \mathbf{\Omega}_\gamma$ such that for this value the function h will be zero. Let $\epsilon'_\gamma = E'_\gamma$ be that value. Therefore

$$h(E'_\gamma, \epsilon_\gamma, \mathbf{\Omega'}_\gamma \cdot \mathbf{\Omega}_\gamma) = 0. \tag{4.25}$$

Also we need

$$\frac{\partial h}{\partial \epsilon'_\gamma}(\epsilon'_\gamma, \epsilon_\gamma, \mathbf{\Omega'}_\gamma \cdot \mathbf{\Omega}_\gamma) = \frac{-1}{[1 + \epsilon'_\gamma(1-\cos\theta)]^2}. \tag{4.26}$$

Then we proceed to the calculation of those $E'_\gamma \in (0,\infty)$ such that $h(E'_\gamma, \epsilon_\gamma, \mathbf{\Omega'}_\gamma \cdot \mathbf{\Omega}_\gamma) = 0$ (for given $\epsilon_\gamma \in (0,\infty)$ and given $\cos\theta = \mathbf{\Omega}'_\gamma \cdot \mathbf{\Omega}_\gamma \in [-1,1]$).

Therefore, we fix $\epsilon_\gamma \in (0,\infty)$ and $C = \cos\theta \in [-1,1]$ and we define $f(x) := h(x, \epsilon_\gamma, C) = \epsilon_\gamma - \frac{x}{1+x(1-C)}$ for $x \in (0,\infty)$. We can get the value of E'_γ by solving the equation $f(x) = 0$.

1. Case $C = 1$.

$$f(x) = \epsilon_\gamma - x = 0 \Longleftrightarrow x = \epsilon_\gamma. \tag{4.27}$$

   Let us call $\tilde{E'}_\gamma = \epsilon_\gamma$

2. Case $C \neq 1$.

   Then we get the following:

$$f(x) = \epsilon_\gamma - \frac{x}{1 + x(1-C)} \text{ for } x \in (0,\infty), \text{ and } f(0) = \epsilon_\gamma > 0 \tag{4.28}$$

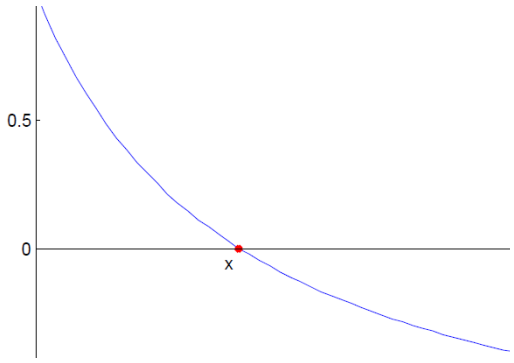

Figure 4.3

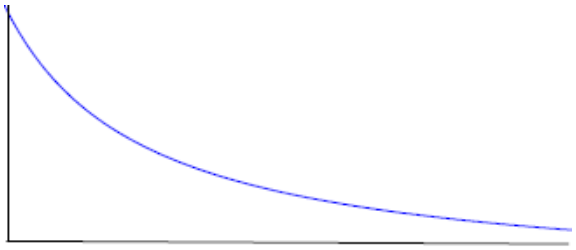

Figure 4.4

$$\lim_{x\to\infty} f(x) = \epsilon_\gamma - \frac{1}{1-C} \tag{4.29}$$

and

$$f'(x) = \frac{-1}{[1+x(1-C)]^2} < 0. \tag{4.30}$$

(a) When $\epsilon_\gamma < \frac{1}{1-C}$ then
$\exists!\ \bar{x} \in (0,\infty)$ such that $f(\bar{x}) = 0$ and $\bar{x} = \frac{\epsilon_\gamma}{1+\epsilon_\gamma(C-1)}$ (see Figure 4.3). Let us call $E'_\gamma \frac{\epsilon_\gamma}{1+\epsilon_\gamma(C-1)}$.

(b) When $\epsilon_\gamma \geq \frac{1}{1-C}$ then
there is no $\bar{x} \in (0,\infty)$ such that $f(\bar{x}) = 0$ (see Figure 4.4).

Also we need:

1. When $C = \cos\theta = \mathbf{\Omega'}_\gamma \cdot \mathbf{\Omega}_\gamma = 1$ then

$$\frac{\partial h}{\partial \epsilon'_\gamma}(\tilde{E'}_\gamma, \epsilon_\gamma, \mathbf{\Omega'}_\gamma \cdot \mathbf{\Omega}_\gamma) = \frac{\partial h}{\partial \epsilon'_\gamma}(\tilde{E'}_\gamma, \epsilon_\gamma, 1) = -1. \tag{4.31}$$

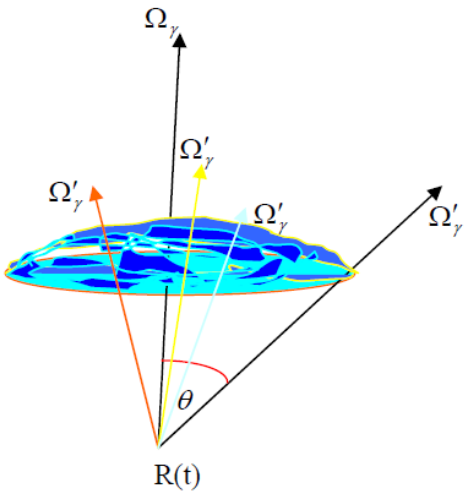

Figure 4.5

2. When $C \in [-1, 1)$ and $\epsilon_\gamma < \frac{1}{1-C}$ then

$$\frac{\partial h}{\partial \epsilon'_\gamma}(E'_\gamma, \epsilon_\gamma, \mathbf{\Omega'}_\gamma \cdot \mathbf{\Omega}_\gamma) = \frac{1}{[1 + \frac{\epsilon_\gamma}{1+\epsilon_\gamma(C-1)}(1-C)]^2} = -[1 + \epsilon_\gamma(C-1)]^2. \tag{4.32}$$

Consequently, for given $\epsilon_\gamma \in (0, \infty)$, $\mathbf{\Omega'}_\gamma$, $\mathbf{\Omega}_\gamma \in S^2$ and $\mathbf{r}(\lambda)$, we get:

$$\begin{aligned}
&\int_0^\infty \tilde{\sigma}_{C,\gamma}(\epsilon'_\gamma, \epsilon_\gamma, \mathbf{\Omega'}_\gamma \cdot \mathbf{\Omega}_\gamma)\psi_\gamma^{(i-1)}(\mathbf{r}(\lambda), \mathbf{\Omega'}_\gamma, \epsilon'_\gamma)\mathrm{d}\epsilon'_\gamma \\
&= \int_0^\infty \sigma_{C,\gamma}(\epsilon'_\gamma, \mathbf{\Omega'}_\gamma \cdot \mathbf{\Omega}_\gamma)\psi_\gamma^{(i-1)}(\mathbf{r}(\lambda), \mathbf{\Omega'}_\gamma, \epsilon'_\gamma)\delta_{C,\gamma}(\epsilon'_\gamma, \epsilon_\gamma, \mathbf{\Omega'}_\gamma \cdot \mathbf{\Omega}_\gamma)\mathrm{d}\epsilon'_\gamma \\
&= \begin{cases}
\sigma_{C,\gamma}(\epsilon_\gamma, 1)\psi_\gamma^{(i-1)}(\mathbf{r}(\lambda), \mathbf{\Omega'}_\gamma, \epsilon_\gamma); & \text{if } \mathbf{\Omega'}_\gamma \cdot \mathbf{\Omega}_\gamma = 1, (\mathbf{\Omega'}_\gamma = \mathbf{\Omega}_\gamma) \\
\dfrac{\sigma_{C,\gamma}(E'_\gamma, C)\psi_\gamma^{(i-1)}(\mathbf{r}(\lambda), \mathbf{\Omega'}_\gamma, E'_\gamma)}{[1 + \epsilon_\gamma(C-1)]^2}; & \text{if } \mathbf{\Omega'}_\gamma \cdot \mathbf{\Omega}_\gamma = \cos\theta = C \neq 1, \text{and } \epsilon_\gamma \in (0, \frac{1}{1-C}) \\
0; & \text{otherwise, } (C \neq 1, \text{and } \epsilon_\gamma \geq \frac{1}{1-C}) \Leftrightarrow (C \leq 1 - \frac{1}{\epsilon_\gamma}),
\end{cases}
\end{aligned} \tag{4.33}$$

where $E'_\gamma = \frac{\epsilon_\gamma}{1+\epsilon_\gamma(C-1)}$.

Note that equation (4.33) define for fixed $\mathbf{\Omega}_\gamma$ a function on S^2 the unit sphere. When the energy ϵ_γ belongs to $(0\,\frac{1}{2}]$ then $C \leq 1 - \frac{1}{\epsilon_\gamma}$ is not possible and the support of the function (4.33) is the whole sphere S^2 but when the energy ϵ_γ is larger than $\frac{1}{2}$ then the support of (4.33) is only part of S^2, as shown in Figure 4.5.

Therefore we get from the above equation (4.33)

$$\begin{aligned} g^{(i-1)}_{\epsilon_\gamma,\mathbf{\Omega}_\gamma}(\lambda) &= \rho_{\mathsf{e}}(\mathbf{r}(\lambda)) \int_0^\infty \int_{S^2} \tilde{\sigma}_{C,\gamma}(\epsilon'_\gamma, \epsilon_\gamma, \mathbf{\Omega'}_\gamma \cdot \mathbf{\Omega}_\gamma) \psi^{(i-1)}_\gamma(\mathbf{r}(\lambda), \mathbf{\Omega}'_\gamma, \epsilon'_\gamma) \mathrm{d}\mathbf{\Omega'}_\gamma \mathrm{d}\epsilon'_\gamma \\ &= \rho_{\mathsf{e}}(\mathbf{r}(\lambda)) \int_{S^2} \int_0^\infty \tilde{\sigma}_{C,\gamma}(\epsilon'_\gamma, \epsilon_\gamma, \mathbf{\Omega}'_\gamma \cdot \mathbf{\Omega}_\gamma) \psi^{(i-1)}_\gamma(\mathbf{r}(\lambda), \mathbf{\Omega}'_\gamma, \epsilon'_\gamma) \mathrm{d}\epsilon'_\gamma \mathrm{d}\mathbf{\Omega}'_\gamma \\ &= \rho_{\mathsf{e}}(\mathbf{r}(\lambda)) \int_D \frac{\sigma_{C,\gamma}(E'_\gamma, C) \psi^{(i-1)}_\gamma(\mathbf{r}(\lambda), \mathbf{\Omega}'_\gamma, E'_\gamma)}{[1+\epsilon_\gamma(C-1)]^2} \mathrm{d}\mathbf{\Omega}'_\gamma. \end{aligned} \tag{4.34}$$

Where $D \subset S^2$ is defined by $D = \left\{ \mathbf{\Omega}'_\gamma \in S^2 : \mathbf{\Omega}'_\gamma \cdot \mathbf{\Omega}_\gamma = \cos\theta = C \neq 1 \text{ and } \epsilon_\gamma \in (0, \frac{1}{1-C}) \right\}$.

4.1.5 Change to spherical coordinates

We change the equation (4.34) to spherical coordinate in here. We take S^2 as a unit sphere then, for point $(x, y, z) \in S^2$, we can put, $x = \rho \sin\varphi \cos\vartheta$, $y = \rho \sin\varphi \sin\vartheta$ and $z = \rho \cos\varphi$ where $\rho = 1$, φ is the zenith angle with $0 \leq \varphi \leq \pi$ and ϑ is the polar angle with $0 \leq \vartheta \leq 2\pi$.

Now,

$$\mathbf{T}_\varphi = \left(\frac{\partial x}{\partial \varphi}, \frac{\partial y}{\partial \varphi}, \frac{\partial z}{\partial \varphi} \right)^T = (\cos\varphi\cos\vartheta, \cos\varphi\sin\vartheta, -\sin\varphi)^T \tag{4.35}$$

$$\mathbf{T}_\vartheta = \left(\frac{\partial x}{\partial \vartheta}, \frac{\partial y}{\partial \vartheta}, \frac{\partial z}{\partial \vartheta} \right)^T = (-\sin\varphi\sin\vartheta, \sin\varphi\cos\vartheta, 0)^T \tag{4.36}$$

$$\begin{aligned} \mathbf{T}_\varphi \times \mathbf{T}_\vartheta &= \begin{bmatrix} \mathbf{e}_1 & \mathbf{e}_2 & \mathbf{e}_3 \\ \cos\varphi\cos\vartheta & \cos\varphi\sin\vartheta & -\sin\varphi \\ -\sin\varphi\sin\vartheta & \sin\varphi\cos\vartheta & 0 \end{bmatrix} \\ &= (\sin^2\varphi\cos\vartheta, -\sin^4\varphi\sin\vartheta, \cos\varphi\sin\vartheta) \end{aligned} \tag{4.37}$$

Therefore,

$$\|\mathbf{T}_\varphi \times \mathbf{T}_\vartheta\| = \sin\varphi \tag{4.38}$$

The given conditions are $\mathbf{\Omega}'_\gamma \cdot \mathbf{\Omega}_\gamma = \cos\theta = C \neq 1$ and $\epsilon_\gamma \in (0, \frac{1}{1-C})$.
Now we get from the above line

$$\begin{aligned} \epsilon_\gamma \in (0, \frac{1}{1-C}) &\Longrightarrow 0 < \epsilon_\gamma < \frac{1}{1-C} \\ &\Longrightarrow \frac{1}{\epsilon_\gamma} > 1 - C \Longrightarrow C > 1 - \frac{1}{\epsilon_\gamma} \end{aligned} \tag{4.39}$$

Therefore,

$$1 - \frac{1}{\epsilon_\gamma} < \cos\theta < 1, \text{ since } \cos\theta \neq 1. \tag{4.40}$$

Since C is a function of $\mathbf{\Omega}'_\gamma$ and E'_γ is a function of C so we write $C(\mathbf{\Omega}'_\gamma)$ and $E'_\gamma(\mathbf{\Omega}'_\gamma)$ instead of C and E'_γ accordingly in the following $H^{(i-1)}(\mathbf{\Omega}'_\gamma)$.

Let

$$H^{(i-1)}(\mathbf{\Omega}'_\gamma) = \frac{\sigma_{\mathsf{C},\gamma}(E'_\gamma(\mathbf{\Omega}'_\gamma), C(\mathbf{\Omega}'_\gamma))\psi_\gamma{}^{(\mathrm{i}-1)}(\mathbf{r}(\lambda), \mathbf{\Omega}'_\gamma, E'_\gamma(\mathbf{\Omega}'_\gamma))}{[1+\epsilon_\gamma(C(\mathbf{\Omega}'_\gamma)-1)]^2} \text{ and } D_1 = \operatorname{supp}\psi_\gamma^{(0)} \tag{4.41}$$

where supp stands for "support".

The explanation of support: Let $f : S^2 \longrightarrow \mathbb{R}$ be a function. Then the support of this function say supp$f$ is defined by $\text{supp}f = \overline{\{\mathbf{\Omega}_\gamma \in S^2 : \ f(\mathbf{\Omega}_\gamma) \neq 0\}}$.

From the energy condition we get

$$1 - \frac{1}{\epsilon_\gamma} < \cos\theta < 1. \tag{4.42}$$

If we look at (4.42) when $\epsilon_\gamma \in (0, \ \frac{1}{2}]$ then the inequality is true for every θ, except $\theta = 0$. In this case, D will be the total S^2 and, for $\epsilon_\gamma > \frac{1}{2}$, D will be $D \subsetneq S^2$ (like an umbrella, see Figure 4.5).

Therefore, by considering the above condition we get from the equation (4.34) by changing to spherical coordinates when $i = 1$

$$g^{(0)}_{\epsilon_\gamma,\mathbf{\Omega}_\gamma}(\lambda) = \begin{cases} \rho_{\mathsf{e}}(\mathbf{r}(\lambda)) \iint_{D_1^\star} \widehat{\mathsf{H}}^{(0)}(\varphi,\vartheta)\sin\varphi\,\mathrm{d}\varphi\,\mathrm{d}\vartheta & \text{when}, \epsilon_\gamma \in (0, \frac{1}{2}], \\ \rho_{\mathsf{e}}(\mathbf{r}(\lambda)) \iint_{(D_1\cap D)^\star} \widehat{\mathsf{H}}^{(0)}(\varphi,\vartheta)\sin\varphi\,\mathrm{d}\varphi\,\mathrm{d}\vartheta & \text{when}, \epsilon_\gamma > \frac{1}{2}, \end{cases} \tag{4.43}$$

where $E'_\gamma = \frac{\epsilon_\gamma}{1+\epsilon_\gamma(C-1)}$ and $C = \mathbf{\Omega'}_\gamma \cdot \mathbf{\Omega}_\gamma \neq 1$.

If we define the function $\zeta : (0, \pi)\times(0, \ 2\pi) \longrightarrow S^2$ given by $\zeta(\varphi, \vartheta) = (\sin\varphi\,\cos\vartheta, \ \sin\varphi\,\sin\vartheta, \ \cos\varphi)$ then $D_1^\star = \zeta^{-1}(D_1)$, $(D_1 \cap D)^\star = \zeta^{-1}(D_1 \cap D)$ and $\widehat{\mathsf{H}}^{(0)}(\varphi, \vartheta) = H^{(0)}(\zeta(\varphi, \ \vartheta))$.

For easy calculation we have used for the integrating area the minimum rectangle containing $D_1^\star$ for $0 < \epsilon_\gamma \leq \frac{1}{2}$ and the minimum rectangle containing $(D_1 \cap D)^\star$ for $\epsilon_\gamma > \frac{1}{2}$.

For $i = 2, 3, ..., M$ we get

$$g^{(\mathrm{i}-1)}_{\epsilon_\gamma,\mathbf{\Omega}_\gamma}(\lambda) = \rho_{\mathsf{e}}(\mathbf{r}(\lambda)) \iint_{D^\star} \widehat{\mathsf{H}}^{(\mathrm{i}-1)}(\varphi,\vartheta)\sin\varphi\,\mathrm{d}\varphi\,\mathrm{d}\vartheta \tag{4.44}$$

for $\epsilon_\gamma \in (0, \ \infty)$. Here also $D^\star = \zeta^{-1}(D)$.

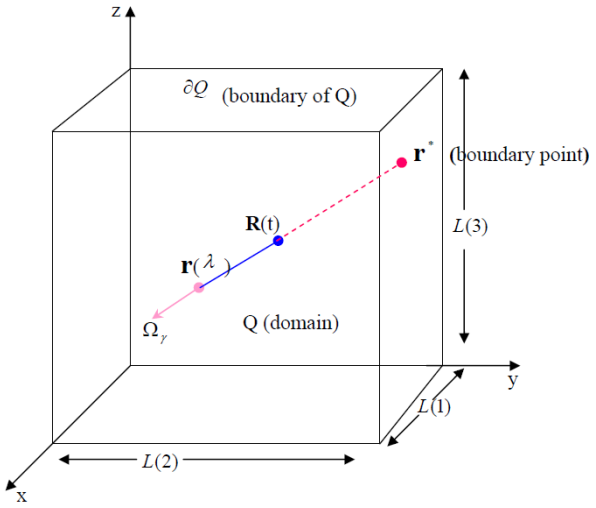

Figure 4.6

4.2 Computation of the boundary point (CBP)

Let Q be our spatial domain. We recall that Q is a rectangular parallelepiped containing water till a height H_W and air in the rest. Let $\mathbf{L}$ be the edge vector of the domain, where $\mathbf{L} = [L(1), L(2), L(3)]$. Clearly the boundary of Q (see Figure (4.6)) consists of six plane surfaces which we will call is the sequel upper face, lower face and lateral faces. We assume that the lower face is located at $z = 0$. Imagine that we want to calculate the number of photons at $\mathbf{r}(\lambda) = \mathbf{r}^\star + \lambda\mathbf{\Omega}_\gamma$ (see Figure 4.2) in the direction of the unit vector $\mathbf{\Omega}_\gamma$. When we expand the direction of $\mathbf{\Omega}_\gamma$ behind $\mathbf{r}(\lambda)$ then this direction will intersect with the boundary plane of the domain and this intersecting is the boundary point, say $\mathbf{r}^\star$ (see Figure 4.2).
When we calculate the number of one time interacting photons at $\mathbf{r}(\lambda)$ then we need to take into account calculate the number of one time interacting photons at all points of the segment joining $\mathbf{r}^\star$ and $\mathbf{r}(\lambda)$.
Let us consider

$$\mathbf{R}(t) = \mathbf{r}^\star + t\mathbf{\Omega}_\gamma, \text{ where } 0 \leq t \leq \lambda \tag{4.45}$$

Here $\mathbf{r}^\star = [r^\star(1),\ r^\star(2),\ r^\star(3)]$ is the boundary point, and let $\mathbf{R}(t) = [R(1),\ R(2),\ R(3)]$ and $\mathbf{\Omega}_\gamma = [\Omega(1),\ \Omega(2),\ \Omega(3)]$.
The number of one time interacting photons at $\mathbf{R}(t)$ influence the value at $\mathbf{r}(\lambda)$ because when a photon (non-interact) comes at $\mathbf{R}(t)$ interacts and goes to the direction of $\mathbf{\Omega}_\gamma$, without suffering more interaction photon it will arrive at $\mathbf{r}(\lambda)$. For two times, or more times interacting photons, analogous assertions hold.

In the following subsections we explain the algorithm which have employed for obtaining the boundary point $\mathbf{r}^\star$.

4.2.1 When $\Omega(3) < 0$

When $\Omega(3) < 0$ then the boundary point $\mathbf{r}^\star$ is located at the upper face or at one of the lateral faces of the domain. If $\mathbf{r}^\star$ is at the upper face of the domain then $r^\star(3) = L(3)$ and equation (4.45) implies

$$t = \frac{R(3) - L(3)}{\Omega(3)} > 0. \tag{4.46}$$

When we put the value of t in (4.45) then we can find the boundary point $\mathbf{r}^\star$. But how can we know whether $\mathbf{r}^\star$ belongs to the upper face or to one of the lateral faces of the domain? For this we can follow the following rules:
Let IPU=[IP(1), IP(2),IP(3)] be the intersecting point between the direction $-\mathbf{\Omega}_\gamma$ from $\mathbf{r}(\lambda)$ and the plane $z = L(3)$. Note that IPU may be outside ∂Q.
Since $IPU(3) = L(3)$ so if we think IPU like as $\mathbf{r}^\star$ then we get from (4.45), IPU=$[R(1) - t\Omega(1),\ R(2) - t\Omega(2),\ L(3)]$ with $t = \frac{R(3)-L(3)}{\Omega(3)}$ given by (4.46) clearly, $\mathbf{r}^\star$=IPU if, and only if, $0 \leq IPU(1) \leq L(1)$ and $0 \leq IPU(2) \leq L(2)$.
If $\mathbf{r}^\star \neq$ IPU then we follow the following rules for finding the boundary point.

1. If $IPU(2) < 0$.
   Note that in this case $\Omega(2)$ must be strictly positive

   (a) If $0 \leq IPU(1) \leq L(1)$ then the direction $-\mathbf{\Omega}_\gamma$ must intersect the lateral face which lies on the plane $y = 0$. So, in this case $r^\star(2) = 0$. If we put this value in (4.45) we get $t = \dfrac{R(2)}{\Omega(2)}$. Therefore we get from (4.45) $\mathbf{r}^\star = [R(1) - t\Omega(1),\ 0,\ R(3) - t\Omega(3)]$ with $t = \dfrac{R(2)}{\Omega(2)}$.

   (b) If $IPU(1) < 0$ which is turn implies $\Omega(1) > 0$ then the direction $-\mathbf{\Omega}_\gamma$ intersects the lateral face of the domain which stays on the plane $x = 0$. For this case $r^\star(1) = 0$, put the value in (4.45) then we get $t = \frac{R(1)}{\Omega(1)}$. So, from the equation (4.45) we get $\mathbf{r}^\star = [0,\ R(2) - t\Omega(2),\ R(3) - t\Omega(3)]$ with $t = \frac{R(1)}{\Omega(1)}$.

   (c) If $IPU(1) > L(1)$ this implies $\Omega(1) < 0$. Then the direction $-\mathbf{\Omega}_\gamma$ intersects the lateral face of the domain which stays on the plane $x = L(1)$. For this case, $r^\star(1) = L(1)$. Put this value in (4.45) to get $t = \frac{R(1)-L(1)}{\Omega(1)}$. Therefore, we get from (4.45) $\mathbf{r}^\star = [L(1),\ R(2) - t\Omega(2),\ R(3) - t\Omega(3)]$, where $t = \frac{R(1)-L(1)}{\Omega(1)}$.

2. If $IPU(2) > L(2)$.

   Note that $\Omega(2) < 0$ in this case.

   (a) If $0 \leq IPU(1) \leq L(1)$, then the direction $-\mathbf{\Omega}_\gamma$ intersects with the lateral face of the domain which stays on the plane $y = L(2)$. For this case, $r^\star(2) = L(2)$. If we put this value in (4.45) we get $t = \frac{R(2)-L(2)}{\Omega(2)}$. Therefore, we get again from (4.45) $\mathbf{r}^\star = [R(1) - t\Omega(1),\ L(2),\ R(3) - t\Omega(3)]$ with $t = \frac{R(2)-L(2)}{\Omega(2)}$.

   (b) If $IPU(1) > L(1)$ (hence $\Omega(1) < 0$) then the direction $-\mathbf{\Omega}_\gamma$ intersects the lateral face of the domain which resides on the plane $x = L(1)$. For this case $r^\star(1) = L(1)$. If we put this value in (4.45) we get $t = \frac{R(1)-L(1)}{\Omega(1)}$ and $\mathbf{r}^\star = [L(1),\ R(2) - t\Omega(2),\ R(3) - t\Omega(3)]$.

   (c) Otherwise, when $IPU(1) < 0$ (hence $\Omega(1) > 0$) then the direction $-\mathbf{\Omega}_\gamma$ must intersect the lateral face which lies on the plane $x = 0$, so $r^\star(1) = 0$. If we put this value in (4.45) we get $t = \frac{R(1)}{\Omega(1)}$ and from there also we get $\mathbf{r}^\star = [0,\ R(2) - t\Omega(2),\ R(3) - t\Omega(3)$ with $t = \frac{R(1)}{\Omega(1)}$.

4.2.2 When $\Omega(3) = 0$

In this case $\mathbf{r}^\star$ belongs to the plane $z = R(3)$, so here $r^\star(3) = R(3)$ for any condition.
Let IPL = $[IPL(1), IPL(2), IPL(3)]$ be the intersecting point between the direction $-\mathbf{\Omega}_\gamma$ and one of the lateral planes containing the face of the domain. Note that IPL may be outside ∂Q.

1. When $\Omega(2) > 0$ then the direction $-\mathbf{\Omega}_\gamma$ must intersect with the plane $y = 0$ then $IPL(2) = 0$. In here we think IPL like as $\mathbf{r}^\star$ then we get from (4.45) $t = \frac{R(2)}{\Omega(2)}$ and IPL = $[R(1) - t\Omega(1),\ 0,\ R(3)]$.

   (a) If $0 \leq IPL(1) \leq L(1)$ then $\mathbf{r}^\star$ = IPL.

   (b) If $IPL(1) < 0$ then the direction $-\mathbf{\Omega}_\gamma$ intersects with the lateral face of the domain which lies on the plane $x = 0$ therefore the boundary point stays on the plane $x = 0$. So, $r^\star(1) = 0$ and when we put this value in (4.45) then we get $t = \frac{R(1)}{\Omega(1)}$. In this case we get $\mathbf{r}^\star = [0,\ R(2) - t\Omega(2),\ R(3)]$ with $t = \frac{R(1)}{\Omega(1)}$.

   (c) If $IPL(1) > L(1)$ then the direction $-\mathbf{\Omega}_\gamma$ intersects with the lateral face of the domain which stays on the plane $x = L(1)$, and therefore the boundary point stays on the plane $x = L(1)$. So $r^\star(1) = L(1)$ and if we put this value in (4.45) we get $t = \frac{R(1)-L(1)}{\Omega(1)}$. Therefore we get also from (4.45), $\mathbf{r}^\star = [L(1),\ R(2) - t\Omega(2),\ R(3)]$ with $t = \frac{R(1)-L(1)}{\Omega(1)}$.

2. When $\Omega(2) = 0$, then $\mathbf{\Omega}_\gamma = [\Omega(1),\ 0,\ 0]$.

   (a) If $\Omega(1) > 0$ then the direction $-\mathbf{\Omega}_\gamma$ intersects with the lateral face of the domain which lies on $x = 0$, so the boundary point stays on the plane $x = 0$, and therefore $r^\star(1) = 0$. Put this value $r^\star(1) = 0$ in (4.45) to get $t = \frac{R(1)}{\Omega(1)}$ and also from (4.45) we get $\mathbf{r}^\star = [0,\ R(2) - t\Omega(2),\ R(3)]$. But here $\Omega(2) = 0$, so $\mathbf{r}^\star = [0,\ R(2),\ R(3)]$.

   (b) If $\Omega(1) < 0$ then the direction $-\mathbf{\Omega}_\gamma$ intersects with the lateral face of the domain which lies on $x = L(1)$ so the boundary point stays on the plane $x = L(1)$. Therefore $r^\star(1) = L(1)$. Put $r^\star(1) = L(1)$ in (4.45) to get $t = \frac{R(1)-L(1)}{\Omega(1)}$. Also from (4.45) we get $\mathbf{r}^\star = [L(1),\ R(2) - t\Omega(2),\ R(3)]$ with $t = \frac{R(1)-L(1)}{\Omega(1)}$, but here $\Omega(2) = 0$ so $\mathbf{r}^\star = [L(1),\ R(2),\ R(3)]$.

   (c) If $\Omega(1) = 0$. It is impossible because if $\Omega(1) = 0$ then $\mathbf{\Omega}_\gamma$ will be zero vector, but $\mathbf{\Omega}_\gamma$ is a unit vector.

3. When $\Omega(2) < 0$ then the direction $-\mathbf{\Omega}_\gamma$ must intersect with the plane $y = L(2)$ then $IPL(2) = L(2)$. In here we think IPL like as $\mathbf{r}^\star$ then we get from (4.45) $t = \frac{R(2)-L(2)}{\Omega(2)}$ and IPL $= [R(1) - t\Omega(1),\ L(2),\ R(3)]$.

   (a) If $0 \le IPL(1) \le L(1)$ then $\mathbf{r}^\star =$ IPL.

   (b) If $IPL(1) < 0$ then the direction $-\mathbf{\Omega}_\gamma$ intersects the lateral face of the domain which lies on the plane $x = 0$. Therefore the boundary point stays on the plane $x = 0$. So, $r^\star(1) = 0$ and when we put this value in (4.45) we get $t = \frac{R(1)}{\Omega(1)}$. In this case we get $\mathbf{r}^\star = [0,\ R(2) - t\Omega(2),\ R(3)]$ with $t = \frac{R(1)}{\Omega(1)}$.

   (c) If $IPL(1) > L(1)$ then the direction $-\mathbf{\Omega}_\gamma$ intersects the lateral face of the domain which stays on the plane $x = L(1)$. Therefore the boundary point is located on the plane $x = L(1)$. So $r^\star(1) = L(1)$ and put this value in (4.45) then we get $t = \frac{R(1)-L(1)}{\Omega(1)}$. Therefore we get also from (4.45), $\mathbf{r}^\star = [L(1),\ R(2) - t\Omega(2),\ R(3)]$ with $t = \frac{R(1)-L(1)}{\Omega(1)}$.

4.2.3 When $\Omega(3) > 0$

Here the boundary point must lie on the lower face or on one of the lateral face. Let IPD $= [IPD(1), IPD(2), IPD(3)]$ be the intersecting point of the direction $-\mathbf{\Omega}_\gamma$ (from $\mathbf{r}(\lambda)$) and the plane $z = 0$. Here $IPD(3) = 0$. We think IPD like as $\mathbf{r}^\star$ to get from (4.45) $t = \frac{R(3)}{\Omega(3)}$. Therefore we get form (4.45) IPD $= [R(1) - t\Omega(1),\ R(2) - t\Omega(2),\ 0]$ with $t = \frac{R(3)}{\Omega(3)}$.

In this case $\mathbf{r}^\star$=IPD if, and only if, $0 \leq IPD(1) \leq L(1)$ and $0 \leq IPD(2) \leq L(2)$. If $\mathbf{r}^\star \neq$ IPU then we follow the following rules for finding the boundary point.

1. If $IPD(2) < 0$.

   (a) If $0 \leq IPD(1) \leq L(1)$ then the direction $-\mathbf{\Omega}_\gamma$ must intersect with the lateral face of the domain which lies on the plane $y = 0$. So, in this case $r^\star(2) = 0$, and putting this value in (4.45) we get $t = \dfrac{R(2)}{\Omega(2)}$. Therefore we get from (4.45) $\mathbf{r}^\star = [R(1) - t\Omega(1),\ 0,\ R(3) - t\Omega(3)]$ with $t = \dfrac{R(2)}{\Omega(2)}$.

   (b) If $IPD(1) < 0$ then the direction $-\mathbf{\Omega}_\gamma$ intersects with the lateral face of the domain which stays on the plane $x = 0$. For this case $r^\star(1) = 0$. If we put this value in (4.45) then we get $t = \frac{R(1)}{\Omega(1)}$. So, from the equation (4.45), we get $\mathbf{r}^\star = [0,\ R(2) - t\Omega(2),\ R(3) - t\Omega(3)]$ with $t = \frac{R(1)}{\Omega(1)}$.

   (c) If $IPD(1) > L(1)$ then the direction $-\mathbf{\Omega}_\gamma$ intersects with the lateral faces of the domain which stays on the plane $x = L(1)$. For this case $r^\star(1) = L(1)$. If we put this value in (4.45) then we get $t = \frac{R(1)-L(1)}{\Omega(1)}$. Therefore, we get from (4.45) $\mathbf{r}^\star = [L(1),\ R(2) - t\Omega(2),\ R(3) - t\Omega(3)]$, where $t = \frac{R(1)-L(1)}{\Omega(1)}$.

2. If $IPD(2) > L(2)$.

   (a) If $0 \leq IPD(1) \leq L(1)$ then the direction $-\mathbf{\Omega}_\gamma$ intersects with the lateral faces of the domain which stays on the plane $y = L(2)$. For this case $r^\star(2) = L(2)$ and putting this value in (4.45) we get $t = \frac{R(2)-L(2)}{\Omega(2)}$. Therefore we get, again from 4.45, $\mathbf{r}^\star = [R(1) - t\Omega(1),\ L(2),\ R(3) - t\Omega(3)]$ with $t = \frac{R(2)-L(2)}{\Omega(2)}$.

   (b) If $IPD(1) > L(1)$ then the direction $-\mathbf{\Omega}_\gamma$ intersects with the lateral face of the domain which resides on the plane $x = L(1)$. For this case $r^\star(1) = L(1)$ and from (4.45) we get $t = \frac{R(1)-L(1)}{\Omega(1)}$ and $\mathbf{r}^\star = [L(1),\ R(2) - t\Omega(2),\ R(3) - t\Omega(3)]$.

   (c) If $IPU(1) < 0$ then the direction $-\mathbf{\Omega}_\gamma$ must intersect with the lateral face which lies on the plane $x = 0$, so $r^\star(1) = 0$ and from (4.45) we get $t = \frac{R(1)}{\Omega(1)}$ and $\mathbf{r}^\star = [0,\ R(2) - t\Omega(2),\ R(3) - t\Omega(3)$ with $t = \frac{R(1)}{\Omega(1)}$.

4.3 Separating the water part of the line segment from $\mathbf{r}^\star$ to $\mathbf{r}(\lambda)$

When we calculate the number of one time interacting photons ($\psi_\gamma^{(1)}$) then we see that the number of one time interacting photons at any point in air is much smaller than the number

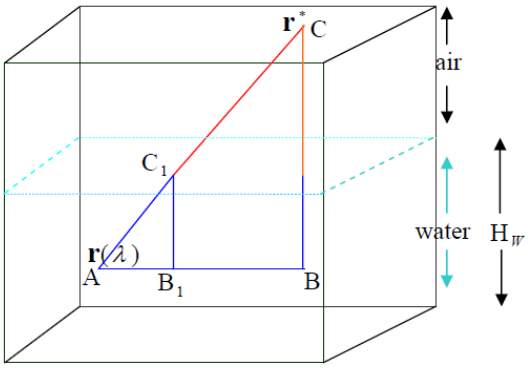

Figure 4.7

of one time interacting photons at any point in water. This is due to the low density of electrons in air when compared to water. The number of one time interacting photons at any point in air is almost zero. This situation is the same for two times interacting photons ($\psi_\gamma^{(2)}$), three times interacting photons ($\psi_\gamma^{(3)}$) or more times interacting photons. So in our MATLAB code we use only the water part of λ for finding the number of one or more times interacting photons. But for finding the number of noninteracting photons ($\psi_\gamma^{(0)}$) we take the total distance from $\mathbf{r}^\star$ to $\mathbf{r}(\lambda)$ (see Figure 4.7). If the boundary point $\mathbf{r}^\star$ is outside the radiative area ABGD (see Figure 4.8) then the number of noninteracting photons at all the points along the direction $\mathbf{\Omega}_\gamma$ between $\mathbf{r}^\star$ and $\mathbf{r}(\lambda)$ is zero. Otherwise if the boundary point $\mathbf{r}^\star$ is inside the radiative area ABGD then the number of noninteracting photons at any point on the λ will give some value which is not near to zero. So, for finding the number of noninteracting photons we take the total λ. Also this value has influence in the value of the number of one time or more times interacting photons (see the equation (4.41) and (4.43)). Let S be the segment joining $\mathbf{r}^\star$ and $\mathbf{r}(\lambda)$. In general one part of S is contained in air and the other part is contained in water. In this section we show how we calculate the water part of S. In the Figure 4.7 we use the points A and C which are exactly $\mathbf{r}(\lambda)$ and $\mathbf{r}^\star$ respectively and $|\overrightarrow{AC_1}|$ is length of the water part of S. From the Figure 4.7 we get the following:
$\lambda = |\overrightarrow{AC}|$ is known because the point

$$\mathrm{A} = \mathbf{r}(\lambda) = [r(1),\ r(2),\ r(3)] \tag{4.47}$$

is given and

$$\mathrm{C} = \mathbf{r}^\star = [r^\star(1),\ r^\star(2),\ r^\star(3)] = \text{boundary point} \tag{4.48}$$

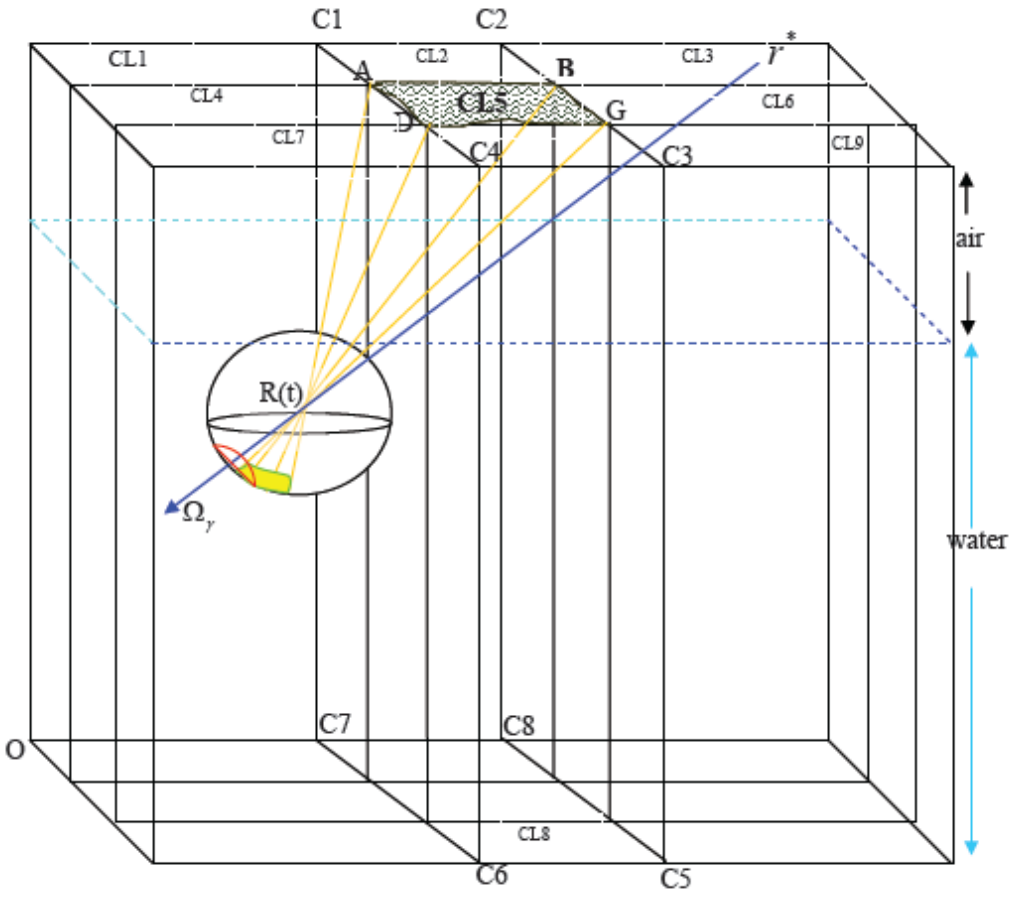

Figure 4.8

is computed. Again we see from the Figure 4.7 that

$$|\overrightarrow{BC}| = r^{\star}(3) - r(3) \text{ and} \tag{4.49}$$

$$|\overrightarrow{B_1C_1}| = H_W - r(3), \tag{4.50}$$

where H_W= height of the water part is given. Now we get from Figure 4.7

$$\frac{|\overrightarrow{AC_1}|}{|\overrightarrow{B_1C_1}|} = \frac{|\overrightarrow{AC}|}{|\overrightarrow{BC}|} \Rightarrow |\overrightarrow{AC_1}| = \frac{\lambda(H_W - r(3))}{r^{\star}(3) - r(3)}. \tag{4.51}$$

From the equation (4.51) we get the length of the water part of S.

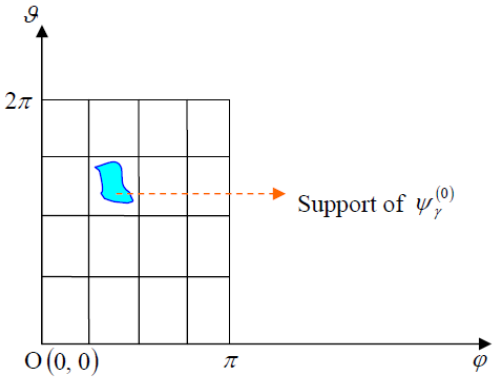

Figure 4.9

4.4 Reduction of the integration domain

From the Figure 4.8 we see that the area ABGD is the radiative area and that the volume of the domain bounded by C1, C2, C3, C4, C5, C6, C7 and C8 contains three columns CL2, CL5 and CL8. There are nine columns in the domain which are CL1, CL2, CL3, CL4, CL5, CL6, CL7, CL8 and CL9. The vector $\mathbf{\Omega}_\gamma$ is the direction of photons, $\mathbf{R}(t)$ is the center of unit sphere and $\mathbf{r}^\star$ is the boundary point. We know that when the boundary point outside from the area ABDG then the number of non interacting photons at $\mathbf{R}(t)$ is zero, i.e., $\psi_\gamma^{(0)} = 0$. The yellow area bounded by the green line represents the support of $\psi_\gamma^{(0)}$. We note that this support of $\psi_\gamma^{(0)}$ does not depend on $\mathbf{\Omega}_\gamma$ and energy but it depends on the position of $\mathbf{R}(t)$ and also on the radiative area ABGD.

We see in (4.43) that the integrand contains $\psi_\gamma^{(0)}$ (for $i = 1$) as a factor, therefore when $\psi_\gamma^{(0)} = 0$ then the integral will be zero. At first we will find the support of $\psi_\gamma^{(0)}$ and then we will take the minimum rectangle in the plane (φ, ϑ) of the spherical coordinate system which contains the support. For the limits of the first integration in (4.43) we will consider this rectangle. Otherwise, in here if we don't consider the support, then we have to take the total surface of the sphere for the limit of the first integral of (4.43). Now, if the radiative area is very small then the support of $\psi_\gamma^{(0)}$ will be very small and computing an accurate value of the integral will be difficult, since it might happen that no nodes of quadrature are located inside the support of $\psi_\gamma^{(0)}$ (see Figure 4.9).

For the second integral of (4.43) when $i = 1$, that means when we are going to calculate the number of one time scattered photons $\psi_\gamma^{(1)}(\mathbf{R}(t), \mathbf{\Omega}_\gamma, \epsilon_\gamma)$ at $\mathbf{R}(t)$ for energy $\epsilon_\gamma > \frac{1}{2}$, then we see that the limiting area of the integration looks like as an umbrella (D say) (see Figure 4.5). Before we mentioned that the support of $\psi_\gamma^{(0)}(\mathbf{R}(t), \mathbf{\Omega}_\gamma, \epsilon_\gamma)$ is called D_1 (see (4.41)).

We get from (4.18)

$$\psi_\gamma^{(1)}(\mathbf{r}(\lambda), \mathbf{\Omega}_\gamma, \epsilon_\gamma) = \int_0^\lambda g^{(0)}_{\epsilon_\gamma, \mathbf{\Omega}_\gamma}(t)\, \mathrm{e}^{-(\int_t^\lambda \rho_{\mathsf{e}}(r(s))\ \mathrm{d}s)\sigma^{\mathrm{tot}}_{C,\gamma}(\epsilon_\gamma)}\ \mathrm{d}t. \tag{4.52}$$

Here,

$$g^{(0)}_{\epsilon_\gamma, \mathbf{\Omega}_\gamma}(\lambda) = \begin{cases} \rho_{\mathsf{e}}(\mathbf{r}(\lambda)) \iint_{D_1^\star} \widehat{\mathsf{H}}^{(0)}(\varphi, \vartheta) \sin\varphi \,\mathrm{d}\varphi \,\mathrm{d}\vartheta & \text{when} \epsilon_\gamma \in (0, \frac{1}{2}], \\ \rho_{\mathsf{e}}(\mathbf{r}(\lambda)) \iint_{(D_1 \cap D)^\star} \widehat{\mathsf{H}}^{(0)}(\varphi, \vartheta) \sin\varphi \,\mathrm{d}\varphi \,\mathrm{d}\vartheta & \text{when} \epsilon_\gamma > \frac{1}{2}, \end{cases} \tag{4.53}$$

where

$$\widehat{\mathsf{H}}^{(0)}(\varphi,\ \vartheta) = H^{(0)}(\zeta(\varphi,\ \vartheta)) \text{ and} \tag{4.54}$$

$$H^{(0)}(\mathbf{\Omega}'_\gamma) = \frac{\sigma_{\mathsf{C},\gamma}(E'_\gamma(\mathbf{\Omega}'_\gamma), C(\mathbf{\Omega}'_\gamma))\psi_\gamma{}^{(0)}(\mathbf{r}(\lambda), \mathbf{\Omega}'_\gamma, E'_\gamma(\mathbf{\Omega}'_\gamma))}{[1 + \epsilon_\gamma(C(\mathbf{\Omega}'_\gamma) - 1)]^2}. \tag{4.55}$$

If we define the function $\zeta : (0,\ \pi)\times(0,\ 2\pi) \longrightarrow S^2$ given by $\zeta(\varphi,\ \vartheta) = (\sin\varphi\cos\vartheta,\ \sin\varphi\sin\vartheta,\ \cos\varphi)$ then $D_1^\star = \zeta^{-1}(D_1),\ (D_1 \cap D)^\star = \zeta^{-1}(D_1 \cap D)$.

From the above equations we can easily see that when $\psi_\gamma^{(0)}$ is zero then $\psi_\gamma^{(1)}$ is zero for all cases. But for energy $\epsilon_\gamma > \frac{1}{2}$, if $D_1 \cap D = \varnothing$ then the number of one time scattered photons $\psi_\gamma^{(1)}$ is zero also.

In the Figure 4.8 we see that the area bounded by the red line is the umbrella D and the area intersected by the red line and the green line is the domain of the integral of (4.53) when energy $\epsilon_\gamma > \frac{1}{2}$.

From the above discussion we see that determining the domain of integration is very important for the accurate value and also for time minimizing.

4.4.1 Calculation of the minimum rectangle containing the support of $\psi_\gamma^{(0)}$

It is difficult to determine the exact shape of supp$\psi_\gamma^{(0)}$ on the $\varphi - \vartheta$ plane (see (a) of Figure 4.12). What we have done instead is to find the smallest rectangle on that plane containing supp$\psi_\gamma^{(0)}$, in order to have at our disposal easy limits of integration when computing the integral with our quadrature formula.

We can find the minimum and maximum polar angle and also minimum and maximum zenith angle of the support of $\psi_\gamma^{(0)}$. We take four straight lines $\varphi =$ maximum zenith angle, $\varphi =$ minimum zenith angle, $\vartheta =$ maximum polar angle and $\vartheta =$ minimum polar angle on

the $\varphi - \vartheta$ plane. The rectangle bounded by the four straight lines will be the minimum rectangle which contains the support of $\psi_\gamma^{(0)}$.

We select a point $\mathbf{R}(t)$ inside the domain Q. Then, we think of calculating the number of photons for a given energy ϵ_γ at $\mathbf{R}(t)$. Take a unit sphere which center is that selected point $\mathbf{R}(t)$ in Figure 4.8. We take a unit vector from $\mathbf{R}(t)$ called $\mathbf{\Omega}_\gamma$. We will calculate the number of photons in this direction $\mathbf{\Omega}_\gamma$ for the energy ϵ_γ. In the previous section we have calculated the boundary point $\mathbf{r}^\star$. At first we take a rectangle on the upper face of the domain and put radiation on the rectangle area. So we see that if the boundary point is located outside the rectangle then $\psi_\gamma^{(0)}$ is zero which implies $g^{(0)}_{\epsilon_\gamma,\mathbf{\Omega}_\gamma}(\lambda)$ is zero also and consequently $\psi_\gamma^{(1)}$ will be zero (see the equation (4.41) and (4.43)). So for minimizing the calculation process and computing time we consider the support of $\psi_\gamma^{(1)}$.

Here $\mathbf{r}^\star$ is the boundary point and we will change the origin at $\mathbf{R}(t)$. We draw the straight lines AR(t), BR(t), GR(t) and DR(t). Find the coordinate of the intersecting points between this straight line AR(t) with the unit sphere which center at $\mathbf{R}(t)$. There are two intersecting points, but we will consider the point which z coordinate is negative. Let A2 be that point. Similarly we will calculate the intersecting points of BR(t), GR(t) and DR(t) with this unit sphere and take the negative one which are B2, G2 and D2 respectively, say. The coordinates of these points are Cartesian coordinates so we will change the coordinates to spherical coordinates.

4.4.2 Change the Cartesian coordinates to spherical coordinates

The coordinate of A2, B2, G2 and D2 are with respect to (0, 0, 0). So will make these coordinate with respect to $\mathbf{R}(t)$. Let $(c1,\ c2,\ c3)$ be the Cartesian coordinates of $\mathbf{R}(t)$ with respect to (0, 0, 0) and any point M with coordinates $(x,\ y,\ z)$ with respect to (0, 0, 0) also. Then the coordinate of M will be $(x - c1,\ y - c2,\ z - c3)$ with respect to $\mathbf{R}(t)$. Now we will change the coordinates $(x - c1,\ y - c2,\ z - c3)$ to spherical coordinates.

Spherical coordinates: (centered at $\mathbf{R}(t)$, see Figure 4.10)

We represent the spherical coordinates to the form $(r,\ \vartheta,\ \varphi)$ where ϑ is a polar angle and φ is the zenith angle. Let

$$x - c1 = X = r\sin\varphi\cos\vartheta, \tag{4.56}$$

$$y - c2 = Y = r\sin\varphi\sin\vartheta, \text{ and} \tag{4.57}$$

$$z - c3 = Z = r\cos\varphi. \tag{4.58}$$

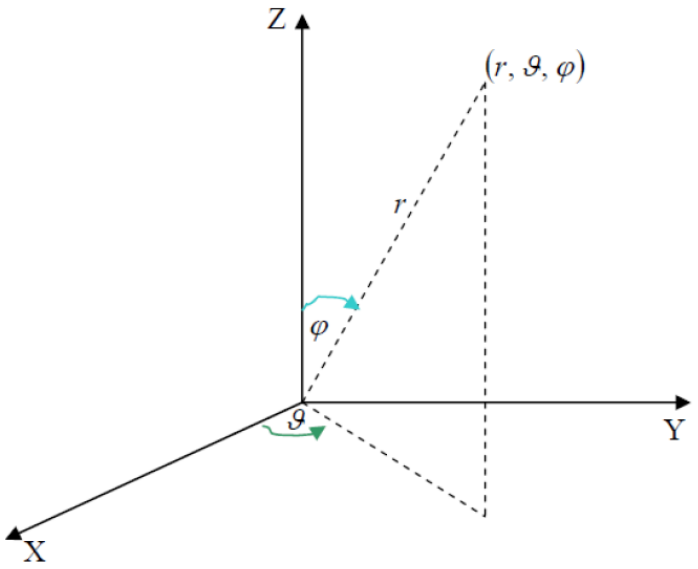

Figure 4.10

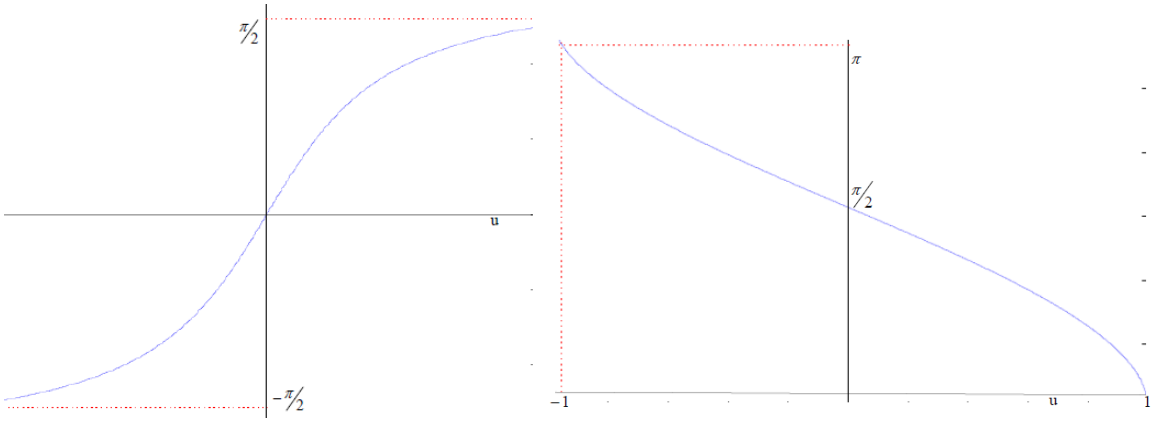

(a) arctan(u) (b) arccos(u)

Figure 4.11

Here φ is the zenith angle and ϑ is the polar angle, $0 \leq \varphi \leq \pi$, $0 \leq \vartheta \leq 2\pi$ and

$$r = \sqrt{(x - c1)^2 + (y - c2)^2 + (z - c3)^2} = \sqrt{X^2 + Y^2 + Z^2}. \tag{4.59}$$

We get from (4.58), $\varphi = \arccos(\frac{Z}{r})$ and we see from the Figure (b) of 4.11 that $\arccos(u) \in [0, \pi]$ so we can find φ directly by the formula since $0 \leq \varphi \leq \pi$. Again we see from the Figure (a) of 4.11 that $\arctan(u) \in \left(-\frac{\pi}{2}, \frac{\pi}{2}\right)$. Since in our case the polar angle $\vartheta \in [0, 2\pi)$, we cannot find the polar angle by the formula $\vartheta = \arctan\left(\frac{Y}{X}\right)$ which we get from (4.56) and (4.57). Therefore we employ the following rules to find the polar angle ϑ.

Now we observe ϑ (polar angle)

1. When $x - c1 = 0 \Longrightarrow X = 0$.

   (a) If $y - c2 > 0 \Longrightarrow Y > 0$.

   Then the point is located on the YZ plane and Y is positive. In this case ϑ will be $\frac{\pi}{2}$.

   (b) If $y - c2 = 0 \Longrightarrow Y = 0$.

   Then the point is on the Z axis. So, we can take any value of $\vartheta \in [0, 2\pi)$. In our program we have used $\vartheta = 0$.

   (c) If $y - c2 < 0 \Longrightarrow Y < 0$.

   Then the point is on the YZ plane where $Y < 0$. In this case $\vartheta = \frac{3\pi}{2}$.

2. When $x - c1 \neq 0 \Longrightarrow X \neq 0$.

   In this case for any value of $\frac{Y}{X}$, $X \neq 0$, we know that $\arctan(Y/X) \in \left(-\frac{\pi}{2}, \frac{\pi}{2}\right)$. But we need $\vartheta \in [0, 2\pi)$. So we apply the following rules:

   (a) when $X > 0$ and $Y \geq 0$.

   In this case $\vartheta = \arctan\left(\frac{Y}{X}\right) \in [0, \frac{\pi}{2})$, which is a valid value for the polar angle.

   (b) when $X < 0$ and $Y \geq 0$.

   Here $\arctan\left(\frac{Y}{X}\right) \in (-\frac{\pi}{2}, 0]$. So, the polar angle is $\vartheta = \pi + \arctan\left(\frac{Y}{X}\right)$.

   (c) when $X < 0$ and $Y < 0$.

   Here $\arctan\left(\frac{Y}{X}\right) \in (0, \frac{\pi}{2})$ is in the correct range $[0, 2\pi)$. But it is quite clear from geometrical considerations that the polar angle is $\vartheta = \pi + \arctan\left(\frac{Y}{X}\right)$.

   (d) when $X > 0$ and $Y < 0$.

   Here $\arctan\left(\frac{Y}{X}\right) \in (-\frac{\pi}{2}, 0)$. In this case, $\vartheta = 2\pi + \arctan\left(\frac{Y}{X}\right)$.

Now we apply the above process for changing the Cartesian coordinate of $\mathbf{R}(t)$, A2, B2, G2 and D2 to spherical coordinates.
Now we use the following process to find the minimum rectangle that contains the support of $\psi_\gamma^{(0)}$. In all the following process $\mathbf{R}(t)$ will be the origin.

- **When $\mathbf{R}(t)$ is in the interior of column CL4 of Figure 4.8 or on the left sided boundary plane of this column or on the right sided boundary plane of this column**

  In this position, we find the plane ADR(t) and the angle between ZX plane and ADR(t) plane. Here we will get two angles but we consider only the larger angle because the support stays under the XY plane for all the position of $\mathbf{R}(t)$ in the domain. We represent the larger angle by the symbol LARG. Let

  $$\text{INZEN} = [\text{zenith angle of A2},\ \text{zenith angle of B2},\ \text{zenith angle of G2},\ \text{zenith angle of D2}],\ \text{and} \tag{4.60}$$

  $$\text{INPOL} = [\text{polar angle of A2},\ \text{polar angle of B2},\ \text{polar angle of G2},\ \text{polar angle of D2}]. \tag{4.61}$$

  We will take four straight lines, $\varphi = \min(\text{INZEN})$, $\varphi = \text{LARG}$, $\vartheta = \min(\text{INPOL})$ and $\vartheta = \max(\text{INPOL})$ on the $\varphi - \vartheta$ plane. The rectangle bounded by the four lines will be the minimum rectangle which contains the support of $\psi_\gamma^{(0)}$.

- **When $\mathbf{R}(t)$ is in the interior of column CL6 of Figure 4.8 or on the left sided boundary plane of this column or on the right sided boundary plane of this column**

  In this case we will find the plane BGR(t) and find the angle between ZX plane and BGR(t) plane. Here we will get two angles but we consider only the larger angle LARG. We will take four straight lines, $\varphi = \min(\text{INZEN})$, $\varphi = \text{LARG}$, $\vartheta = \min(\text{INPOL})$ and $\vartheta = \max(\text{INPOL})$ on the $\varphi - \vartheta$ plane. The rectangle bounded by the four lines will be the minimum rectangle containing the support of $\psi_\gamma^{(0)}$.

- **When $\mathbf{R}(t)$ is in the interior of column CL2 of Figure 4.8 or on the front sided boundary plane of this column or on the back sided boundary plane of this column**

  In this case we will find the plane ABR(t) and find the angle between ABR(t) and ZY plane and will take the larger angle LARG like as before. We will take four straight lines, $\varphi = \min(\text{INZEN})$, $\varphi = \text{LARG}$, $\vartheta = \min(\text{INPOL})$ and $\vartheta = \max(\text{INPOL})$ on the $\varphi - \vartheta$ plane. The rectangle bounded by the four lines will be the minimum rectangle containing the support of $\psi_\gamma^{(0)}$.

- **When $\mathbf{R}(t)$ is in the interior of column CL8 of Figure 4.8 or on the front sided boundary plane of this column or on the back sided boundary plane of this column**

  In this case we make a plane DGR(t) and find the angle between DGR(t) and the YZ plane and we will consider the larger angle LARG between the two angles like as before. For making the limit of the polar angle we will have to divide two parts of this polar angle because in this case the ZX; $X > 0$ plane divide this polar angle in two parts. Here two rectangles contain the supp$\psi_\gamma^{(0)}$ together. One of them bounded by the four straight lines, $\varphi = \min(\text{INZEN})$, $\varphi = \text{LARG}$, $\vartheta = 0$ and $\vartheta = \max[\text{polar angle of A2, polar angle of D2}]$ on the $\varphi - \vartheta$ plane. And the other rectangle is bounded by $\varphi = \min(\text{INZEN})$, $\varphi = \text{LARG}$, $\vartheta = 2\pi$ and $\vartheta = \min[\text{polar angle of B2, polar angle of G2}]$ on the $\varphi - \vartheta$ plane.

- **When $\mathbf{R}(t)$ is in the interior of column CL5 of Figure 4.8**

  In this position the minimum rectangle containing the supp$\psi_\gamma^{(0)}$ will be bounded by the lines $\varphi = \min(\text{INZEN})$, $\varphi = \pi$, $\vartheta = 0$ and $\vartheta = 2\pi$ on the $\varphi - \vartheta$ plane.

- **When $\mathbf{R}(t)$ is on the right sided plane of the column CL7 of Figure 4.8**

  We observed that here the support is contained in the left side of the ZX plane, and the minimum rectangle containing the supp$\psi_\gamma^{(0)}$ is bounded by the four lines, $\vartheta =$ polar angle of G2, $\vartheta = 2\pi$, $\varphi = \min(\text{INZEN})$ and $\varphi = \max(\text{INZEN})$ in the $\varphi - \vartheta$ plane.

- **When $\mathbf{R}(t)$ is on the left sided plane of the column CL9 of Figure 4.8**

  In this case the support is stay in the right side of the ZX plane. In this case the minimum rectangle containing the supp$\psi_\gamma^{(0)}$ is bounded by the four lines, $\vartheta = 0$, $\vartheta =$ MAX[polar angle of A2, polar angle of D2], $\varphi = \min$ (INZEN) and $\varphi = \max$ (INZEN) in the $\varphi - \vartheta$ plane. And for all other positions we will have to take the four lines, $\varphi = \min$ (INZEN), $\varphi = \max$ (INZEN), $\vartheta = \min$ (INPOL) and $\vartheta = \max$ (INPOL) as a boundary of the minimum rectangle which contains the supp$\psi_\gamma^{(0)}$.

Let us consider the minimum rectangle containing the support of $\psi_\gamma^{(0)}$ be REC0.

4.4.3 Calculation of the support of the integrand for the second integral of (4.43)

In this case, the limit for polar angle is from 0 to 2π and for the zenith angle from 0 to $\arccos(1 - \frac{1}{\epsilon_\gamma})$, here $\epsilon_\gamma \in (\frac{1}{2},\ \infty)$ is the energy of the photon. If we think this limiting area on a sphere then this area looks like an umbrella (see Figure 4.5).

For calculating the number of one time interacting photons we see that the integrand of the integral in (4.43) contains $\psi_\gamma^{(0)}$ so when $\psi_\gamma^{(0)} = 0$ then the value of integration will be 0. That means that if this umbrella does not intersect with the support of the $\psi_\gamma^{(0)}$ then the value of $g^{(0)}_{\epsilon_\gamma, \mathbf{\Omega}_\gamma}(\lambda)$ will be 0. Because in this case the boundary point of any direction of one time interacting photons going from $\mathbf{R}(t)$ to any point inside the umbrella stays outside the radiative area. If they are intersecting to each other then the intersecting area will be the support of this integrand when If the support of $\psi_\gamma^{(0)}$ and the umbrella don't intersect then the integral will be zero.

Now we will calculate the minimum rectangle containing this umbrella. Let REC1 be this rectangle.

4.4.4 Calculation of the minimum rectangle containing the umbrella

We see (Figure 4.5) that the direction $\mathbf{\Omega}_\gamma$ points towards the center of the umbrella from the point $\mathbf{R}(t)$. Since we know the unit vector $\mathbf{\Omega}_\gamma$ (given) so we can find the zenith angle (ZOME say) and polar angle (POME say) of it. Also we know $\theta \in \left[0, \arccos\left(1 - \frac{1}{\epsilon_\gamma}\right)\right]$ (see Figure 4.5). So the maximum value of θ is $\arccos\left(1 - \frac{1}{\epsilon_\gamma}\right)$ (ANG say). Now we take the

four straight lines $\varphi = ZOME - ANG$, $\varphi = ZOME + ANG$, $\vartheta = POME - ANG$ and $\vartheta = POME + ANG$. The rectangle bounded by the four lines is the minimum rectangle containing the umbrella. Let we mention this rectangle as REC1.

Therefore the domain of the second integral of (4.43), when $i = 1$, will be the intersecting rectangle of REC0 and REC1 ($REC0 \cap REC1$) and for the first integral the domain will be the REC0.

The above two processes are applicable only for $g^{(0)}_{\epsilon_\gamma,\mathbf{\Omega}_\gamma}(\lambda)$ and this $g^{(0)}_{\epsilon_\gamma,\mathbf{\Omega}_\gamma}(\lambda)$ is needed for calculating $\psi^{(1)}_\gamma$.

For calculating $\psi^{(2)}_\gamma$ we need the value of $g^{(1)}_{\epsilon_\gamma,\mathbf{\Omega}_\gamma}(\lambda)$ (see equation(4.44)). In this case the integrand contain $\psi^{(1)}_\gamma$ and the support of $\psi^{(1)}_\gamma$ is the total sphere. So, in here only the umbrella will be the domain of the integral when the energy $\epsilon_\gamma \in (\frac{1}{2},\ \infty)$ (see Figure 4.5). So we take the minimum rectangle REC1 for the integration area of $g^{(1)}_{\epsilon_\gamma,\mathbf{\Omega}_\gamma}$. For $\psi^{(i)}_\gamma$ where $i = 3, 4, .., M$ we use the same process like $\psi^{(2)}_\gamma$.

When the energy $\epsilon_\gamma \in \left(0, \frac{1}{2}\right]$ then for finding the number of two or more time intersecting photons we will have to take the total surface of the unit sphere for the integrating domain. Because in this case the integrand doesn't contain $\psi^{(0)}_\gamma$ but it contains $\psi^{(i)}_\gamma$ for $i = 2, 3, 4, ...$ and this one or more times interacting photons ($\psi^{(i)}_\gamma$ for $i = 2, 3, 4, ...$) may come from any direction to $\mathbf{R}(t)$.

4.5 The Matlab code

We have made a MATLAB code about approximately 6000 lines to solve the Boltzmann transport equation for photons. We calculate the number of noninteracting photons, one time interacting photons, two times interacting photons and three times interacting photons by this MATLAB code. This total code contains 16 m-files. We use the the following names for those m-files are PSI0, PSI1, PSI2, PSI3, PS1, PS2, PS3, H1, H2, H3, g0, g1, g2, CBP, EX and main2. We discuss about the m-files in the following:

1. In main2 we give the necessary data (input data) and get output in here.
   For input data we use some symbol in this m-file which are L, ED, R, OME, E, HW, Nx, Ny, Nx1, Ny1, Nx2, Ny2, NW1, NW2 and NW3. All the notations and the meaning of those are following:
   (a) L=[Lx,Ly,Lz], where Lx, Ly and Lz are the length of three edges of the cube (domain).
   (b) ED is the length of edge of irradiate square on the upper surface of the cube.

(c) R is the point inside the domain where we want to calculate the number of photons (in the Figure 4.8 point $\mathbf{R}$ is $\mathbf{R}(t)$).

(d) We calculate the number of photons at a fixed direction. OME is the unit vector in that direction. In the Figure 4.8 it is $\mathbf{\Omega}_\gamma$.

(e) E is the energy of photon.

(f) In the cube (domain) we use two parts one of that is water and the other is air. HW is the length of height of the water part.
For calculating $\psi_\gamma^{(1)}$ we need to calculate $g^{(0)}_{\epsilon_\gamma,\mathbf{\Omega}_\gamma}(\lambda)$ (see (4.18)) and in the formulation of $g^{(0)}_{\epsilon_\gamma,\mathbf{\Omega}_\gamma}(\lambda)$ we see that there are two integrations one for polar angle and one for zenith angle. Here we use y for polar angle and x for zenith angle (4.19)).

(g) Nx is the division number of the range of x of the domain of the integral in the formulation of $g^{(0)}_{\epsilon_\gamma,\mathbf{\Omega}_\gamma}(\lambda)$.

(h) Ny is the division number of the range of y of the domain of the integral in the formulation of $g^{(0)}_{\epsilon_\gamma,\mathbf{\Omega}_\gamma}(\lambda)$.
For calculating $\psi_\gamma^{(2)}$ we need to calculate $g^{(1)}_{\epsilon_\gamma,\mathbf{\Omega}_\gamma}(\lambda)$ and in the formula of $g^{(1)}_{\epsilon_\gamma,\mathbf{\Omega}_\gamma}(\lambda)$ has two integrations one for polar angle and one for zenith angle. Here we use y1 for polar angle and x1 for zenith angle.

(i) Nx1 is the division number of the range of x1 of the domain of the integral in the formulation of $g^{(1)}_{\epsilon_\gamma,\mathbf{\Omega}_\gamma}(\lambda)$.

(j) Ny1 is the division number of the range of y1 of the domain of the integral in the formulation of $g^{(1)}_{\epsilon_\gamma,\mathbf{\Omega}_\gamma}(\lambda)$.
We use x2 and y2 for the zenith and polar angle respectively in the integral involving in the formula of $g^{(2)}_{\epsilon_\gamma,\mathbf{\Omega}_\gamma}(\lambda)$ to calculate $\psi_\gamma^{(3)}$.

(k) Nx2 is the division number of the range of x2 of the domain of the integral in the formulation of $g^{(2)}_{\epsilon_\gamma,\mathbf{\Omega}_\gamma}(\lambda)$.

(l) Ny2 is the division number of the range of y2 of the domain of the integral in the formulation of $g^{(1)}_{\epsilon_\gamma,\mathbf{\Omega}_\gamma}(\lambda)$.
We observe that the value of $\psi_\gamma^{(1)}$ at a point inside air is much smaller than the value of $\psi_\gamma^{(1)}$ at a point inside water. It is almost zero. So, in our MATLAB code we use only the points which are inside in water to calculate $\psi_\gamma^{(i)}$, where $i = 1, 2, 3, ..., M$.
In the equation (4.18) there is an integration with respect to t and the limit of

this integration is from 0 to λ. But by the above discussion we will take the part of λ which inside in the water.

(m) NW1 is the number of divisions of the water part of λ which is the range of the integral domain involved in the formula of $\psi_\gamma^{(1)}$.

(n) NW2 is the number of divisions of the water part of λ which is the range of the integral domain involved in the formula of $\psi_\gamma^{(2)}$.

(o) NW3 is the number of divisions of the water part of λ which is the range of the integral domain involved in the formula of $\psi_\gamma^{(3)}$.

2. In CBP we find the boundary point $\mathbf{r}^\star$.

3. In EX we obtain the exponential part of the formula of $\psi_\gamma^{(0)}(\mathbf{r}(\lambda), \mathbf{\Omega}_\gamma, \epsilon_\gamma)$ (see equation (4.12)). In the exponential part, there exist a line integral and the limit of this integral is from 0 to λ (λ is the distance from boundary point $\mathbf{r}^\star$ to $\mathbf{R}(t)$, see Figure 4.8). If the domain that contains the sigment $[0, \lambda]$ is heterogeneous then the electron density is different for different media. In making this program we have taken this fact into consideration.

4. In PSI0, we solve the number of non-interacting photons by using CBP and EX.

5. In g0 we find $g^{(0)}_{\epsilon_\gamma, \mathbf{\Omega}_\gamma}(\lambda)$ by using this PSI0. Here we use the support (mentioned in previous section) to calculate the integration of g0.

6. To calculate g0 we need the value of integrand at the limiting points of the domain of integral. In H1 we find this value.

7. In PSI1 we find the number of one time interacting photons by using g0 and EX.

8. To find PSI1, we need the value of the integrand involving in PSI1 at the limiting points of the domain of the integral. We calculate this value in PS1.

9. In g1 we find $g^{(1)}_{\epsilon_\gamma, \mathbf{\Omega}_\gamma}(\lambda)$ by using this PSI1. Here we use the support (mentioned in previous section) to calculate the integration of g1.

10. To calculate g1 we need the value of integrand involving in the formula of $g^{(1)}_{\epsilon_\gamma, \mathbf{\Omega}_\gamma}(\lambda)$ at the limiting point of the integral domain. In H2 we find this value.

11. In PSI2 we find the number of two time interacting photons by using g1 and EX.

12. To find PSI2, we need the value of the integrand of the integration involving in PSI2 at the limiting points of the integrating domain. We have calculated that value in PS2.

N_x	N_t	Numerical value	Error
10	10	0.1675	8.3333e-004
20	20	0.1669	2.0833e-004
30	30	0.1668	9.2593e-005
40	40	0.1667	5.2083e-005
50	50	0.1667	3.3333e-005
100	100	0.1667	8.3333e-006
200	200	0.1667	2.0833e-006
500	500	0.1667	3.3333e-007
1000	1000	0.1667	8.3333e-008

Table 4.1

Similarly, we calculate the g2, PSI3, PS3 and H3 like as g1, PSI2, PS2 and H2 respectively. In main2 we give the necessary data (input data) and get output from here.

4.6 Checking the numerical quadrature code

For solving the integration numerically we use the 2D composite trapezoidal rule. In this section we check that our numerical code regarding this part works well.
Let N_x and N_y be the number of divisions of the range of x and y respectively. We give the following three examples.

1. We find the value of
$$\int_0^1 \int_0^1 xy^2 dx\, dy = 0.166666... \tag{4.62}$$
Table 4.1 gives the numerical result of the integral (4.62) which is solved by 2D composite trapezoidal rule.

2. We calculate by hand and see that the value of
$$\int_0^3 \int_0^2 (x^3 + y^3) dx\, dy = 52.5. \tag{4.63}$$
Table 4.2 gives the numerical result of the integral (4.63) which is solved by 2D composite trapezoidal rule.

3. We calculate and observe that
$$\int_1^3 \int_1^3 (x^2 \cos(y) + y^2 \sin(x)) dx\, dy = 7.1928. \tag{4.64}$$

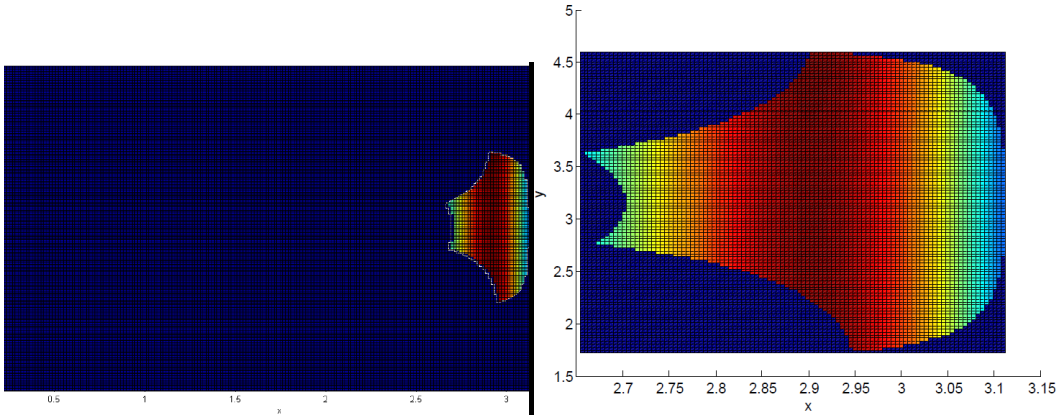

(a) (b)

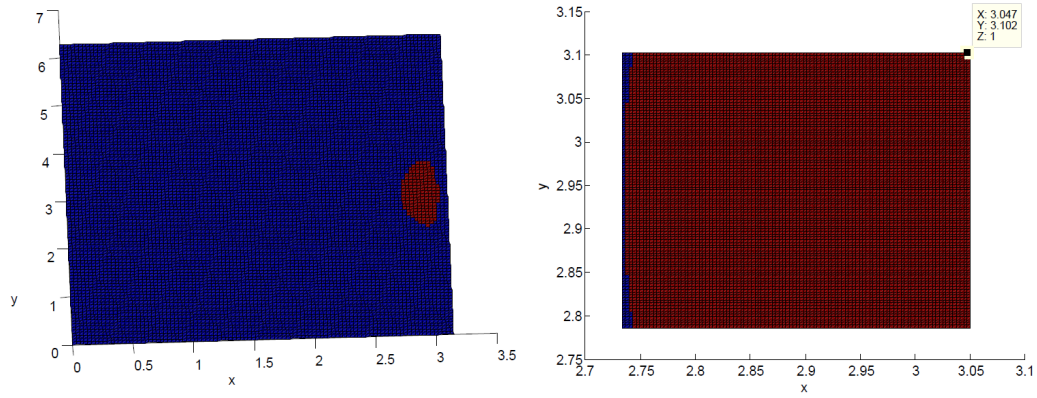

(c) (d)

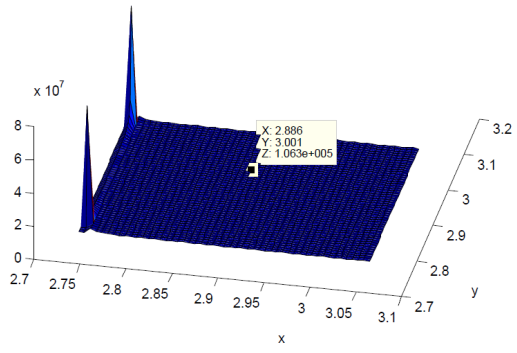

(e)

Figure 4.12

N_x	N_t	Numerical value	Error
10	10	53.0250	0.5250
20	20	52.6313	0.1313
30	30	52.5583	0.0583
40	40	52.5328	0.0328
50	50	52.5210	0.0210
100	100	52.5053	0.0053
150	150	52.5023	0.0023
200	200	52.5013	0.0013
300	300	52.5006	5.8333e-004
500	500	52.5002	2.1000e-004
1000	1000	52.5000	5.2500e-005
1050	1050	52.5000	4.7619e-005
1100	1100	52.5000	4.3388e-005

Table 4.2

Table 4.3 gives the numerical result of the integral (4.64) which is solved by 2D composite trapezoidal rule.

Therefore, we see that the numerical results of each of the three examples are converge with order 2 to their exact result.

4.7 Discussion about Figure 4.12

1. **Graph(a).** This graph represents the total domain and the support of $\psi_\gamma^{(0)}$ (the part which is not blue) inside the domain.

2. **Graph(b).** This graph represents the minimum rectangle (say REC0) containing the support of $\psi_\gamma^{(0)}$.

3. **Graph(c).** This graph represents the total domain and the umbrella of Figure 4.5 (the part which is not blue) inside the domain .

4. **Graph(d).** This graph represents the minimum rectangle (say REC1) containing this umbrella.

5. **Graph(e).** This graph represents the intersecting rectangle = REC0 $\cap$ REC1.

N_x	N_t	Numerical value	Error
10	10	7.1977	0.0129
20	20	7.1896	0.0032
30	30	7.1914	0.0014
40	40	7.1920	7.6061e-004
50	50	7.1923	4.7000e-004
60	60	7.1925	3.1217e-004
70	70	7.1926	2.1701e-004
80	80	7.1926	1.5525e-004
90	90	7.1927	1.1290e-004
100	100	7.1927	8.2618e-005
110	110	7.1927	6.0210e-005
120	120	7.1928	4.3167e-005
150	150	7.1928	1.0890e-005
200	200	7.1928	1.4214e-005

Table 4.3

4.8 Characteristics of computer

All computations have been performed on a personal computer with the following characteristics:

1. **Operating system**: Microsoft Windows XP.

2. **Processor**: Intel duel cor T4200 @ 200 GHz.

3. **Memory**: 2GB RAM.

4. **Hard disk**: 250GB.

4.9 Numerical results

Here we show the numerical result of BTE for photons. We find the number of noninteracting photons ($\psi_\gamma^{(0)}(\mathbf{r}, \mathbf{\Omega}_\gamma, \epsilon_\gamma)$), one time interacting photons ($\psi_\gamma^{(1)}(\mathbf{r}, \mathbf{\Omega}_\gamma, \epsilon_\gamma)$), two times interacting photons ($\psi_\gamma^{(2)}(\mathbf{r}, \mathbf{\Omega}_\gamma, \epsilon_\gamma)$) and three times interacting photons ($\psi_\gamma^{(3)}(\mathbf{r}, \mathbf{\Omega}_\gamma, \epsilon_\gamma)$). We see that the computing time to find the three time interacting photons is high. The number of three times interaction photons is much smaller than the number of noninteracting, one time interacting and two times interacting photons which has been shown in here

for some points. Let

$$PHOT(1) = \psi_\gamma^{(0)}(\mathbf{r}, \mathbf{\Omega}_\gamma, \epsilon_\gamma) + \psi_\gamma^{(1)}(\mathbf{r}, \mathbf{\Omega}_\gamma, \epsilon_\gamma) + \psi_\gamma^{(2)}(\mathbf{r}, \mathbf{\Omega}_\gamma, \epsilon_\gamma) \text{ and} \tag{4.65}$$

$$PHOT(2) = \psi_\gamma^{(0)}(\mathbf{r}, \mathbf{\Omega}_\gamma, \epsilon_\gamma) + \psi_\gamma^{(1)}(\mathbf{r}, \mathbf{\Omega}_\gamma, \epsilon_\gamma) + \psi_\gamma^{(2)}(\mathbf{r}, \mathbf{\Omega}_\gamma, \epsilon_\gamma) + \psi_\gamma^{(3)}(\mathbf{r}, \mathbf{\Omega}_\gamma, \epsilon_\gamma). \tag{4.66}$$

The tests have been carried out by using the following boundary condition, which has been adapted from the one of reference [26]

$$\psi_\gamma^{(0)}(\mathbf{r}^\star, \mathbf{\Omega}_\gamma, \epsilon_\gamma) = \begin{cases} 10^5 \mathrm{e}^{\{-10(1+\cos\theta)^2\}} \text{ when } \mathbf{r}^\star \in \Gamma \text{ and } \pi/2 < \theta \leq \pi, \\ 0 \text{ when } \mathbf{r}^\star \in \Lambda \text{ and } \pi/2 < \theta \leq \pi, \end{cases} \tag{4.67}$$

and we solve (4.4) for different M ($M = 2$ and $M = 3$). Here θ is the angle between the outward normal vector at the radiative point and the direction of the unit vector $\mathbf{\Omega}_\gamma$.
Notice that the value of $\psi_\gamma(\mathbf{r}, \mathbf{\Omega}_\gamma, \epsilon_\gamma)$ is given when $\mathbf{r} \in \partial Q$ and $\mathbf{\Omega}_\gamma \cdot \boldsymbol{n}(\mathbf{r}) < 0$, that is to say, the value of $\psi_\gamma(\mathbf{r}, \mathbf{\Omega}_\gamma, \epsilon_\gamma)$ is known at the boundary points only for ingoing direction $\mathbf{\Omega}_\gamma$ (entering inside the domain Q). For outgoing direction $\mathbf{\Omega}_\gamma$ (such that $\mathbf{\Omega}_\gamma \cdot \boldsymbol{n}(\mathbf{r}) \geq 0$) we need to compute $\psi_\gamma(\mathbf{r}, \mathbf{\Omega}_\gamma, \epsilon_\gamma)$.
The approximate development of the photon transport equation is based on the observation that photon has large mean free paths which are in the range about 10 to 50 cm. So the entering photon in the patient body is only subject to a few Compton scattering events say 1 to 3, or even none, before it leaves the body [18]. In this memory we chose $M = 2$ but also for our observation we calculate the three times interacting photons and this result is given in here.
We have taken a cube which each edge length is 3 m (Figure 4.8). O is the origin, ABGD is the irradiated area and AB=BG=DG=AD=0.2 m. We consider two layers one of air and other one of water and the thickness of air is 1.5 m and water is 1.5 m. The following four examples are given here.
Notice that in the following four examples we use small values for Nx, Ny, $Nx1$, $Ny1$, $Nw1$, and $Nw2$. Since our radiation area is small (0.04 m^2) so the support of the integration is very small. For this reason we get good approximations even for small number of divisions (coarse mesh of integration). In the first one of those four examples if we take (Nx, Ny, $Nw1$) = (300, 300, 100) and

$$\epsilon_\gamma = 12 \iff \text{energy} = 6.132\,\text{MeV}$$

then the exact value of $\psi_\gamma^{(1)} = 215.8170$ and the corresponding time is 1350 seconds. So, to find $\psi_\gamma^{(2)}$ we need much more time. But when we take $(Nx,\, Ny,\, Nw1) = (2,\, 10,\, 3)$ then the value of $\psi_\gamma^{(1)} = 215.9039$ and the corresponding time is only 0.0122 seconds. This value is very near to the exact value. Here if we take $(Nx,\, Ny,\, Nx1,\, Ny1\, Nw1,\, Nw2) = (2,\, 10,\, 3,\, 50,\, 50,\, 2)$ then the exact value of $\psi_\gamma^{(2)} = 10.1498$ and the corresponding time is 63 seconds. But if we take $(Nx,\, Ny,\, Nx1,\, Ny1\, Nw1,\, Nw2) = (2,\, 10,\, 3,\, 7,\, 1,\, 2)$ then $\psi_\gamma^{(2)} = 10.0572$ and the corresponding time is 0.42 seconds. So we see from the above discussion that the error is very small.

1. We take a unit vector

$$\mathbf{\Omega}_\gamma = \left[0,\ \frac{-0.05}{1.5608},\ \frac{-1.56}{1.5608}\right]. \tag{4.68}$$

Then the number of photons at [1.5, 1.45, 1.44] ($\mathbf{R}(t)$) going to this direction are given in Table 4.4 for some different energies. We observe that the value of integral involving in the formula of $\psi_\gamma^{(1)}(\mathbf{r}, \mathbf{\Omega}_\gamma, \epsilon_\gamma)$ and $\psi_\gamma^{(2)}(\mathbf{r}, \mathbf{\Omega}_\gamma, \epsilon_\gamma)$ is a good approximation to the exact value for

$$(Nx,\, Ny,\, Nx1,\, Ny1,\, Nw1,\, Nw2) = (2,\, 10,\, 7,\, 1,\, 3,\, 1). \tag{4.69}$$

So in here we use this data. This point ($\mathbf{R}(t)$) is inside the column CL5 and the boundary point $\mathbf{r}^\star$ is inside the radiative area ABGD (Figure 4.8). Here, $\psi_\gamma^{(3)} = 0.1243$

Energy, MeV	$\psi_\gamma^{(0)}$	$\psi_\gamma^{(1)}$	$\psi_\gamma^{(2)}$	$PHOT(1)$	Time (seconds)
3	7.9393e+004	191.8405	9.3377	7.9594e+004	0.25
4	8.2495e+004	202.4116	7.6265	8.2705e+004	0.25
5	8.4692e+004	209.8232	6.5878	8.4909e+004	0.25
6	8.6344e+004	215.2895	6.2183	8.6566e+004	0.25
10	9.0282e+004	227.3801	4.4317	9.0541e+004	0.25
15	9.2717e+004	233.1860	3.1842	9.2954e+004	0.25
20	9.4115e+004	235.0480	2.4945	9.4353e+004	0.25

Table 4.4

for

$$(Nx,\, Ny,\, Nx1,\, Ny1,\, Nx2,\, Ny2,\, Nw1,\, Nw2,\, Nw3) = (2,\, 10,\, 7,\, 1,3,\, 3,\, 3,\, 1,\, 2) \tag{4.70}$$

when $\epsilon_\gamma = 6$ MeV. The corresponding time is 8 seconds in this case. The comparative size of $\psi_\gamma^{(3)}$ with respect $PHOT(1)$ is $\frac{\psi_\gamma^{(3)}}{PHOT(1)} = 1.4359\text{e} - 006$, which is very small. Now we show in Figure 4.13 the combination of the number of photons going to the

Energy, MeV	$\psi_\gamma^{(0)}$	$\psi_\gamma^{(1)}$	$\psi_\gamma^{(2)}$	$PHOT(1)$	Time (seconds)
3	0	166.7789	6.6483	173.4272	0.05
4	0	173.5893	5.4628	179.0521	0.05
5	0	178.0782	4.6470	182.7252	0.05
6	0	181.1521	4.0480	185.2001	0.05
10	0	186.4472	2.6799	189.1271	0.05
15	0	186.6012	.9402	187.5414	0.05
20	0	184.222	1.3290	185.5511	0.05

Table 4.5

direction

$$\mathbf{\Omega}_\gamma \left[0,\ \frac{-0.05}{1.5608},\ \frac{-1.56}{1.5608}\right] \tag{4.71}$$

on some different planes for energy 6 MeV and discuss. In the Figure 4.13, (a) shows the value of ψ_γ on XY plane inside water and (b) inside air. Then (c), (d), (e) show ψ_γ left sided plane of the column CL5, (d) plane inside the column CL5 and (e) right sided plane of the column CL5 accordingly. The (f), (g), (h) show ψ_γ on vertical planes parallal to YZ plane: (f) is the back sided of the column CL5, the plane (g) is inside the column CL5 and the plane showed by (h) is the front sided of the column CL5 (Figure 4.8).

2. We take a unit vector

$$\mathbf{\Omega}_\gamma = \left[0,\ \frac{-0.151}{1.5573},\ \frac{-1.55}{1.5573}\right]. \tag{4.72}$$

Then the number of photons at [1.5, 1.45, 1.45] ($\mathbf{R}(t)$) going to this direction are shown in Table 4.5 for some different energies. We observe that the value of integral involving in the formula of $\psi_\gamma^{(1)}(\mathbf{r}, \mathbf{\Omega}_\gamma, \epsilon_\gamma)$ and $\psi_\gamma^{(2)}(\mathbf{r}, \mathbf{\Omega}_\gamma, \epsilon_\gamma)$ converge for

$$(Nx,\ Ny,\ Nx1,\ Ny1,\ Nw1,\ Nw2) = (3,\ 10,\ 2,\ 1,\ 1,\ 1). \tag{4.73}$$

So in here we use this data. This point ($\mathbf{R}(t)$) is inside the column CL5 and the boundary point $\mathbf{r}^\star$ is outside of the radiative area ABGD (Figure 4.8). Here, $\psi_\gamma^{(3)} = 0.1830$ for $\epsilon_\gamma = 6$ MeV, where

$$(Nx,\ Ny,\ Nx1,\ Ny1,\ Nx2,\ Ny2,\ Nw1,\ Nw2,\ Nw3) = (3,\ 10,\ 2,\ 1,\ 3,\ 3,\ 1,\ 1,\ 2) \tag{4.74}$$

and the corresponding time is 2 seconds. The comparative size of $\psi_\gamma^{(3)}$ with respect $PHOT(1)$ is $\frac{\psi_\gamma^{(3)}}{PHOT(1)} = 9.8812\text{e}-004$, which is very small.

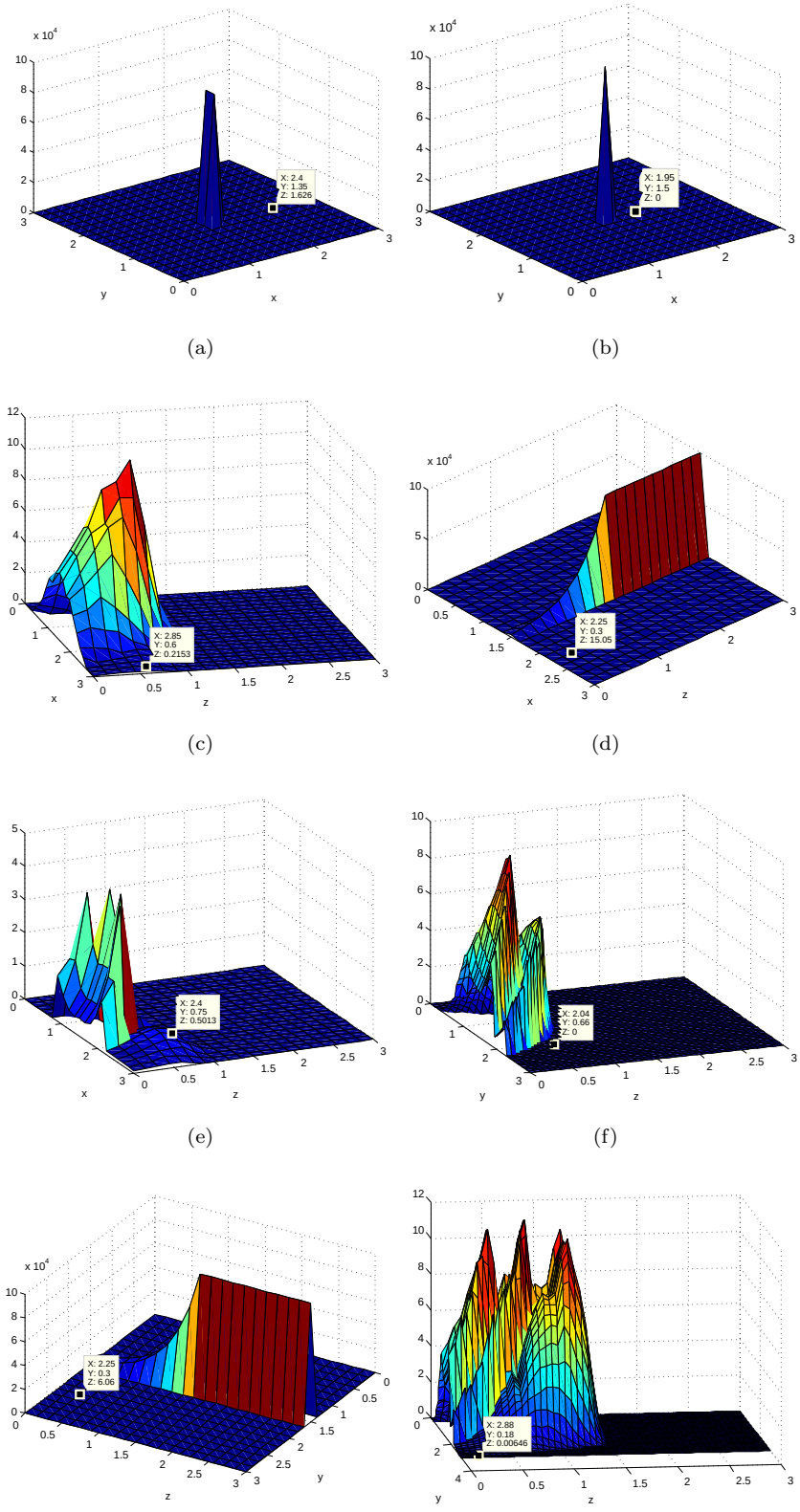
x 10^4
X: 2.4
Y: 1.35
Z: 1.626
(a)
x 10^4
X: 1.95
Y: 1.5
Z: 0
(b)
X: 2.85
Y: 0.6
Z: 0.2153
(c)
x 10^4
X: 2.25
Y: 0.3
Z: 15.05
(d)
X: 2.4
Y: 0.75
Z: 0.5013
(e)
X: 2.04
Y: 0.66
Z: 0
(f)
x 10^4
X: 2.25
Y: 0.3
Z: 6.06
(g)
X: 2.88
Y: 0.18
Z: 0.00646
(h)

Figure 4.13

Energy, MeV	$\psi_\gamma^{(0)}$	$\psi_\gamma^{(1)}$	$\psi_\gamma^{(2)}$	$PHOT(1)$	Time (seconds)
3	1.4279e+004	110.7736	8.1909	1.4398e+004	44
4	1.9724e+004	169.9053	13.6027	1.9908e+004	44
5	2.4615e+004	228.4460	17.7111	2.4862e+004	44
6	2.8969e+004	284.3090	22.2070	2.9275e+004	44
10	4.2186e+004	471.4149	33.0116	4.2690e+004	44
15	5.2797e+004	634.3340	36.5042	5.3468e+004	44
20	5.9893e+004	744.6039	37.2615	6.0675e+004	44

Table 4.6

3. We take a unit vector

$$\mathbf{\Omega}_\gamma = \left[\frac{0.08}{2.024}, \frac{-0.3}{2.024}, \frac{-2}{2.024}\right]. \tag{4.75}$$

Then the number of photons at $[1.5,\ 1.2,\ 1]$ ($\mathbf{R}(t)$) going to this direction are given in Table 4.6 for some different energies. We observe that the value of integral involving in the formula of $\psi_\gamma^{(1)}(\mathbf{r}, \mathbf{\Omega}_\gamma, \epsilon_\gamma)$ and $\psi_\gamma^{(2)}(\mathbf{r}, \mathbf{\Omega}_\gamma, \epsilon_\gamma)$ converge for

$$(Nx,\ Ny,\ Nx1,\ Ny1,\ Nw1,\ Nw2) = (10,\ 8,\ 4,\ 4,\ 30,\ 15). \tag{4.76}$$

So in here we use this data. This point ($\mathbf{R}(t)$) is outside the column CL5 and the boundary point $\mathbf{r}^\star$ is inside the radiative area ABGD (Figure 4.8). Here, $\psi_\gamma^{(3)} = 0.4533$ for $\epsilon_\gamma = 3$ MeV, where

$$(Nx,\ Ny,\ Nx1,\ Ny1,\ Nx2,\ Ny2,\ Nw1,\ Nw2,\ Nw3) = (10,\ 8,\ 4,\ 4,\ 3,\ 3,\ 30,\ 15,\ 2) \tag{4.77}$$

and the corresponding time is 1400 seconds. The comparative size of $\psi_\gamma^{(3)}$ with respect $PHOT(1)$ is $\frac{\psi_\gamma^{(3)}}{PHOT(1)} = 3.1484\text{e} - 005$, which is very small.

4. We take a unit vector

$$\mathbf{\Omega}_\gamma = \left[0, \frac{-0.7}{1.7007}, \frac{-1.55}{1.7007}\right]. \tag{4.78}$$

Then the number of photons at $[1.5,\ 1,\ 1.45]$ ($\mathbf{R}(t)$) going to this direction are given in Table 4.7 for some different energies. We observe that the value of integral involving in the formula of $\psi_\gamma^{(1)}(\mathbf{r}, \mathbf{\Omega}_\gamma, \epsilon_\gamma)$ and $\psi_\gamma^{(2)}(\mathbf{r}, \mathbf{\Omega}_\gamma, \epsilon_\gamma)$ converge for

$$(Nx,\ Ny,\ Nx1,\ Ny1,\ Nw1,\ Nw2) = (25,\ 5,\ 4,\ 3,\ 1,\ 1). \tag{4.79}$$

So in here we use this data. This point ($\mathbf{R}(t)$) is outside the column CL5 and the

Energy, MeV	$\psi_\gamma^{(0)}$	$\psi_\gamma^{(1)}$	$\psi_\gamma^{(2)}$	$PHOT(1)$	Time (seconds)
3	0	146.3158	7.5128	153.8286	0.35
4	0	151.6629	4.9370	156.5999	0.35
5	0	154.7981	4.0720	158.8701	0.35
6	0	156.5922	2.3215	158.9137	0.35
10	0	151.2835	1.5818	158.8653	0.35
15	0	152.6300	1.0842	158.9137	0.35
6	0	156.5922	2.3215	158.9137	0.35

Table 4.7

boundary point $\mathbf{r}^\star$ is outside of the radiative area ABGD (Figure 4.8). Here, $\psi_\gamma^{(3)} = 0.4533$ for $\epsilon_\gamma = 6$ MeV, where

$$(Nx,\, Ny,\, Nx1,\, Ny1,\, Nx2,\, Ny2,\, Nw1,\, Nw2,\, Nw3) = (25,\, 5,\, 4,\, 3,\, 3,\, 3,\, 1,\, 1,\, 2) \tag{4.80}$$

and the corresponding time is 10 seconds. The comparative size of $\psi_\gamma^{(3)}$ with respect $PHOT(1)$ is $\frac{\psi_\gamma^{(3)}}{PHOT(1)} = 2.3409\text{e} - 004$, which is very small.

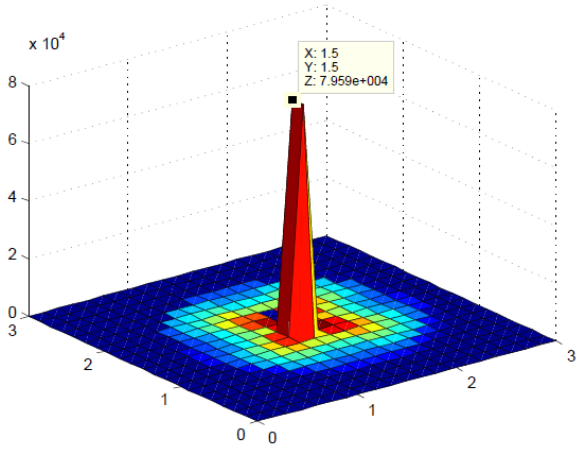

(a)

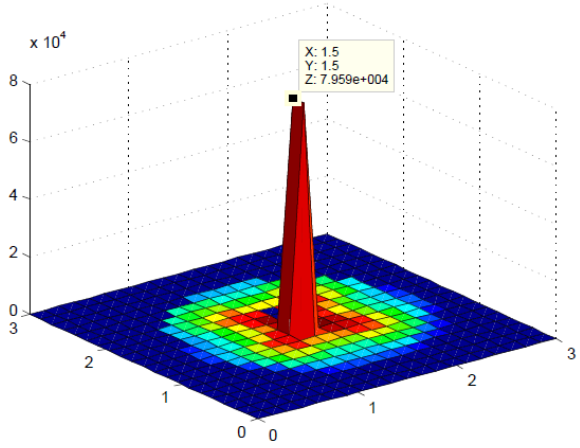

(b)

Figure 4.14

We see in the Tables 4.4, 4.5, 4.6 and 4.7 that the number of three time interacting photons is much smaller than the number of $PHOT(1)$ and the comparatively value is near to zero which we show in this four tables. The (a) and (b) of Figure 4.14 represent the value of ψ_γ on the plane ($Z = 1.44$ plane). We use $PHOT(1)$ for (a) and $PHOT(2)$ for (b) of the Figure 4.14. Here the Z axis represents the number of photons. We observed that

$$(X, Y) = (1.5,\ 1.5) \text{ which implies } Z = 7.959\text{e} + 004 \tag{4.81}$$

on the both graphics (a) and (b). Therefore we see that the number of photons are same at the same points on the both graphics (a) and (b). The result $PHOT(1)$ is not affected by $\psi_\gamma^{(3)}$. We use the data for computing which we use for the Table 4.4, in both cases.

The two graphics are indistinguishable, but the computing times are very different:

1. Computing (a) takes 0.54 seconds.

2. Computing (b) takes 1800 seconds.

In here we observe that the result is same but the time difference is very high. In both graphics we use the number of divisions in the X direction is 20 and the number of divisions in the Y direction is 20. If we increase the number of those divisions then of course the computing time also increases, and the increasing rate is very high. Also the difference between computing times for (a) and (b) would become larger.

Chapter 5

A finite difference scheme for a degenerate final value problem

This chapter is devoted to search finite difference schemes which can be used to discretize the differential operators appearing in the Fokker-Planck equation for electrons. Also, we show the mathematical model for the Compton source term of the Fokker-Planck approximation in this chapter. The mean free path of electrons is much smaller than the mean free path of photons, so we cannot solve the BTE for electrons by using the same process which we used for solving the BTE for photons. Alternatively, one can solve instead the Fokker-Planck equation, which is an approximation of the BTE based on the fact that the scattering process for electrons are very forward-peaked. For solving this equation numerically, we are researching to find the appropriate method. For this we have solved some differential equations numerically. One of them, the one which is some difficult due to degeneracy is

shown in this chapter with its numerical scheme and error of the result.

$$\begin{aligned}\boldsymbol{\Omega}_{\mathsf{e}} \cdot \nabla\psi_{\mathsf{e}}(\mathbf{r}, \boldsymbol{\Omega}_{\mathsf{e}}, \epsilon_{\mathsf{e}}) =& \rho_{\mathsf{e}}(\mathbf{r}) \int_0^\infty \int_{S^2_{1/2}} \tilde{\sigma}_{C,\mathsf{e}}(\epsilon'_\gamma, \epsilon_{\mathsf{e}}, \boldsymbol{\Omega}'_\gamma \cdot \boldsymbol{\Omega}_{\mathsf{e}})\psi_\gamma(\mathbf{r}, \boldsymbol{\Omega}'_\gamma, \epsilon'_\gamma)\ \mathrm{d}\boldsymbol{\Omega}'_\gamma\ \mathrm{d}\epsilon'_\gamma \\ &+ \rho_{\mathsf{e}}(\mathbf{r}) \int_{\epsilon_s}^\infty \int_{S^2_{1/4}} \tilde{\sigma}_{\mathrm{M}}(\epsilon'_{\mathsf{e}}, \epsilon_{\mathsf{e}}, \boldsymbol{\Omega}'_{\mathsf{e}} \cdot \boldsymbol{\Omega}_{\mathsf{e}})\psi_{\mathsf{e}}(\mathbf{r}, \boldsymbol{\Omega}'_{\mathsf{e}}, \epsilon'_{\mathsf{e}})\ \mathrm{d}\boldsymbol{\Omega}'_{\mathsf{e}}\ \mathrm{d}\epsilon'_{\mathsf{e}} \\ &+ \rho_{\mathsf{e}}(\mathbf{r}) \int_{\epsilon_s}^\infty \int_{S^2_{2/4}} \tilde{\sigma}_{\mathrm{M},\delta}(\epsilon'_{\mathsf{e}}, \epsilon_{\mathsf{e}}, \boldsymbol{\Omega}'_{\mathsf{e}} \cdot \boldsymbol{\Omega}_{\mathsf{e}})\psi_{\mathsf{e}}(\mathbf{r}, \boldsymbol{\Omega}'_{\mathsf{e}}, \epsilon'_{\mathsf{e}})\ \mathrm{d}\boldsymbol{\Omega}'_{\mathsf{e}}\ \mathrm{d}\epsilon'_{\mathsf{e}} \\ &+ \rho_{\mathsf{c}}(\mathbf{r}) \int_{S^2} \sigma_{\mathrm{Mott}}(\mathbf{r}, \epsilon_{\mathsf{e}}, \boldsymbol{\Omega}'_{\mathsf{e}} \cdot \boldsymbol{\Omega}_{\mathsf{e}})\psi_{\mathsf{e}}(\mathbf{r}, \boldsymbol{\Omega}'_{\mathsf{e}}, \epsilon_{\mathsf{e}})\ \mathrm{d}\boldsymbol{\Omega}'_{\mathsf{e}} \\ &- \rho_{\mathsf{e}}(\mathbf{r})\sigma^{\mathrm{tot}}_{\mathrm{M}}(\epsilon_{\mathsf{e}})\psi_{\mathsf{e}}(\mathbf{r}, \boldsymbol{\Omega}_{\mathsf{e}}, \epsilon_{\mathsf{e}}) \\ &- \rho_{\mathsf{c}}(\mathbf{r})\sigma^{\mathrm{tot}}_{\mathrm{Mott}}(\mathbf{r}, \epsilon_{\mathsf{e}})\psi_{\mathsf{e}}(\mathbf{r}, \boldsymbol{\Omega}_{\mathsf{e}}, \epsilon_{\mathsf{e}}). \end{aligned} \tag{5.1}$$

where ρ_{c} is the density of atomic cores in the medium, $\tilde{\sigma}_{C,\mathsf{e}}$ is the scattering cross section differential in angle and energy for Compton scattering of electrons. $\tilde{\sigma}_{\mathrm{M}}$ is the scattering cross section for primary electrons differential in angle and energy for Møller scattering and $\tilde{\sigma}_{\mathrm{M},\delta}$ is the cross section for secondary electrons (delta-rays). The scattering cross section for Mott scattering σ_{Mott} is only differential in angle, because Mott scattering is an elastic scattering. The total cross section for Møller and Mott scattering are $\sigma^{\mathrm{tot}}_{\mathrm{M}}$ and $\sigma^{\mathrm{tot}}_{\mathrm{Mott}}$ respectively.

The meaning of notations $S^2_{1/2}$, $S^2_{1/4}$ and $S^2_{2/4}$ is explained in [15]. Since it will be needed in the following section, it is useful to include in here that, for fixed Ω_e,

$$S^2_{1/2} = \left\{\boldsymbol{\Omega}'_\gamma \in S^2 : \boldsymbol{\Omega}'_\gamma \cdot \Omega_e \geq 0\right\} \tag{5.2}$$

The electrons have forward peaked scattering and small energy loss, so for finding the number of electrons we take Fokker-Planck equation instead of Boltzmann transport equation

$$\begin{aligned}\boldsymbol{\Omega}_{\mathsf{e}} \cdot \nabla\psi_{\mathsf{e}}(\mathbf{r}, \boldsymbol{\Omega}_{\mathsf{e}}, \epsilon_{\mathsf{e}}) - [T_{\mathrm{Mott}}(\mathbf{r}, \epsilon_{\mathsf{e}}) + T_{\mathrm{M}}(\mathbf{r}, \epsilon_{\mathsf{e}})]L\psi_{\mathsf{e}} \\ - \frac{\partial}{\partial\epsilon_{\mathsf{e}}}[S_{\mathrm{M}}(\mathbf{r}, \epsilon_{\mathsf{e}})\psi_{\mathsf{e}}] = Q(\mathbf{r}, \boldsymbol{\Omega}_{\mathsf{e}}, \epsilon_{\mathsf{e}}),\end{aligned} \tag{5.3}$$

where L is the Laplace operator on the sphere

$$L = \frac{\partial}{\partial\mu_{\mathsf{e}}}(1-\mu^2_{\mathsf{e}})\frac{\partial}{\partial\mu_{\mathsf{e}}} + \frac{1}{1-\mu^2_{\mathsf{e}}}\frac{\partial^2}{\partial\varphi^2_{\mathsf{e}}}, \qquad \mu_{\mathsf{e}} = \cos\vartheta_{\mathsf{e}}, \tag{5.4}$$

and

$$0 \leq \vartheta_{\mathsf{e}} \leq \pi. \tag{5.5}$$

For fixed $\mathbf{\Omega}_{\mathsf{e}}$, $\mathbf{\Omega}_{\mathsf{e}} \cdot \nabla\psi_{\mathsf{e}}(\mathbf{r}, \mathbf{\Omega}_{\mathsf{e}}, \epsilon_{\mathsf{e}})$ represents the directional derivative in the direction $\mathbf{\Omega}_{\mathsf{e}}$. Thus if $\mathbf{r}^{\star} \in \partial Q$ and

$$\mathbf{r}(\lambda) = \mathbf{r}^{\star} + \lambda\mathbf{\Omega}_{\mathsf{e}}, \tag{5.6}$$

where $\lambda \in [0,\, L]$ for some positive value of L, we have that

$$\mathbf{\Omega}_{\mathsf{e}} \cdot \nabla\psi_{\mathsf{e}}(\mathbf{r}(\lambda), \mathbf{\Omega}_{\mathsf{e}}, \epsilon_{\mathsf{e}}) = \frac{\partial\psi_{\mathsf{e}}(\mathbf{r}(\lambda), \mathbf{\Omega}_{\mathsf{e}}, \epsilon_{\mathsf{e}})}{\partial\lambda} \tag{5.7}$$

and consequently the Fokker-Planck equation (5.3) reads as follows:

$$\frac{\partial\psi_{\mathsf{e}}(\mathbf{r}(\lambda), \mathbf{\Omega}_{\mathsf{e}}, \epsilon_{\mathsf{e}})}{\partial\lambda} - [T_{\mathrm{Mott}}(\mathbf{r}(\lambda), \epsilon_{\mathsf{e}}) + T_{\mathrm{M}}(\mathbf{r}(\lambda), \epsilon_{\mathsf{e}})]L\psi_{\mathsf{e}} - \frac{\partial}{\partial\epsilon_{\mathsf{e}}}[S_{\mathrm{M}}(\mathbf{r}(\lambda), \epsilon_{\mathsf{e}})\psi_{\mathsf{e}}] = Q(\mathbf{r}(\lambda), \mathbf{\Omega}_{\mathsf{e}}, \epsilon_{\mathsf{e}}). \tag{5.8}$$

Here, $Q(\mathbf{r}, \mathbf{\Omega}_{\mathsf{e}}, \epsilon_{\mathsf{e}})$ is the Compton source term which is given by

$$\begin{aligned} Q(\mathbf{r}, \mathbf{\Omega}_{\mathsf{e}}, \epsilon_{\mathsf{e}}) =& \rho_{\mathsf{e}}(\mathbf{r}) \int_0^{\infty} \int_{S^2_{1/2}} \tilde{\sigma}_{C,\mathsf{e}}(\epsilon'_{\gamma}, \epsilon_{\mathsf{e}}, \mathbf{\Omega}_{\gamma} \cdot \mathbf{\Omega}'_{\mathsf{e}})\psi_{\gamma}(\mathbf{r}, \mathbf{\Omega}'_{\gamma}, \epsilon'_{\gamma})\, \mathrm{d}\mathbf{\Omega}'_{\gamma}\, \mathrm{d}\epsilon'_{\gamma} \\ =& \rho_{\mathsf{e}}(\mathbf{r}) \int_{S^2_{1/2}} \int_0^{\infty} \tilde{\sigma}_{C,\mathsf{e}}(\epsilon'_{\gamma}, \epsilon_{\mathsf{e}}, \mathbf{\Omega}_{\gamma} \cdot \mathbf{\Omega}'_{\mathsf{e}})\psi_{\gamma}(\mathbf{r}, \mathbf{\Omega}'_{\gamma}, \epsilon'_{\gamma})\, \mathrm{d}\epsilon'_{\gamma}\, \mathrm{d}\mathbf{\Omega}'_{\gamma}. \end{aligned} \tag{5.9}$$

A rigorous mathematical deduction of Fokker-Planck from the Boltzmann transport equation can be found in the paper [27] by Pomraning.

5.1 Mathematical model of Compton source term

To calculate the Compton source term (5.9) we need the flux density of photons (ψ_{γ}) which we get from Chapter 4. Here there is another term in the differential cross section for Compton scattering containing the Dirac delta function. Therefore we need some mathematical calculation for this differential cross section which we show in this section. The process is similar to the one employed for calculating (4.19). We know from [15] that

$$\tilde{\sigma}_{C,\mathsf{e}}(\epsilon'_{\gamma}, \epsilon_{\mathsf{e}}, \mathbf{\Omega'}_{\gamma} \cdot \mathbf{\Omega}_{\mathsf{e}}) = \sigma_{C,\mathsf{e}}(\epsilon'_{\gamma}, \mathbf{\Omega'}_{\gamma} \cdot \mathbf{\Omega}_{\mathsf{e}})\delta_{C,\mathsf{e}}(\epsilon'_{\gamma}, \epsilon_{\mathsf{e}}) \tag{5.10}$$

with

$$\sigma_{C,\mathsf{e}}(\epsilon'_\gamma, \boldsymbol{\Omega}'_\gamma \cdot \boldsymbol{\Omega}_\mathsf{e}) = \frac{4r_\mathsf{e}^2(1+\epsilon'_\gamma)^2}{\cos^3\theta_\mathsf{e}} \frac{1}{(a(\epsilon'_\gamma,\theta_\mathsf{e})+2\epsilon'_\gamma)^2} \left[1 - \frac{2}{a(\epsilon'_\gamma,\theta_\mathsf{e})} + \frac{2}{a^2(\epsilon'_\gamma,\theta_\mathsf{e})} + \frac{2\epsilon_\gamma^2}{a(\epsilon'_\gamma,\theta_\mathsf{e})(a(\epsilon'_\gamma,\theta_\mathsf{e})+2\epsilon'_\gamma)}\right] \tag{5.11}$$

$$\delta_{C,\mathsf{e}}(\epsilon'_\gamma, \epsilon_\mathsf{e}) := \delta\left(\epsilon_\mathsf{e} - \frac{2{\epsilon'}_\gamma^2}{2\epsilon'_\gamma + a(\epsilon'_\gamma,\theta_\mathsf{e})}\right) \tag{5.12}$$

where

$$a(\epsilon'_\gamma, \theta_\mathsf{e}) := (1+\epsilon'_\gamma)^2 \tan^2\theta_\mathsf{e} + 1 \tag{5.13}$$

and $\boldsymbol{\Omega}'_\gamma \cdot \boldsymbol{\Omega}_\mathsf{e} = \cos\theta_\mathsf{e} = C$.

Therefore,

$$\tan^2\theta_\mathsf{e} = \frac{1-C^2}{C^2} \text{ and } \delta_{C,\mathsf{e}}(\epsilon'_\gamma, \epsilon_\mathsf{e}) := \delta\left(\epsilon_\mathsf{e} - \frac{2C^2{\epsilon'}_\gamma^2}{{\epsilon'}_\gamma^2 - C^2{\epsilon'_\gamma}^2 + 2\epsilon'_\gamma + 1}\right). \tag{5.14}$$

We can write from [12]

$$\int_0^\infty G(\epsilon'_\gamma)\delta(h(\epsilon'_\gamma, \epsilon_\mathsf{e}, C))\, \mathrm{d}\epsilon'_\gamma = \sum \frac{G(E'_\gamma)}{|\frac{\partial h}{\partial \epsilon'_\gamma}(E'_\gamma, \epsilon_\mathsf{e}, C)|}, \tag{5.15}$$

where the sum is taken over all those E'_γ such that $h(E'_\gamma, \epsilon_\mathsf{e}, C) = 0$. In case there exist no E'_γ such that $h(E'_\gamma, \epsilon_\mathsf{e}, C) = 0$ then

$$\int_0^\infty G(\epsilon'_\gamma)\delta(h(\epsilon'_\gamma, \epsilon_\mathsf{e}, C))\, \mathrm{d}\epsilon'_\gamma = 0.$$

Let

$$h(\epsilon'_\gamma, \epsilon_\mathsf{e}, C) = \epsilon_\mathsf{e} - \frac{2C^2{\epsilon'}_\gamma^2}{{\epsilon'}_\gamma^2 - C^2{\epsilon'_\gamma}^2 + 2\epsilon'_\gamma + 1} \tag{5.16}$$

$$\therefore \quad \frac{\partial h(\epsilon'_\gamma, \epsilon_\mathsf{e}, C)}{\partial \epsilon'_\gamma} = \frac{-4C^2\epsilon'_\gamma(\epsilon'_\gamma+1)}{({\epsilon'}_\gamma^2 - C^2{\epsilon'_\gamma}^2 + 2\epsilon'_\gamma + 1)^2}. \tag{5.17}$$

Now we are going to calculate those E'_γ such that $h(E'_\gamma, \epsilon_\mathsf{e}, C) = 0$. According to (5.16) we must solve the following equation:

$$h(E'_\gamma, \epsilon_\mathsf{e}, C) = \epsilon_\mathsf{e} - \frac{2C^2{E'}_\gamma^2}{{E'}_\gamma^2 - C^2{E'}_\gamma^2 + 2E'_\gamma + 1} = 0. \tag{5.18}$$

Since E'_γ is an energy we must look for $E'_\gamma \in (0,\infty)$. We fix $\epsilon_\mathsf{e} \in (0,\infty)$ and $\cos\theta_\mathsf{e} = \mathbf{\Omega}'_\gamma \cdot \mathbf{\Omega}_\mathsf{e} = C \in [-1,1]$. Let

$$f(x) = h(x,\epsilon_\mathsf{e},C) = \epsilon_\mathsf{e} - \frac{2C^2x^2}{x^2(1-C^2)+2x+1},\ \forall\ x \in (0,\infty). \tag{5.19}$$

Now we will find the solution of $f(x) = 0$.

1. If $C = \pm 1$, then

$$f(x) = \epsilon_\mathsf{e} - \frac{2x^2}{2x+1} = 0 \tag{5.20}$$

$$\Rightarrow\ \ x = \frac{1}{2}(\epsilon_\mathsf{e} \pm \sqrt{\epsilon_\mathsf{e}^2 + 2\epsilon_\mathsf{e}}), \tag{5.21}$$

but only we take

$$x = \frac{1}{2}(\epsilon_\mathsf{e} + \sqrt{\epsilon_\mathsf{e}^2 + 2\epsilon_\mathsf{e}}) = \widetilde{E'_\gamma}\ (say) \tag{5.22}$$

because $x \in (0,\infty)$.

Therefore we get, by using (5.17),

$$\frac{\partial h(\widetilde{E'_\gamma},\epsilon_\mathsf{e},C)}{\partial \epsilon'_\gamma} = \frac{-4C^2\widetilde{E'_\gamma}(\widetilde{E'_\gamma}+1)}{(\widetilde{E'_\gamma}^{\,2} - C^2\widetilde{E'_\gamma}^{\,2} + 2\widetilde{E'_\gamma}+1)^2}. \tag{5.23}$$

2. If $C \in (-1,1)$, then we must solve

$$f(x) = \epsilon_\mathsf{e} - \frac{2C^2x^2}{x^2(1-C^2)+2x+1} = 0. \tag{5.24}$$

Notice that

$$f(0) = \epsilon_\mathsf{e},\ \ \lim_{x\to\infty} f(x) = \epsilon_\mathsf{e} - \frac{2C^2}{1-C^2} \text{ and} \tag{5.25}$$

$$f'(x) = \frac{-4C^2x(1+x)}{[x^2(1-C^2)+2x+1]^2} < 0;\ \text{ since } x \in (0,\infty) \text{ and } -1 < C < 1. \tag{5.26}$$

(a) When $\epsilon_\mathsf{e} < \frac{2C^2}{1-C^2}$ then there is only one $\bar{x}$ such that $f(\bar{x}) = 0$ (see Figure 5.1).

$$\Rightarrow\ \bar{x} = \frac{\epsilon_\mathsf{e} \pm \sqrt{C^2\epsilon_\mathsf{e}(2+\epsilon_\mathsf{e})}}{2C^2 - \epsilon_\mathsf{e} + C^2\epsilon_\mathsf{e}}; \tag{5.27}$$

since $\bar{x}$ is always positive so, we will take only the positive value $\bar{x}$.

$$\therefore\ \ \bar{x} = \frac{\epsilon_\mathsf{e} + \sqrt{C^2\epsilon_\mathsf{e}(2+\epsilon_\mathsf{e})}}{2C^2 - \epsilon_\mathsf{e} + C^2\epsilon_\mathsf{e}} = E'_\gamma\ (say), \tag{5.28}$$

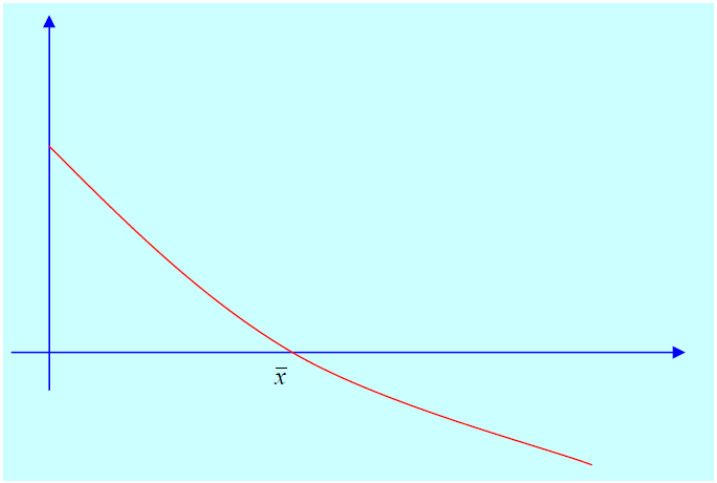

Figure 5.1

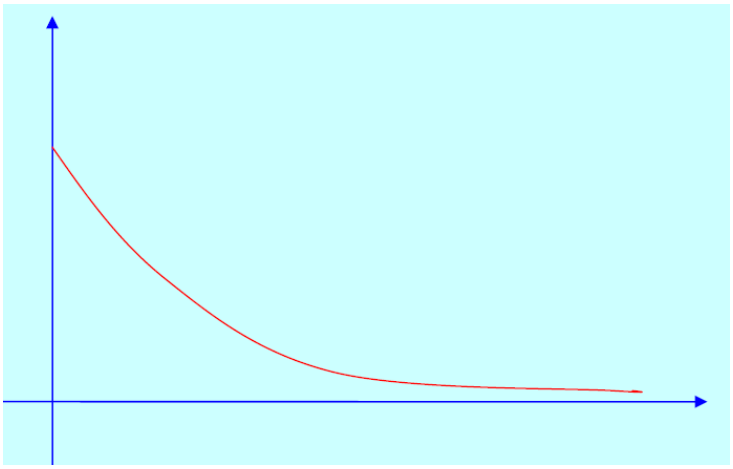

Figure 5.2

because this denominator is always greater than zero since $\epsilon_e < \frac{2C^2}{1-C^2}$ and in the numerator $\sqrt{C^2\epsilon_e(2+\epsilon_e)} > \epsilon_e$.

Therefore we find by using (5.17)

$$\frac{\partial h(E'_\gamma, \epsilon_e, C)}{\partial \epsilon'_\gamma} = \frac{-4C^2E'_\gamma(E'_\gamma+1)}{({E'_\gamma}^2 - C^2{E'_\gamma}^2 + 2E'_\gamma + 1)^2}. \tag{5.29}$$

(b) When $\epsilon_e \geq \frac{2C^2}{1-C^2}$ then there exists no $\bar{x}$ for which $f(\bar{x}) = 0$ (see Figure 5.2).

Therefore we get from (5.9), (5.10) and (5.15)

$$\int_0^\infty \tilde{\sigma}_{C,\mathsf{e}}\big(\epsilon'_\gamma, \epsilon_\mathsf{e}, \boldsymbol{\Omega}_\gamma \cdot \boldsymbol{\Omega}'_\mathsf{e}\big)\psi_\gamma\big(\mathbf{r}, \boldsymbol{\Omega}'_\gamma, \epsilon'_\gamma\big)\,\mathrm{d}\epsilon'_\gamma = \begin{cases} \frac{\sigma_{C,\mathsf{e}}(\widetilde{E'_\gamma}, \pm 1)\psi_\gamma(\mathbf{r}, \boldsymbol{\Omega}'_\gamma, \widetilde{E'_\gamma})(2\widetilde{E'_\gamma}+1)^2}{4\widetilde{E'_\gamma}(\widetilde{E'_\gamma}+1)} & \text{if } \boldsymbol{\Omega}'_\gamma \cdot \boldsymbol{\Omega}_\mathsf{e} = \pm 1 \\ \frac{\sigma_{C,\mathsf{e}}(E'_\gamma, C)\psi_\gamma(\mathbf{r}, \boldsymbol{\Omega}'\gamma, E'_\gamma)[(1-C^2)E'^2_\gamma + 2E'_\gamma + 1]^2}{4E'_\gamma C^2(1+E'_\gamma)} & \text{if } \boldsymbol{\Omega}'_\gamma \cdot \boldsymbol{\Omega}_\mathsf{e} = \\ & C \neq \pm 1 \text{ and} \\ & \epsilon_\mathsf{e} \in (0, \frac{2C^2}{1-C^2}) \\ 0 & \text{if } C \neq \pm 1 \\ & \text{and } \epsilon_\mathsf{e} \geq \frac{2C^2}{1-C^2}, \end{cases} \tag{5.30}$$

where $\widetilde{E'_\gamma}$, E'_γ are given by (5.22) and (5.28) respectively.
When we integrate with respect to $\boldsymbol{\Omega}'_\gamma$ then for fixed $\boldsymbol{\Omega}_\mathsf{e}$, $\boldsymbol{\Omega}_\mathsf{e} \cdot \boldsymbol{\Omega}'_\gamma = \pm 1$ indicates only two points on the sphere so it is not important in here. Consequently, we get from (5.9) and (5.30)

$$Q(\mathbf{r}, \boldsymbol{\Omega}_\mathsf{e}, \epsilon_\mathsf{e}) = \rho_\mathsf{e}(\mathbf{r}) \int_{D \subset S^2_{1/2}} \frac{\sigma_{C,\mathsf{e}}(E'_\gamma, C)\psi_\gamma(\mathbf{r}, \boldsymbol{\Omega}'\gamma, E'_\gamma)[(1-C^2)E'^2_\gamma + 2E'_\gamma + 1]^2}{4E'_\gamma C^2(1+E'_\gamma)} \mathrm{d}\boldsymbol{\Omega}'_\gamma, \tag{5.31}$$

where

$$C = C(\boldsymbol{\Omega}'_\gamma) = \boldsymbol{\Omega}_\mathsf{e} \cdot \boldsymbol{\Omega}'_\gamma \text{ and} \tag{5.32}$$

$$E'_\gamma = E'_\gamma(\boldsymbol{\Omega}'_\gamma) \text{ is given by (5.28)} \tag{5.33}$$

being

$$D = \left\{ \boldsymbol{\Omega}'_\gamma \in S^2_{1/2} : C \neq \pm 1 \text{ and } \epsilon_\mathsf{e} \in \left(0, \frac{2C^2}{1-C^2}\right) \right\}. \tag{5.34}$$

Since

$$\epsilon_\mathsf{e} \in \left(0, \frac{2C^2}{1-C^2}\right) \;\Leftrightarrow 0 < \epsilon_\mathsf{e} < \frac{2C^2}{1-C^2} \;\Leftrightarrow |\, C \,| > \sqrt{\frac{\epsilon_\mathsf{e}}{2+\epsilon_\mathsf{e}}}. \tag{5.35}$$

Hence either

$$1 > C > \left(\frac{\epsilon_\mathsf{e}}{2+\epsilon_\mathsf{e}}\right)^{1/2} \tag{5.36}$$

or

$$-1 < C < -\left(\frac{\epsilon_\mathsf{e}}{2+\epsilon_\mathsf{e}}\right)^{1/2}. \tag{5.37}$$

We will take only (5.36) because

$$C = \boldsymbol{\Omega}'_\gamma \cdot \Omega_e \geq 0 \text{ when } \boldsymbol{\Omega}'_\gamma \in S^2_{1/2}. \tag{5.38}$$

Therefore we will have to take, $0 < \theta_{\mathsf{e}} < \arccos\left[\left(\frac{\epsilon_{\mathsf{e}}}{2+\epsilon_{\mathsf{e}}}\right)^{1/2}\right]$, begin θ_e the angle between $\mathbf{\Omega}'_\gamma$ and Ω_e.

5.2 The partial differential equation

In this section we use some notation for the Fokker-Planck equation (5.8) and discuss. A numerical scheme based on finite differences for this equation is given here. We have tested the numerical scheme for an exact test. If we consider

$$\mu_{\mathsf{e}} = \cos(\text{zenith angle}) = x;\ \varphi_{\mathsf{e}} = \text{polar angle} = y;\ \lambda = z,\ \text{energy} = \epsilon_{\mathsf{e}} = t\ \ \psi_{\mathsf{e}} = u,$$
$$T_{\text{Mott}} + T_{\text{M}} = \text{constant} = T \text{ and } \frac{\partial S_{\text{M}}}{\partial \epsilon_{\mathsf{e}}} = \text{constant} = B \tag{5.39}$$

then equation (5.8) become

$$\frac{\partial u}{\partial z} - T\left[\frac{\partial}{\partial x}(1-x^2)\frac{\partial}{\partial x} + \frac{1}{1-x^2}\frac{\partial^2}{\partial y^2}\right]u - S_{\text{M}}\frac{\partial u}{\partial t} - Bu = Q \tag{5.40}$$

where $-1 \le x \le 1,\ 0 \le y < 2\pi,\ 0 \le z \le \lambda$.

To solve the equation (5.40) we need to select an appropriate method. For choosing the method we solved some partial differential equations which are related to the equation (5.40). One of them is the following:

$$\frac{\partial u}{\partial t} + \frac{\partial}{\partial x}\left[(1-x^2)\frac{\partial u}{\partial x}\right] = M(t,x), \tag{5.41}$$

where $x \in [-1,\ 1]$ and $t \in [0,\ T]$ (say). This equation is similar to the heat equation. We know the heat equation

$$\frac{\partial u}{\partial t} - \frac{\partial}{\partial x}\left[k(x)\frac{\partial u}{\partial x}\right] = M(t,x), \tag{5.42}$$

where the $k(x) > 0$ is heat conductivity. Our equation contains '+' sign in front of $\frac{\partial}{\partial x}$ instead of the '−' sign of the heat equation.

It is well known that for solving the heat equation an initial condition is needed. What we need now is a final condition due to the fact that we have a '+' sign in front of $\frac{\partial}{\partial x}$ instead of '−' sign.

Thus we will consider the following final condition associated with the partial difference equation (5.41):

$$u(T,x) = u_T(x). \tag{5.43}$$

Let, on the other hand,

$$a(x) = (1 - x^2) \geq 0 \quad (\text{since} \quad -1 \leq x \leq 1). \tag{5.44}$$

We see that equation (5.41) contains a first order partial derivative with respect to t and a second order partial derivative with respect to x. Typically to solve this kind of equations we need a final condition and two boundary conditions, one at $x = -1$ and other at $x = 1$. However, this is a degenerate parabolic PDE, it is degenerate because here $a(x) = 0$ at the boundary of $[-1, 1]$, and for this reason the boundary values are not needed in here. Therefore for choosing an appropriate numerical scheme we cannot choose any numerical scheme which is used to solve heat equation. We choose a numerical scheme which takes into account that $a(x) = 0$ at the boundary. As in the case of the heat equation, implicit schemes give better result than explicit ones.

5.2.1 The numerical scheme of the degenerate parabolic PDE

Here we discuss about some details concerning our numerical scheme. We look for a difference scheme of order in t and order 2 in x. Regarding the x discretization, note that at the boundary of $[-1, 1]$ we cannot use the centered difference formula for the first order derivative with respect to x. So at -1 we use the forward difference formula for the first order derivative with respect to x and at 1 we use the backward difference formula for the first order derivative with respect to x (see [14], page 207). For the interior nodes of $[-1, 1]$, that is to say, for the nodes belonging to the open interval $(-1, 1)$, we use the appropriate centered difference formula.

Let n_x be the number of nodes in $[-1, 1]$ and let $n_t - 1$ be the number of "time" steps covering $[0, T]$. We use the notations

$$\begin{aligned} x_i &= -1 + (i-1)h, \text{ where } i = 1, ..., n_x \text{ and } \Delta x = h = \frac{2}{n_x - 1}, \\ t_j &= (j-1)k, \text{ where } j = 1, ..., n_t \text{ and } \Delta t = k = \frac{T}{n_t - 1}. \end{aligned} \tag{5.45}$$

- **For** $i = 1$

  The numerical scheme of (5.41)

$$\frac{u(t_{j+1}, x_i) - u(t_j, x_i)}{k} \approx \frac{-3a(x_i)\frac{\partial}{\partial x}u(t_j, x_i) + 4a(x_{i+1})\frac{\partial}{\partial x}u(t_j, x_{i+1}) - a(x_{i+2})\frac{\partial}{\partial x}u(t_j, x_{i+2})}{-2h} + M(t_j, x_i). \tag{5.46}$$

Despite having explicit appearance, this is an implicit approximation because we are solving a final value problem. We use the following notations:

$$u(t_j, x_i) \approx U_i^j,\ a(x_i) = a_i,\ \text{and } M(t_j, x_i) = M_i^j. \tag{5.47}$$

Note that here

$$a(x_i) = a(x_1) = a_1 = a(-1) = 0. \tag{5.48}$$

Therefore we get from (5.46)

$$\begin{aligned}\frac{u(t_{j+1}, x_i) - u(t_j, x_i)}{k} \approx & \frac{-1}{2h}\left[4a_{i+1}\frac{u(t_j, x_{i+2}) - u(t_j, x_i)}{2h} - a_{i+2}\frac{u(t_j, x_{i+3}) - u(t_j, x_{i+1})}{2h}\right] \\ & + M(t_j, x_i),\end{aligned} \tag{5.49}$$

which suggests the following numerical scheme:

$$\frac{U_i^{j+1} - U_i^j}{k} = \frac{-1}{2h}\left[4a_{i+1}\frac{U_{i+2}^j - U_i^j}{2h} - a_{i+2}\frac{U_{i+3}^j - U_{i+1}^j}{2h}\right] + M_i^j, \tag{5.50}$$

$$\Leftrightarrow \left(\frac{a_{i+1}}{-h^2} - \frac{1}{k}\right)U_i^j = \frac{a_{i+1}}{-h^2}U_{i+2}^j + \frac{a_{i+2}}{4h^2}\left(U_{i+3}^j - U_{i+1}^j\right) - \frac{1}{k}U_i^{j+1} + M_i^j. \tag{5.51}$$

- **For** $i = 2$

  The numerical scheme of (5.41)

$$\frac{u(t_{j+1}, x_i) - u(t_j, x_i)}{k} \approx \frac{a_{i+1}\frac{\partial}{\partial x}u(t_j, x_{i+1}) - a_{i-1}\frac{\partial}{\partial x}u(t_j, x_{i-1})}{-2h} + M_i^j. \tag{5.52}$$

  Note that

$$a_{i-1} = a_1 = a(x_1) = a(-1) = 0. \tag{5.53}$$

  Then we get from equation (5.52)

$$\begin{aligned}&\frac{u(t_{j+1}, x_i) - u(t_j, x_i)}{k} \approx \frac{-1}{2h}\left[a_{i+1}\left(\frac{u(t_j, x_{i+2}) - u(t_j, x_i)}{2h}\right)\right] + M_i^j \\ &\Rightarrow \frac{U_i^{j+1} - U_i^j}{k} = \frac{1}{-2h}\left[a_{i+1}\left(\frac{U_{i+2}^j - U_i^j}{2h}\right)\right] + M_i^j \\ &\Leftrightarrow \left(\frac{a_{i+1}}{-4h^2} - \frac{1}{k}\right)U_i^j + \frac{a_{i+1}}{4h^2}U_{i+2}^j = \frac{1}{-k}U_i^{j+1} + M_i^j.\end{aligned} \tag{5.54}$$

- **For** $3 \leq i \leq n_x - 2$

  Now we consider

$$\frac{u(t_{j+1}, x_i) - u(t_j, x_i)}{k} \approx \frac{a(x_{i+\frac{1}{2}})\frac{\partial u}{\partial x}(t_j, x_{i+\frac{1}{2}}) - a(x_{i-\frac{1}{2}})\frac{\partial u}{\partial x}(t_j, x_{i-\frac{1}{2}})}{-h} + M_i^j, \quad (5.55)$$

  where $x_{i+\frac{1}{2}} = x_i + \frac{h}{2}$ and $x_{1-\frac{1}{2}} = x_i - \frac{h}{2}$. Which leads to

$$\begin{aligned}\frac{u(t_{j+1}, x_i) - u(t_j, x_i)}{k} \approx & \frac{-1}{h}\left[a(x_{i+\frac{1}{2}})\frac{u(t_j, x_{i+1}) - u(t_j, x_i)}{h}\right. \\ & \left. -a(x_{i-\frac{1}{2}})\frac{u(t_j, x_i) - u(t_j, x_{i-1})}{h}\right] + M_i^j. \quad (5.56)\end{aligned}$$

  By employing the natural notations $a_{i+\frac{1}{2}} = a(x_{i+\frac{1}{2}})$, $a_{i-\frac{1}{2}} = a(x_{i-\frac{1}{2}})$, we arrive at

$$\frac{U_i^{j+1} - U_i^j}{k} = \frac{-1}{h^2}\left[a_{i+\frac{1}{2}}(U_{i+1}^j - U_i^j) - a_{i-\frac{1}{2}}(U_i^j - U_{i-1}^j)\right] + M_i^j \quad (5.57)$$

$$\Leftrightarrow \frac{a_{i-\frac{1}{2}}}{h^2}U_{i-1}^j - \left(\frac{1}{k} + \frac{1}{h^2}(a_{i+\frac{1}{2}} + a_{i-\frac{1}{2}})\right)U_i^j + \frac{a_{i+\frac{1}{2}}}{h^2}U_{i+1}^j = \frac{-1}{k}U_i^{j+1} + M_i^j. \quad (5.58)$$

- **For** $i = n_x - 1$

  This is analogous to the case $i = 2$

$$\frac{u(t_{j+1}, x_i) - u(t_j, x_i)}{k} \approx \frac{a_{i+1}\frac{\partial}{\partial x}u(t_j, x_{i+1}) - a_{i-1}\frac{\partial}{\partial x}u(t_j, x_{i-1})}{-2h} + M_i^j \quad (5.59)$$

  Note that here

$$a_{i+1} = a_{n_x} = a(x_{n_x}) = a(1) = 0. \quad (5.60)$$

  Therefore we get from (5.59)

$$\frac{u(t_{j+1}, x_i) - u(t_j, x_i)}{k} \approx \frac{1}{2h}\left[a_{i-1}\frac{u(t_j, x_i) - u(t_j, x_{i-2})}{2h}\right] + M_i^j, \quad (5.61)$$

$$\Rightarrow \frac{U_i^{j+1} - U_i^j}{k} = \frac{a_{i-1}}{4h^2}(U_i^j - U_{i-2}^j) + M_i^j, \quad (5.62)$$

$$\Leftrightarrow \left(\frac{a_{i-1}}{-4h^2} - \frac{1}{k}\right)U_i^j + \frac{a_{i-1}}{4h^2}U_{i-2}^j = \frac{1}{-k}U_i^{j+1} + M_i^j. \quad (5.63)$$

- **For** $i = n_x$

  This is analogous to the case $i = 1$,

$$\frac{u(t_{j+1}, x_i) - u(t_j, x_i)}{k} \approx \frac{a_{i-2}\frac{\partial}{\partial x}u(t_j, x_{i-2}) - 4a_{i-1}\frac{\partial}{\partial x}u(t_j, x_{i-1}) + 3a_i\frac{\partial}{\partial x}u(t_j, x_i)}{-2h} + M_i^j. \tag{5.64}$$

  Note that here

$$a_i = a_{n_x} = a(x_{n_x}) = a(1) = 0. \tag{5.65}$$

  So we get from (5.64)

$$\frac{u(t_{j+1}, x_i) - u(t_j, x_i)}{k} \approx \frac{-1}{2h}\left[a_{i-2}\frac{u(t_j, x_{i-1}) - u(t_j, x_{i-3})}{2h} - 4a_{i-1}\frac{u(t_j, x_i) - u(t_j, x_{i-2})}{2h}\right] + M_i^j. \tag{5.66}$$

$$\Rightarrow \frac{U_i^{j+1} - U_i^j}{k} = \frac{-a_{i-2}}{4h^2}(U_{i-1}^j - U_{i-3}^j) + \frac{a_{i-1}}{h^2}(U_i^j - U_{i-2}^j) + M_i^j, \tag{5.67}$$

$$\Leftrightarrow \left(\frac{a_{i-1}}{-h^2} - \frac{1}{k}\right)U_i^j = \frac{a_{i-2}}{-4h^2}\left(U_{i-1}^j - U_{i-3}^j\right) - \frac{a_{i-1}}{h^2}U_{i-2}^j - \frac{1}{k}U_i^{j+1} + M_i^j. \tag{5.68}$$

Equation (5.41), together with (5.43) is a final value problem, so we know the value of U_i^j when $j = n_t$. Now we will find the value of U_i^j when $j = n_t - 1$ (at $t = T - k$).

When $j = n_t - 1$ then we get from (5.54), (5.58) and (5.63) the following system of equations:

1. **For** $i = 2$

$$\left(\frac{a_{i+1}}{-4h^2} - \frac{1}{k}\right)U_i^{n_t-1} + \frac{a_{i+1}}{4h^2}U_{i+2}^{n_t-1} = \frac{1}{-k}U_i^{n_t} + M_i^{n_t-1}, \tag{5.69}$$

2. **For** $3 \le i \le n_x - 2$

$$\frac{a_{i-\frac{1}{2}}}{h^2}U_{i-1}^{n_t-1} - \left(\frac{1}{k} + \frac{1}{h^2}(a_{i+\frac{1}{2}} + a_{i-\frac{1}{2}})\right)U_i^{n_t-1} + \frac{a_{i+\frac{1}{2}}}{h^2}U_{i+1}^{n_t-1} = \frac{-1}{k}U_i^{n_t} + M_i^{n_t-1}, \tag{5.70}$$

   and

3. **For** $i = n_x - 1$

$$\frac{a_{i-1}}{4h^2}U_{i-2}^{n_t-1} - \left(\frac{a_{i-1}}{4h^2} + \frac{1}{k}\right)U_i^{n_t-1} = \frac{1}{-k}U_i^{n_t} + M_i^{n_t-1} \tag{5.71}$$

accordingly.
We see from (5.69), (5.70) and (5.71) that the number of equations is $n_x - 2$. We know the value of $U_i^{n_t}$, for every $i = 1, 2, ..., n_x$ and the value of M_i^j for every $i = 1, 2, ..., n_x$, $j = 1, 2, ..., n_t$. Therefore the right hand sides of the three equations (5.69), (5.70) and (5.71) are known and the number of unknowns is $n_x - 2$ also. So we can write equations (5.69), (5.70) and (5.71) in a square matrix form easily:

$$\begin{bmatrix} \frac{-a_3}{4h^2} - \frac{1}{k} & 0 & \frac{a_3}{4h^2} & \cdots & 0 & 0 & 0 & 0 \\ \frac{a_{3-\frac{1}{2}}}{h^2} & -\left(\frac{1}{k} + \frac{1}{h^2}(a_{3+\frac{1}{2}} + a_{3-\frac{1}{2}})\right) & \frac{a_{3+\frac{1}{2}}}{h^2} & \cdots & 0 & 0 & 0 & 0 \\ \vdots & \vdots & \vdots & \cdots & \vdots & \frac{a_{(n_x-2)-\frac{1}{2}}}{h^2} & -\left(\frac{1}{k} + \frac{1}{h^2}(a_{(n_x-2)+\frac{1}{2}} + a_{(n_x-2)-\frac{1}{2}})\right) & \frac{a_{(n_x-2)+\frac{1}{2}}}{h^2} \\ 0 & 0 & 0 & \cdots & 0 & \frac{a_{n_x-2}}{4h^2} & 0 & -\left(\frac{a_{n_x-2}}{4h^2} + \frac{1}{k}\right) \end{bmatrix}$$

$$\times \begin{bmatrix} U_2^{n_t-1} \\ U_3^{n_t-1} \\ \vdots \\ U_{n_x-2}^{n_t-1} \\ U_{n_x-1}^{n_t-1} \end{bmatrix} = \begin{bmatrix} \frac{-1}{k}U_2^{n_t} + M_2^{n_t-1} \\ \frac{-1}{k}U_3^{n_t} + M_3^{n_t-1} \\ \vdots \\ \frac{-1}{k}U_{n_x-2}^{n_t} + M_{n_x-2}^{n_t-1} \\ \frac{-1}{k}U_{n_x-1}^{n_t} + M_{n_x-1}^{n_t-1}. \end{bmatrix} \tag{5.72}$$

We solve the equation (5.72) and find

$$U_2^{n_t-1}, U_3^{n_t-1}, ..., U_{n_x-2}^{n_t-1} \text{ and } U_{n_x-1}^{n_t-1}. \tag{5.73}$$

Again we get from (5.51) and (5.68) when $j = n_t - 1$

1. **For** $i = 1$

$$\left(\frac{a_2}{-h^2} - \frac{1}{k}\right)U_1^{n_t-1} = \frac{a_2}{-h^2}U_3^{n_t-1} + \frac{a_3}{4h^2}\left(U_4^{n_t-1} - U_2^{n_t-1}\right) - \frac{1}{k}U_1^{n_t} + M_1^{n_t-1}, \tag{5.74}$$

and

2. **For** $i = n_x$

$$\left(\frac{a_{n_x-1}}{-h^2} - \frac{1}{k}\right)U_{n_x}^{n_t-1} = \frac{a_{n_x-2}}{-4h^2}\left(U_{n_x-1}^{n_t-1} - U_{n_x-3}^{n_t-1}\right) - \frac{a_{n_x-1}}{h^2}U_{n_x-2}^{n_t-1} - \frac{1}{k}U_{n_x}^{n_t} + M_{n_x}^{n_t-1} \tag{5.75}$$

accordingly.

From (5.74) and (5.75) we can find $U_1^{n_t-1}$ and $U_{n_x}^{n_t-1}$ respectively by using (5.73). Similarly we can find the value of U_i^j for all i and for $j = n_t - 2, n_t - 3, .., 2, 1$.

Matlab code

We have made a MATLAB code to solve the equation (5.41) with the final value condition (5.43) that means to solve (5.72), (5.74) and (5.75). The code is made of 4 m-files. The name of those m-files are benchmark, Exact2, FM2 and data.

1. In the benchmark m-file exact and approximate solutions are compared.

2. In the data m-file we give the input data for the program. Here we use the following notations:

   (a) We use enx for the number of nodes in $[x1, x2]$. Where $x1$ is the lower limit and $x2$ is the upper limit of the range of x which is used in (5.41).

   (b) We use ent where ent-1 is the number of time steps covering $[t1, t2]$. Where $t1$ is the lower limit and $t2$ is the upper limit of the range of t use in (5.41)

3. In Exact2 we put the exact solution $u(t, x)$ for testing our Matlab code.

4. In FM2 we put function $M(t, x)$. For exact test function $M(t, x)$ is computed with (5.41) for a given $u(t, x)$.

Numerical results

We test our Matlab code for three exact tests. Let $u(t, x)$ be a given function and put this $u(t, x)$ in (5.41) in order to find the function $M(t, x)$. By using $M(t, x)$ we can find an approximate value of

$$u(t_j, x_i), \text{ where } i = 1, 2, ..., n_x \text{ and } j = 1, 2, ..., n_t - 1.$$

by using our Matlab code. Also we can find the exact value of $u(x_i, t_j)$ directly. We compare those two values of $u(t_j, x_i)$ and give the difference of the two values which is the error. We compute the error by means of the infinite norm over the grid (t_j, x_i).

1. We take $u(t, x) = \sin(t^2 + x^3)$ then we get by using (5.41)

$$M(t, x) = 2(t + 3x - 6x^3)\cos(t^2 + x^3) - 9x^4(1 - x^2)\sin(t^2 + x^3). \tag{5.76}$$

   Now we use this $u(t, x)$ and $M(t, x)$ in our Matlab code and find the error which we show in the table (5.1).

n_x	n_t	Error	Time
11	11	0.2180	0.04 sec.
31	101	0.0426	0.08 sec.
91	1001	0.0037	1.64 sec.
271	10001	2.8624e-004	184 sec.

Table 5.1

n_x	n_t	Error	Time
11	11	0.2634	0.03 sec.
31	101	0.0244	0.08 sec.
91	1001	0.0022	1.56 sec.
271	10001	2.0290e-004	177 sec.

Table 5.2

Numerical results show that

$$\text{error} \approx O(\Delta t) + O((\Delta x)^2), \tag{5.77}$$

as expected. In here we see that if we reduce ten times the value of Δt and ten times the value of $(\Delta x)^2$ then the error will reduce approximate ten times. But for reducing ten times the value of $(\Delta x)^2$ need to increase three times of n_x approximately. Which we represent in the following table 5.1. We see in the table $n_x = 11, 31, 91, 271$ because $\Delta x = h = \frac{x_2 - x_1}{n_x - 1}$ and also we use $n_t = 11, 101, 1001, 10001$ because $\Delta t = k = \frac{t2 - t1}{n_t - 1}$.

2. We take $u(t, x) = t^2 + x^3$ then we get by using (5.41)

$$M(t, x) = 2t + 6x + 12x^3. \tag{5.78}$$

Now we use this $u(t, x)$ and $M(t, x)$ in our Matlab code and find the error which we show in the table (5.2).

3. We take $u(t, x) = \sin(x^2)$ then we get by using (5.41)

$$M(t, x) = 4x^2(x^2 - 1)\sin(x^2) + 2(1 - 3x^2)\cos(x^2). \tag{5.79}$$

Now we use this $u(t, x)$ and $M(t, x)$ in our Matlab code and find the error which we

n_x	n_t	Error	Time
11	11	0.1162	0.05 sec.
31	101	0.0152	0.08 sec.
91	1001	0.0011	1.53 sec.
271	10001	8.4993e-005	177 sec.

Table 5.3

show in the table (5.3).

Conclusions and future work

5.3 Conclusions

We have solved the Boltzmann transport equation (BTE) for photons and successfully find the values of $\psi_\gamma^{(0)}$, $\psi_\gamma^{(1)}$, $\psi_\gamma^{(2)}$ and $\psi_\gamma^{(3)}$. We have seen that the value of $\psi_\gamma^{(3)}$ is very small comparatively with $\psi_\gamma = \psi_\gamma^{(0)} + \psi_\gamma^{(1)} + \psi_\gamma^{(2)}$ but the computation time of $\psi_\gamma^{(3)}$ is very high. The value of $\psi_\gamma^{(i)}$ when $i \geq 4$ is even smaller than $\psi_\gamma^{(3)}$ and the computing time is extremely large. So, for total number of photons we use simply $\psi_\gamma = \psi_\gamma^{(0)} + \psi_\gamma^{(1)} + \psi_\gamma^{(2)}$ instead of $\psi_\gamma = \sum_{i=0}^{N} \psi_\gamma^{(i)}$.
We cannot solve the BTE for electrons by the same process which we use to solve the BTE for photons due to the smaller mean free path of electron than the mean free path of photon. An alternative is to solve instead the Fokker-Planck equation, which is an approximation of the BTE based on the fact that scattering of electrons is very forward-peaked. To solve this equation we are looking a proper finite difference scheme. For this reason we have solved a degenerate parabolic partial differential equation, built of some selected differential operators appearing in the Fokker-Planck equation, with an appropriate numerical scheme, and the results have been shown in this memory.

5.4 Future work

We have found good approximations of $\psi_\gamma^{(0)}$ and $\psi_\gamma^{(1)}$ but due to the limitations of my computer we could not check very well the value of $\psi_\gamma^{(2)}$, because my computer takes many time to calculate $\psi_\gamma^{(2)}$. Since $\psi_\gamma^{(1)}$ is well calculated so we think $\psi_\gamma^{(2)}$ is more or less good, because $\psi_\gamma^{(2)}$ depends on $\psi_\gamma^{(1)}$ for each integrating node. In any case, we think that it would be good to check whether the value of ψ^2 has been computed till convergence or not, by using a more powerful computer.

In our program we have used a cubic domain. We will work on our program in order to adapt it to more complex domains.

Another point to be developed is the quadrature formulas. We have used the composite trapezoidal quadrature formula for integration in our program, but perhaps other formulas could give better results. For instance, we can think of adaptive formulas or on formulas especially designed for integrating on the sphere, like the Lebedev formulas. The objective would be always the same: to reduce computing time.

In our memory we show the numerical scheme of a degenerate parabolic partial differential equation which is near to the Fokker-Planck equation. In the future we want to calculate some other PDE which are more near than the degenerate parabolic partial differential equation and then we will solve the Fokker-Planck equation to find the number of electrons which is needed for the dose calculation of cancer treatment. In fact, in order to obtain an accurate dose it is probably needed a better approximation than plain Fokker-Planck.

Appendix A

5.4.1 Differential cross section for Compton scattering of photons

Literature: [7].

$$\tilde{\sigma}_{\mathsf{C},\gamma}(\epsilon'_\gamma, \epsilon_\gamma, \boldsymbol{\Omega'}_\gamma \cdot \boldsymbol{\Omega}_\gamma) = \sigma_{\mathsf{C},\gamma}(\epsilon'_\gamma, \boldsymbol{\Omega'}_\gamma \cdot \boldsymbol{\Omega}_\gamma)\delta_{\mathsf{C},\gamma}(\epsilon'_\gamma, \epsilon_\gamma) \tag{5.1}$$

with

$$\sigma_{\mathsf{C},\gamma}(\epsilon'_\gamma, \boldsymbol{\Omega'}_\gamma \cdot \boldsymbol{\Omega}_\gamma) = \frac{r_\mathsf{e}^2}{2}\left[\frac{1}{1+\epsilon'_\gamma(1-\cos\vartheta_\gamma)}\right]^3\left[1+\cos^2\vartheta_\gamma + \frac{\epsilon'^2_\gamma(1-\cos\vartheta\gamma)^2}{1+\epsilon'_\gamma(1-\cos\vartheta_\gamma)}\right] \tag{5.2}$$

and

$$\delta_{\mathsf{C},\gamma}(\epsilon'_\gamma, \epsilon_\gamma) := \delta\left(\epsilon_\gamma - \frac{\epsilon'_\gamma}{1+\epsilon'_\gamma(1-\cos\vartheta_\gamma)}\right). \tag{5.3}$$

5.4.2 Total cross section for Compton scattering of photons

Literature: [7].

$$\sigma^{\mathsf{tot}}_{\mathsf{C},\gamma}(\epsilon_\gamma) = 2\pi r_\mathsf{e}^2\left[\frac{1+\epsilon_\gamma}{\epsilon_\gamma^2}\left(\frac{2(1+\epsilon_\gamma)}{1+2\epsilon_\gamma} - \frac{1}{\epsilon_\gamma}\mathsf{ln}(1+2\epsilon_\gamma)\right) + \frac{1}{2\epsilon_\gamma}\mathsf{ln}(1+2\epsilon_\gamma) - \frac{1+3\epsilon_\gamma}{(1+2\epsilon_\gamma)^2}\right]. \tag{5.4}$$

5.4.3 Differential cross section for Compton scattering of electrons

$$\tilde{\sigma}_{\mathsf{C},\mathsf{e}}(\epsilon'_\gamma, \epsilon_\mathsf{e}, \boldsymbol{\Omega'_\mathsf{e}} \cdot \boldsymbol{\Omega}_\mathsf{e}) = \sigma_{\mathsf{C},\mathsf{e}}(\epsilon'_\gamma, \boldsymbol{\Omega'}_\gamma \cdot \boldsymbol{\Omega}_\mathsf{e})\delta_{\mathsf{C},\mathsf{e}}(\epsilon'_\gamma, \epsilon_\mathsf{e}) \tag{5.5}$$

with

$$\sigma_{\mathsf{C,e}}(\epsilon'_\gamma, \mathbf{\Omega}'_\mathsf{e} \cdot \mathbf{\Omega}_\mathsf{e}) = \frac{4r_\mathsf{e}^2(1+\epsilon'_\gamma)^2}{\cos^3\vartheta_\mathsf{e}} \frac{1}{(a(\epsilon'_\gamma,\vartheta_\mathsf{e})+2\epsilon'_\gamma)^2} \tag{5.6}$$

$$\times \left[1 - \frac{2}{a(\epsilon'_\gamma,\vartheta_\mathsf{e})} + \frac{2}{a^2(\epsilon'_\gamma,\vartheta_\mathsf{e})} + \frac{2\epsilon_\gamma^2}{a(\epsilon'_\gamma,\vartheta_\mathsf{e})(a(\epsilon'_\gamma,\vartheta_\mathsf{e})+2\epsilon'_\gamma)}\right] \tag{5.7}$$

$$\delta_{\mathsf{C,e}}(\epsilon'_\gamma, \epsilon_\gamma) := \delta\left(\epsilon_\mathsf{e} - \frac{2\epsilon_\gamma'^2}{2\epsilon'_\gamma + a(\epsilon'_\gamma,\vartheta_\mathsf{e})}\right) \tag{5.8}$$

where

$$a(\epsilon'_\gamma, \vartheta_\mathsf{e}) := (1+\epsilon'_\gamma)^2 \tan^2\vartheta_\mathsf{e} + 1. \tag{5.9}$$

5.4.4 Differential cross section for Møller scattering of primary electrons, i.e., $\epsilon_\mathsf{e} > (\epsilon'_\mathsf{e} - \epsilon_\mathsf{B})/2$

Literature:[20] and [25].

$$\tilde{\sigma}_\mathsf{M}(\epsilon'_\mathsf{e}, \epsilon_\mathsf{e}, \mathbf{\Omega}'_\mathsf{e} \cdot \mathbf{\Omega}_\mathsf{e}) = \sigma_\mathsf{M}(\epsilon'_\mathsf{e}, \epsilon_\mathsf{e}) \delta_\mathsf{M}(\mu_\mathsf{e}, \mu_p) \frac{1}{2\pi}, \quad \mu_\mathsf{e} = \mathbf{\Omega}'_\mathsf{e} \cdot \mathbf{\Omega}_\mathsf{e} \tag{5.10}$$

with

$$\sigma_\mathsf{M}(\epsilon'_\mathsf{e}, \epsilon_\mathsf{e}) = \frac{2\pi r_\mathsf{e}^2(\epsilon'_\mathsf{e}+1)^2}{\epsilon'_\mathsf{e}(\epsilon'_\mathsf{e}+2)} \left[\frac{1}{\epsilon_\mathsf{e}^2} + \frac{1}{(\epsilon'_\mathsf{e}-\epsilon_\mathsf{e})^2} + \frac{1}{(\epsilon'_\mathsf{e}+1)^2} - \frac{2\epsilon'_\mathsf{e}+1}{(\epsilon'_\mathsf{e}+1)^2\epsilon_\mathsf{e}(\epsilon'_\mathsf{e}-\epsilon_\mathsf{e})}\right] \tag{5.11}$$

$$\delta_{\mathsf{M},\delta}(\mu_\mathsf{e}, \mu_\delta) = \delta\left(\mu_\mathsf{e} - \sqrt{\frac{\epsilon_\mathsf{e}}{\epsilon'_\mathsf{e}} \frac{\epsilon'_\mathsf{e}+2}{\epsilon_\mathsf{e}+2}}\right), \ \epsilon_\mathsf{e} > (\epsilon'_\mathsf{e} - \epsilon_\mathsf{B})/2. \tag{5.12}$$

5.4.5 Differential cross section for Møller scattering of secondary electrons, i.e., $\epsilon_\mathsf{e} < (\epsilon'_\mathsf{e} - \epsilon_\mathsf{B})/2$

Literature:[20] and [25].

$$\tilde{\sigma}_{\mathsf{M},\delta}(\epsilon'_\mathsf{e}, \epsilon_\mathsf{e}, \mathbf{\Omega}'_\mathsf{e} \cdot \mathbf{\Omega}_\mathsf{e}) = \sigma_\mathsf{M}(\epsilon'_\mathsf{e}, \epsilon_\mathsf{e}) \delta_{\mathsf{M},\delta}(\mu_\mathsf{e}, \mu_\delta) \frac{1}{2\pi}, \quad \mu_\mathsf{e} = \mathbf{\Omega}'_\mathsf{e} \cdot \mathbf{\Omega}_\mathsf{e} \tag{5.13}$$

with

$$\sigma_\mathsf{M}(\epsilon'_\mathsf{e}, \epsilon_\mathsf{e}) = \frac{2\pi r_\mathsf{e}^2(\epsilon'_\mathsf{e}+1)^2}{\epsilon'_\mathsf{e}(\epsilon'_\mathsf{e}+2)} \left[\frac{1}{\epsilon_\mathsf{e}^2} + \frac{1}{(\epsilon'_\mathsf{e}-\epsilon_\mathsf{e})^2} + \frac{1}{(\epsilon'_\mathsf{e}+1)^2} - \frac{2\epsilon'_\mathsf{e}+1}{(\epsilon'_\mathsf{e}+1)^2\epsilon_\mathsf{e}(\epsilon'_\mathsf{e}-\epsilon_\mathsf{e})}\right] \tag{5.14}$$

$$\delta_{\mathsf{M},\delta}(\mu_\mathsf{e},\mu_\delta)=\delta\left(\mu_\mathsf{e}-\sqrt{\frac{\epsilon_\mathsf{e}}{\epsilon'_\mathsf{e}}\frac{\epsilon'_\mathsf{e}+2}{\epsilon_\mathsf{e}+2}}\right),\ \epsilon_\mathsf{e}<(\epsilon'_\mathsf{e}-\epsilon_\mathsf{B})/2. \tag{5.15}$$

5.4.6 Total cross section for Møller scattering of electrons

Calculation based on [20] and [25]

$$\sigma^{\mathsf{tot}}_{\mathsf{M}}(\epsilon_\mathsf{e})=\int_{\epsilon_\mathsf{B}}^{(\epsilon_\mathsf{e}-\epsilon_\mathsf{B})/2}\sigma_{\mathsf{M}}(\epsilon_\mathsf{e},\epsilon'_\mathsf{e})\ \mathrm{d}\epsilon'_\mathsf{e}. \tag{5.16}$$

The lower limit of integration is due to the fact that the primary electron can only be scattered if at lest the binding energy ϵ_B is transferred to the secondary electron (of a tissue molecule). Besides the evident motivation of this choice based on our model, this is a standard way to avoid singularities in calculating total cross section (see e.g. [35], section 5.1). The upper limit of integration is due to the fact that the primary electron has larger energy than the secondary electron and that the binding energy ϵ_B was introduced into the scattering processes (usually the upper limit is $\epsilon'_\mathsf{e}/2$). One gets

$$\begin{aligned}\sigma^{\mathsf{tot}}_{\mathsf{M}}(\epsilon_\mathsf{e})=&\frac{2\pi r_\mathsf{e}^2(\epsilon_\mathsf{e}+1)^2}{\epsilon_\mathsf{e}(\epsilon_\mathsf{e}+2)}\left\{\frac{1}{\epsilon_\mathsf{B}}-\frac{3}{\epsilon_\mathsf{e}-\epsilon_\mathsf{B}}+\frac{2}{\epsilon_\mathsf{e}+\epsilon_\mathsf{B}}+\frac{\epsilon_\mathsf{e}-3\epsilon_\mathsf{B}}{2(\epsilon_\mathsf{e}+1)^2}+\frac{2\epsilon_\mathsf{e}+1}{\epsilon_\mathsf{e}(\epsilon_\mathsf{e}+1)}\right.\\&\left.\times\left[\ln\frac{\epsilon_\mathsf{e}+\epsilon_\mathsf{B}}{\epsilon_\mathsf{e}-\epsilon_\mathsf{B}}-\ln\frac{\epsilon_\mathsf{e}-\epsilon_\mathsf{B}}{\epsilon_\mathsf{B}}\right]\right\}.\end{aligned} \tag{5.17}$$

5.4.7 Differential cross section for Mott scattering of electrons

Literature: [24] and [22].

$\alpha\approx 1/137$ is the fine structure constant, Z is the atomic number of the irradiate medium. Z depends on $\mathbf{r}$ to account for heterogeneous media.

$$\begin{aligned}\sigma_{\mathsf{Mott}}(\mathbf{r},\epsilon_\mathsf{e},\mathbf{\Omega}'_\mathsf{e}\cdot\mathbf{\Omega}_\mathsf{e})=&\frac{Z^2(\mathbf{r})r_\mathsf{e}^2(mc^2)^2}{4p^2c^2\beta^2\sin^4(\frac{\vartheta_\mathsf{e}}{2})}\left[1-\beta^2\sin^2\frac{\vartheta_\mathsf{e}}{2}+Z\pi\alpha\beta\sin\frac{\vartheta_\mathsf{e}}{2}(1-\sin\frac{\vartheta_\mathsf{e}}{2})\right]\\\approx&\frac{Z^2(\mathbf{r})r_\mathsf{e}^2(mc^2)^2}{4p^2c^2\beta^2\sin^4\frac{\vartheta_\mathsf{e}}{2}}\left[1-\beta^2\sin^2\frac{\vartheta_\mathsf{e}}{2}\right],\end{aligned} \tag{5.18}$$

with $\beta^2=\frac{\epsilon_\mathsf{e}(\epsilon+2)}{(\epsilon+1)^2}$. The last approximation is justified, because in the energy range studied here and for typical low-Z media like water only small errors are made.

To avoid the singularity at $\vartheta_\mathsf{e}=0$ a screening parameter η can be introduced (see [36]) that models the screening effect of the electron and the atomic shell:

$$\sigma_{\mathsf{Mott}}(\mathbf{r},\epsilon_\mathsf{e},\mathbf{\Omega}'_\mathsf{e}\cdot\mathbf{\Omega}_\mathsf{e})=\frac{Z^2(\mathbf{r})r_\mathsf{e}^2(1+\epsilon_\mathsf{e})^2}{4[\epsilon_\mathsf{e}(\epsilon_\mathsf{e}+2)]^2(1+2\eta(\mathbf{r},\epsilon_\mathsf{e})-\cos\vartheta_\mathsf{e})^2}\left[1-\frac{\epsilon_\mathsf{e}(\epsilon_\mathsf{e}+2)}{(1+\epsilon_\mathsf{e})^2}\sin^2\frac{\vartheta_\mathsf{e}}{2}\right], \tag{5.19}$$

where

$$\eta(\mathbf{r}, \epsilon_{\mathsf{e}}) = \frac{\pi^2 \alpha^2 Z^{\frac{2}{3}}(r)}{\epsilon_{\mathsf{e}}(\epsilon_{\mathsf{e}} + 2)}. \tag{5.20}$$

5.4.8 Total cross section for Mott scattering of electrons

$$\begin{aligned}\sigma^{\mathsf{tot}}_{\mathsf{Mott}}(\mathbf{r}, \epsilon_{\mathsf{e}}) = &\frac{\pi (Z(r) r_{\mathsf{e}})^2}{\epsilon_{\mathsf{e}}(\epsilon_{\mathsf{e}} + 2)} \left[\frac{(\epsilon_{\mathsf{e}} + 1)^2}{(\pi\alpha)^2 Z^{\frac{2}{3}}(r)(1 + \eta(\mathbf{r}, \epsilon_{\mathsf{e}}))} + \frac{1}{1 + \eta(\mathbf{r}, \epsilon_{\mathsf{e}})} \right. \\ &\left. + \ln \eta(\mathbf{r}, \epsilon_{\mathsf{e}}) - \ln(1 + \eta(\mathbf{r}, \epsilon_{\mathsf{e}})) \right]. \end{aligned} \tag{5.21}$$

Appendix B

The coefficients are defined according to [27].

5.4.9 The Møller coefficient T_{M}

Since the secondary (outgoing) electron has the lower energy ($\epsilon'_{\mathsf{e}} < \frac{\epsilon-\epsilon_{\mathsf{B}}}{2}$), energy is restricted to $[\epsilon_{\mathsf{B}}, \frac{\epsilon_{\mathsf{e}}-\epsilon_{\mathsf{B}}}{2}]$:

$$T_{\mathsf{M}}(\mathbf{r}, \epsilon_{\mathsf{e}}) = \pi\rho_{\mathsf{e}}(\mathbf{r}) \int_{\epsilon_{\mathsf{B}}}^{(\epsilon_{\mathsf{e}}-\epsilon_{\mathsf{B}})/2} \int_{-1}^{1} (1-\mu)\tilde{\sigma}_{\mathsf{M}}(\epsilon_{\mathsf{e}}, \epsilon'_{\mathsf{e}}, \mu) d\mu\, d\epsilon'_{\mathsf{e}}. \tag{5.22}$$

Using the definition (see equations 5.10, 5.11 and 5.12) of the Møller scattering cross section one gets

$$T_{\mathsf{M}}(\mathbf{r}, \epsilon_{\mathsf{e}}) = \frac{\rho_{\mathsf{e}}(\mathbf{r})}{2} \int_{\epsilon_{\mathsf{B}}}^{(\epsilon_{\mathsf{e}}-\epsilon_{\mathsf{B}})/2} \left(1 - \sqrt{\frac{\epsilon_{\mathsf{e}} - \epsilon'_{\mathsf{e}}}{\epsilon_{\mathsf{e}}} \frac{\epsilon_{\mathsf{e}}+2}{\epsilon_{\mathsf{e}}-\epsilon'_{\mathsf{e}}+2}}\right) \sigma_{\mathsf{M}}(\epsilon_{\mathsf{e}}, \epsilon'_{\mathsf{e}}) d\epsilon'_{\mathsf{e}}. \tag{5.23}$$

This integral can in principle be calculated analytically.

5.4.10 The Mott coefficient T_{Mott}

$$T_{\mathsf{Mott}}(\mathbf{r}, \epsilon_{\mathsf{e}}) = \pi\rho_{\mathsf{c}}(\mathbf{r}) \int_{-1}^{1} (1-\mu)\sigma_{\mathsf{Mott}}(\epsilon_{\mathsf{e}}, \mu) d\mu. \tag{5.24}$$

The angular integration can be done analytically and one gets

$$T_{\mathsf{Mott}}(\mathbf{r}, \epsilon_{\mathsf{e}}) = -\frac{\pi Z^2(\mathbf{r}) r_{\mathsf{e}}^2 \rho_{\mathsf{c}}(\mathbf{r})(\epsilon_{\mathsf{e}}+1)^2}{{\epsilon_{\mathsf{e}}}^2(\epsilon_{\mathsf{e}}+2)^2(1+\eta)} \tag{5.25}$$

$$\times \{1 + \beta^2(1+2\eta) + (1+\eta)(1+2\beta^2\eta)[\ln 2\eta - \ln(2+2\eta)]\}, \tag{5.26}$$

with $\beta^2 = \frac{\epsilon_{\mathsf{e}}(\epsilon_{\mathsf{e}}+2)}{(\epsilon_{\mathsf{e}}+1)^2}$ and $\eta = \eta(\mathbf{r}, \epsilon_{\mathsf{e}})$ as defined in equation (5.20).

5.4.11 The Møller stopping power S_{M}

Instead of using the definition of Pomraning (1992) it is convenient to use the standard definition of the stopping power:

$$S_{\mathsf{M}}(\mathbf{r},\epsilon_{\mathsf{e}}) = \rho_{\mathsf{e}}(\mathbf{r}) \int_{\epsilon_{\mathsf{B}}}^{(\epsilon_{\mathsf{e}}-\epsilon_{\mathsf{B}})/2} \epsilon'_{\mathsf{e}} \sigma_{\mathsf{M}}(\epsilon_{\mathsf{e}},\epsilon'_{\mathsf{e}})\,\mathrm{d}\epsilon'_{\mathsf{e}}. \tag{5.27}$$

Of course both definitions are equivalent.

This integral can be evaluated analytically, too, and one gets

$$\begin{aligned} S_{\mathsf{M}}(\mathbf{r},\epsilon_{\mathsf{e}}) =& \frac{2\pi r_{\mathsf{e}}^2 \rho_{\mathsf{e}}(\mathbf{r})(\epsilon_{\mathsf{e}}+1)^2}{\epsilon_{\mathsf{e}}(\epsilon_{\mathsf{e}}+2)} \left[\frac{2\epsilon_{\mathsf{e}}}{\epsilon_{\mathsf{e}}-\epsilon_{\mathsf{B}}} + 2\ln\frac{\epsilon_{\mathsf{e}}-\epsilon_{\mathsf{B}}}{2} - \ln\epsilon_{\mathsf{B}} - \frac{\epsilon_{\mathsf{e}}}{\epsilon_{\mathsf{e}}-\epsilon_{\mathsf{B}}} - \ln(\epsilon_{\mathsf{e}}-\epsilon_{\mathsf{B}}) \right. \\ & \left. + \frac{1}{2(\epsilon_{\mathsf{e}}+1)^2} \left(\frac{(\epsilon_{\mathsf{e}}-\epsilon_{\mathsf{B}})^2}{4} - \epsilon_B^2 \right) + \frac{2\epsilon_{\mathsf{e}}+1}{(\epsilon_{\mathsf{e}}+1)^2} \left(\ln\frac{\epsilon_{\mathsf{e}}-\epsilon_B}{2} - \ln(\epsilon_{\mathsf{e}}-\epsilon_B) \right) \right]. \end{aligned} \tag{5.28}$$

Anexo. Resumen en castellano

El objetivo de este trabajo es resolver numéricamente la ecuación de transporte de Boltzmann para fotones, así como cierto tipo de ecuaciones parabólicas degeneradas que guardan relación con la ecuación de Fokker–Planck.

Desde el punto de vista de las aplicaciones, esta tesis puede enmarcarse dentro del campo del tratamiento de cáncer con radioterapia externa de fotones, porque nuestro punto de partida es el trabajo de Hensel, Iza–Teran y Siedow [15], en el que los autores proponen un modelo matemático para el cálculo de la dosis absorbida por el paciente que incluye ecuaciones del tipo que se estudian en nuestro trabajo.

En los capítulos 1 y 2 se hace un recorrido por los principios de la radiobiología y por los fenómenos de interacción de la radiación con la materia. Los capítulos 3 y 4 se dedican a describir el modelo matemático para el cálculo de la dosis absorbida y a la resolución numérica de la ecuación de transporte de Boltzmann para fotones. Finalmente, en el capítulo 5 se muestra un esquema numérico de diferencias finitas para resolver un problema de valor final, parabólico y degenerado, que proviene de seleccionar ciertos operadores diferenciales presentes en la ecuación de Fokker–Planck, y da evidencias numéricas del orden de convergencia de dicho esquema. La ecuación de Fokker–Planck es una aproximación de la ecuación de transporte de Boltzmann para electrones, ecuación más difícil de resolver que la de fotones.

Pasamos ahora a explicar con más detalle los contenidos de los diferentes capítulos.

Resumen del capítulo 1. Principios de la Radiobiología.

El capítulo 1 comienza con una breve perspectiva histórica del tratamiento de radioterapia, desde que Röntgen descubrió los rayos X en 1895, y continúa con una descripción de los diferentes tipos de radioterapia: teleterapia o radioterapia externa, braquiterapia o radioterapia interna y terapia sistémica de radioisótopos. Los modelos matemáticos que se estudian en esta tesis están pensados para la radioterapia externa de fotones. Después, se explican los

efectos biológicos de la radiación, es decir, el daño que la radiación produce en las células, tanto cancerígenas como sanas. Especial interés tiene el hecho de que las primeras sean más sensibles a la radiación que las segundas, lo que hace que el tratamiento por radioterapia sea utilizado con tanto éxito.

La radiación, cuando alcanza el cuerpo humano, puede dañar el material genético de las células, impidiendo que estas se reproduzcan o provocando alteraciones en el proceso de reproducción. Por lo tanto, la radiación puede ser usada para eliminar células cancerígenas, con el objetivo de hacer desaparecer tumores o, al menos, de reducirlos. Claro está que la radiación daña también las células normales o sanas, y por ese motivo el tratamiento por radioterapia está sujeto a rígidos protocolos y su éxito depende grandemente de la medida de precisión en la localización del tumor y en el cálculo de la dosis absorbida.

Cuando la radiación afecta a la célula, no lo hace siempre de forma directa, es decir, no siempre la radiación daña directamente las cadenas de ADN; otras veces, lo que sucede es que se rompen las moléculas de agua (aproximadamente el 80% de una célula es agua), liberando H y OH que pueden recombinarse para formar peróxido de hidrógeno (H_2O_2), que es tóxico y contribuye a la destrucción celular.

Como dijimos antes, las células cancerígenas son por regla general más sensibles a la radiación que las células sanas. Uno de lo motivos que hay detrás es que las células son más subceptibles de ser dañadas mientras se reproducen, y precisamente las células cancerígenas tienden a reproducirse muy rápidamente y fuera de control.

Resumen del capítulo 2. Interacción de la radiación con la materia.

El capítulo 2 tiene un perfil menos médico–biológico y más físico, pues recoge los principos básicos de la interacción entre materia y radiación. Nos centramos en las interacciones que nos interesan en este trabajo, que son aquellas que se dan entre la materia y los fotones y electrones. Cuando los fotones (luz) o las partículas subatómicas chocan con la materia, sufren diferentes procesos que modifican su trayectoria (es el *scattering*) y su energía. Las trayectorias acaban siendo tramos de líneas rectas que se quiebran por los eventos de *scattering*. Otros términos clave son el de sección eficaz (*cross section*), cantidad que mide la probabilidad de *scattering*, y el camino libre medio (*mean free path*), que mide la capacidad de penetración de la radiación en la materia antes de sufrir un evento de *scattering*. La comprensión de estos aspectos es necesaria para entender a su vez el significado de los diferentes

términos de las ecuaciones posteriores.

Las principales interacciones de los fotones con la materia son: el efecto fotoeléctrico, el *scattering* de Compton, el *scattering* de Thompson, el *scattering* de Rayleigh y la producción de pares. De todos estos mecanismos, el dominante en los rangos de energía de un acelerador lineal es el *scattering* de Compton.

Las principales interacciones de los electrones con la materia son: la ionización, el *scattering* de Møller, el *scattering* de Mott, el *scattering* de Bhabha, la aniquilación electrón–positrón y el *bremsstrahlung* o radiación de frenado. Los electrones pueden también emitir radiación, la llamada radiación de Cherenkov, cuando son acelerados dentro de un medio a una velocidad superior a la de la luz en ese medio. De entre estos mecanismos, los que debemos considerar en radioterapia son el *scattering* de Møller y el *scattering* de Mott.

Resumen del capítulo 3. Ecuaciones de transporte. Depósito de la energía y dosis absorbida.

El capítulo 3 presenta el modelo matemático que se sigue en la memoria para el cálculo de la dosis absorbida. El esquema para ese cálculo, de acuerdo con [15], es el siguiente:

1. Primero se resuelve la ecuación del transporte de Boltzmann (ETB) para fotones. El *output* es ψ_γ, la densidad media de fotones dentro del dominio espacial.

2. En segundo lugar,

   (a) Se resuelve la ETB para electrones

   o bien, aprovechando la Física que hay detrás,

   (b) Se resuelve la aproximación de Fokker–Planck de la ETB para electrones.

   El *output* del paso 1, ψ_γ, entra como un término fuente en el paso 2. Por lo tanto, este es un plan secuencial; es preciso completar el paso 1 antes de abordar el paso 2.

   El *output* del paso 2 es ψ_e, la densidad media de electrones en el dominio.

3. En tercer lugar, la función ψ_e se usa para calcular la dosis de radiación absorbida mediante una fórmula explícita que tiene en cuenta el tiempo de exposición a la radiación.

A partir de ahí, esta memoria se centra especialmente en la resolución del paso 1 (capítulo 4), si bien toca muy someramente, en el capítulo 5, el tema de la discretización mediante

diferencias finitas de algunos de los operadores diferenciales presentes en la ecuación de Fokker–Planck.

Se adopta una aproximación al problema que es *determinista*, lo cual quiere decir que, dejando aparte errores de redondeo del ordenador y errores de discretización de los métodos numéricos empleados, uno obtiene siempre la misma solución para el mismo conjunto de datos.

Hasta ahora, los cálculos de dosis más precisos se han obtenido mayoritariamente resolviendo la ecuación de Boltzmann mediante métodos *estocásticos* (no deterministas) de tipo Monte Carlo. Mientras que el método de Monte Carlo proporciona muy buenas aproximaciones de la dosis absorbida, este método presenta el inconveniente de que el tiempo de cálculo que requiere es elevado para ser empleado en usos clínicos. Algunos autores argumentan que es posible calcular la dosis absorbida en tiempos menores resolviendo ecuaciones cinéticas de tipo Boltzmann con métodos numéricos basados en mallas, librando de paso a la solución de ruido estocástico. Siguiendo esa línea, científicos de Los Alamos han desarrollado códigos como Attila© y Acuros™, a los que no tenemos acceso libre. Al respecto, pueden consultarse a día de hoy (16 de julio de 2012) las páginas *web*

http://www.varian.com/media/oncology/brachytherapy/pdf/AcurosBrochure_SP.pdf

y

http://www.lanl.gov/news/newsletter/110507.pdf.

La última sección de este capítulo está dedicada a explicar cómo se deposita la energía en las moléculas, lo que lleva finalmente a la fórmula para el cálculo de la dosis absorbida.

Resumen del capítulo 4. Resolución numérica de la ecuación del transporte de Boltzmann para fotones.

Con esas bases, en el capítulo 4 se resuelve, en un dominio tridimensional y posiblemente heterogéneo, la siguiente ecuación de Boltzmann para fotones, donde la incógnita es ψ_γ:

$$\mathbf{\Omega}_\gamma \cdot \nabla \psi_\gamma(\mathbf{r}, \mathbf{\Omega}_\gamma, \epsilon_\gamma) = [\mathrm{IS}(\psi_\gamma)](\mathbf{r}, \mathbf{\Omega}_\gamma, \epsilon_\gamma) - [\mathrm{OS}(\psi_\gamma)](\mathbf{r}, \mathbf{\Omega}_\gamma, \epsilon_\gamma), \tag{5.29}$$

siendo

$$[\mathrm{IS}(\psi_\gamma)](\mathbf{r}, \mathbf{\Omega}_\gamma, \epsilon_\gamma) = \rho_\mathrm{e}(\mathbf{r}) \int_0^\infty \int_{S^2} \widetilde{\sigma}_{\mathrm{C},\gamma}(\epsilon'_\gamma, \epsilon_\gamma, \mathbf{\Omega}'_\gamma \cdot \mathbf{\Omega}_\gamma)\ \psi_\gamma(\mathbf{r}, \mathbf{\Omega}'_\gamma, \epsilon'_\gamma)\ \mathrm{d}\mathbf{\Omega}'_\gamma\ \mathrm{d}\epsilon'_\gamma, \tag{5.30}$$

$$[\mathrm{OS}(\psi_\gamma)](\mathbf{r}, \mathbf{\Omega}_\gamma, \epsilon_\gamma) = \rho_\mathrm{e}(\mathbf{r})\ \sigma^{\mathrm{tot}}_{\mathrm{C},\gamma}(\epsilon_\gamma)\ \psi_\gamma(\mathbf{r}, \mathbf{\Omega}_\gamma, \epsilon_\gamma). \tag{5.31}$$

La ecuación (5.29) expresa el balance para la variación de ψ_γ en la dirección $\mathbf{\Omega}_\gamma$ (i. e., $\mathbf{\Omega}_\gamma \cdot \nabla\psi_\gamma$), y resulta útil verla como un conjunto infinito de ecuaciones, una para cada dirección $\mathbf{\Omega}_\gamma \in S^2$. El término IS($\psi_\gamma$) tiene en cuenta las ganancias debidas al *in–scattering* (fotones viajando en una dirección $\mathbf{\Omega}'_\gamma \neq \mathbf{\Omega}_\gamma$ que cambian su dirección hacia $\mathbf{\Omega}_\gamma$ debido a alguna colisión), y el término OS(ψ_γ) representa las pérdidas debidas al efecto contrario, el *out–scattering*.

Además:

1. $\mathbf{r} = (r_1, r_2, r_3)$ es el vector de posición en el espacio.

2. $\mathbf{\Omega}_\gamma$ es la dirección del movimiento de los fotones.

3. ϵ_γ es la energía, reescalada por la energía en reposo del electrón $mc^2 = 0.511$ MeV, siendo m la masa del electrón en reposo y c la velocidad de la luz en el vacío. Quiere esto decir que la energía real viene dada por $\epsilon_\gamma mc^2$ MeV; por ejemplo, un valor de $\epsilon_\gamma = 1$ (adimensional) indica una energía de 0.511 MeV.

4. S^2 es la esfera unidad $\mathbb{R}^3$. Los vectores $\mathbf{\Omega}_\gamma$ y $\mathbf{\Omega}'_\gamma$ viven en S^2; por lo tanto son siempre unitarios y, además, $\mathbf{\Omega}'_\gamma \cdot \mathbf{\Omega}_\gamma = \cos\vartheta_\gamma$, siendo ϑ_γ el ángulo en $[0, \pi]$ que forman $\mathbf{\Omega}'_\gamma$ y $\mathbf{\Omega}_\gamma$.

5. El operador ∇ indica gradiente con respecto a las tres variables espaciales.

6. $\psi_\gamma(\mathbf{r}, \mathbf{\Omega}_\gamma, \epsilon_\gamma)$ [fotones/(m^3 sr MeV)] es la densidad de flujo angular de fotones, es decir, el número medio de fotones por unidad de volumen, de ángulo sólido y de energía en el punto $\mathbf{r}$, volando en dirección $\mathbf{\Omega}_\gamma$ y con energía ϵ_γ. La integral

$$\int_0^\infty \int_{S^2} \psi_\gamma(\mathbf{r}, \mathbf{\Omega}'_\gamma, \epsilon'_\gamma)\ \mathrm{d}\mathbf{\Omega}'_\gamma\ \mathrm{d}\epsilon'_\gamma \tag{5.32}$$

   da el número medio de fotones por unidad de volumen en la posición $\mathbf{r}$. Otra forma de explicar el significado de ψ_γ es, de acuerdo con [15], decir que

$$\psi_\gamma(\mathbf{r}, \mathbf{\Omega}_\gamma, \epsilon_\gamma) \cos\Theta\ \mathrm{d}A\ \mathrm{d}\mathbf{\Omega}_\gamma\ \mathrm{d}\epsilon_\gamma$$

   es el número medio de fotones que se mueven a través del área $\mathrm{d}A$ en el elemento de ángulo sólido $\mathrm{d}\mathbf{\Omega}_\gamma$ en torno a $\mathbf{\Omega}_\gamma$ con energía en el intervalo $(\epsilon_\gamma, \epsilon_\gamma + \mathrm{d}\epsilon_\gamma)$, siendo Θ el ángulo entre $\mathbf{\Omega}_\gamma$ y el vector normal exterior a $\mathrm{d}A$.

7. ρ_e [electrones/m^3] es la densidad de electrones en el medio.

8. $\widetilde{\sigma}_{\mathrm{C},\gamma}$ [m^2/(sr MeV electrón)] es la sección eficaz diferencial para el *scattering Compton* de fotones. Está dada por las fórmulas siguientes (ver [15] y [7]):

$$\widetilde{\sigma}_{\mathrm{C},\gamma}(\epsilon'_\gamma, \epsilon_\gamma, \mathbf{\Omega}'_\gamma \cdot \mathbf{\Omega}_\gamma) = \sigma_{\mathrm{C},\gamma}(\epsilon'_\gamma, \mathbf{\Omega}'_\gamma \cdot \mathbf{\Omega}_\gamma)\ \delta_{\mathrm{C}}(\epsilon'_\gamma, \epsilon_\gamma, \mathbf{\Omega}'_\gamma \cdot \mathbf{\Omega}_\gamma), \tag{5.33}$$

donde

$$\sigma_{\mathrm{C},\gamma}(\epsilon'_\gamma, \mathbf{\Omega}'_\gamma \cdot \mathbf{\Omega}_\gamma) = \frac{r_{\mathrm{e}}^2}{2}\left[\frac{1}{1+\epsilon'_\gamma(1-\cos\vartheta_\gamma)}\right]^3\left[1+\cos^2\vartheta_\gamma + \frac{{\epsilon'_\gamma}^2(1-\cos\vartheta_\gamma)^2}{1+\epsilon'_\gamma(1-\cos\vartheta_\gamma)}\right] \tag{5.34}$$

y

$$\delta_{\mathrm{C}}(\epsilon'_\gamma, \epsilon_\gamma, \mathbf{\Omega}'_\gamma \cdot \mathbf{\Omega}_\gamma) = \delta\left(\epsilon_\gamma - \frac{\epsilon'_\gamma}{1+\epsilon'_\gamma(1-\cos\vartheta_\gamma)}\right), \tag{5.35}$$

donde δ es la delta de Dirac (ver punto 11).

En las fórmulas precedentes, se ha empleado en varias ocasiones la identidad $\mathbf{\Omega}'_\gamma \cdot \mathbf{\Omega}_\gamma = \cos\vartheta_\gamma$ explicada en el punto 4.

9. $\sigma_{\mathrm{C},\gamma}^{\mathrm{tot}}$ [m^2/electrón] es la sección eficaz total para el *scattering Compton* de fotones. Está dada por la fórmula siguiente (ver [15] y [7]):

$$\sigma_{\mathrm{C},\gamma}^{\mathrm{tot}}(\epsilon_\gamma) = 2\pi r_{\mathrm{e}}^2\left[\frac{1+\epsilon_\gamma}{{\epsilon_\gamma}^2}\left(\frac{2(1+\epsilon_\gamma)}{1+2\epsilon_\gamma} - \frac{1}{\epsilon_\gamma}\ln(1+2\epsilon_\gamma)\right) + \frac{1}{2\epsilon_\gamma}\ln(1+2\epsilon_\gamma) - \frac{1+3\epsilon_\gamma}{(1+2\epsilon_\gamma)^2}\right]. \tag{5.36}$$

10. En los puntos 8 y 9, r_{e} simboliza el radio clásico del electrón: $r_{\mathrm{e}} = 2.8179 \times 10^{-15}$ m.

11. La delta de Dirac que aparece en la Ecuación (5.35) debe ser entendida como se explica en [12, página 184]: si $f : (a,b) \to \mathbb{R}$, con $\varnothing \neq (a,b) \subseteq \mathbb{R}$, es una función diferenciable con N raíces $x_1, \ldots, x_N$ en (a,b), todas ellas simples, entonces

$$\int_a^b \phi(x)\ \delta(f(x))\ \mathrm{d}x = \sum_{n=1}^{N} \frac{\phi(x_n)}{|f'(x_n)|}, \tag{5.37}$$

siendo el resultado igual a 0 cuando f no tiene ninguna raíz en (a,b).

Aunque en esta memoria se muestran resutados numéricos para un dominio tridimensional y rectangular, el método se puede extender a dominios convexos generales. Con mayor precisión, podemos pensar que la ecuación se plantea en un dominio $Q \subset \mathbb{R}^3$ no vacío, abierto, acotado y convexo. Bajo esas hipótesis, su frontera ∂Q es Lipschitz, y por tanto la normal exterior unitaria $\boldsymbol{n}(\mathbf{r})$ en $\mathbf{r} \in \partial Q$ está bien definida en casi todo punto con respecto a la medida de superficie (también bien definida) sobre ∂Q.

Consideramos que la frontera ∂Q se divide en dos partes disjuntas: una parte Γ, donde se localiza la fuente de radiación entrante, y el resto de la superficie, que denotamos Λ, por la que no entra ninguna radiación. Se tiene por tanto que $\partial Q = \Gamma \sqcup \Lambda$, donde $\sqcup$ simboliza "unión disjunta".

Para cerrar la ecuación (5.29), se considera la siguiente condición de contorno:

$$\psi_\gamma(\mathbf{r}, \mathbf{\Omega}_\gamma, \epsilon_\gamma) = \begin{cases} \psi_\gamma^{\text{in}}(\mathbf{r}, \mathbf{\Omega}_\gamma, \epsilon_\gamma) & \text{si } \mathbf{r} \in \Gamma \text{ y } \mathbf{\Omega}_\gamma \cdot \boldsymbol{n} < 0, \\ 0 & \text{si } \mathbf{r} \in \Lambda \text{ y } \mathbf{\Omega}_\gamma \cdot \boldsymbol{n} < 0, \end{cases} \tag{5.38}$$

donde ψ_γ^{in} es la densidad de fotones que entran en Q a través de Γ (fotones entrantes) y $\boldsymbol{n} = \boldsymbol{n}(\mathbf{r})$ es la normal exterior unitaria en el punto $\mathbf{r} \in \partial Q$. Hacemos notar que la condición $\mathbf{\Omega}_\gamma \cdot \boldsymbol{n} < 0$ significa que $\mathbf{\Omega}_\gamma$ es una dirección que se dirige hacia el interior del dominio Q.

En el contexto de la radioterapia externa, es fácil imaginarse que Q es la parte irradiada del paciente, típicamente conteniendo estrictamente el tumor en consideración, y que Γ es la parte de la piel que recibe la radiación externa. Sin embargo, es mejor considerar que Q es la extensión de ese dominio que resulta de añadir al anterior el espacio que hay entre la piel del paciente y el acelerador lineal; en ese caso, Γ es la parte del acelerador que emite los fotones (rayos X de alta energía).

El método que empleamos para resolver la ecuación (5.29) junto con la condición de contorno (5.38) tiene su base en ciertas consideraciones físicas. Concretamente, se basa en que el camino libre medio de los fotones dentro del aire y del cuerpo humano es muy grande, lo cual quiere decir un fotón se desvía muy pocas veces, raramente más de dos o tres, al atravesar esos medios[1]. En consecuencia, para calcular el número total de fotones basta sumar, a los que no se han desviado, los que se han desviado una, dos o, más raramente, tres veces. En terminología matemática, es claro que podemos expandir ψ_γ como

$$\psi_\gamma(\mathbf{r}, \mathbf{\Omega}_\gamma, \epsilon_\gamma) = \sum_{i=0}^{N} \psi_\gamma^{(i)}(\mathbf{r}, \mathbf{\Omega}_\gamma, \epsilon_\gamma), \tag{5.39}$$

siendo

- $\psi_\gamma^{(0)}(\mathbf{r}, \mathbf{\Omega}_\gamma, \epsilon_\gamma)$ la densidad de fotones (en $\mathbf{r}$, moviéndose con dirección $\mathbf{\Omega}_\gamma$ y con energía ϵ_γ) que no han sufrido *scattering*,
- $\psi_\gamma^{(i)}(\mathbf{r}, \mathbf{\Omega}_\gamma, \epsilon_\gamma)$, para $i = 1, \ldots, N-1$, la densidad de fotones que han sufrido *scattering*

[1] Esta afirmación está naturalmente ligada a las escalas espaciales. El cuerpo humano ya delimita una escala espacial lo bastante pequeña para que la afirmación sea cierta, es decir, para que los fotones realmente se desvíen muy pocas veces dentro del cuerpo. En cuanto al aire, la escala espacial que se maneja en radioterapia es también pequeña (distancia entre acelerador lineal y paciente).

exactamente i veces, y

- $\psi_\gamma^{(N)}(\mathbf{r}, \mathbf{\Omega}_\gamma, \epsilon_\gamma)$ la densidad de fotones que han sufrido *scattering* al menos N veces (i. e., N veces o más).

Si suponemos que en la expansión anterior N es estrictamente mayor que M, es posible obtener una buena aproximación de ψ_γ de

$$\psi_\gamma(\mathbf{r}, \mathbf{\Omega}_\gamma, \epsilon_\gamma) \approx \sum_{i=0}^{M} \psi_\gamma^{(i)}(\mathbf{r}, \mathbf{\Omega}_\gamma, \epsilon_\gamma) \tag{5.40}$$

tomando $M = 2$ o $M = 3$. En esta tesis hemos comprobado que la elección $M = 2$ nos proporciona resultados muy precisos en nuestros ejemplos de prueba.

La posibilidad de obtener aproximaciones muy precisas con números bajos de M es crucial para la viabilidad del método, ya que el coste computacional que exige el cálculo de $\psi_\gamma^{(i)}$ crece muy rápidamente con i. En particular, esa es la razón por la que este método no puede ser empleado para resolver la ecuación de Boltzmann para electrones, los cuales tienen un camino libre medio mucho menor que el de los fotones.

Para obtener los valores de $\psi_\gamma^{(i)}$ es necesario calcular integrales sobre partes de la esfera S^2 que pueden ser muy pequeñas, ya que dependen de la zona irradiada, que es pequeña en comparación con el dominio total. Cuando el soporte del integrando es muy pequeño, no es conveniente aplicar una fórmula de cuadratura tomando como dominio toda la esfera o, hablando en términos de la parametrización de S^2 en coordenadas esféricas, no es conveniente aplicar la cuadratura en todo el rectángulo $[0, \pi] \times [0, 2\pi]$, ya que el número de puntos de la malla que caen dentro del soporte de la función puede ser muy pequeño o incluso nulo, dando lugar por tanto a aproximaciones poco precisas de la integral. Para salvar este problema, lo ideal es aplicar la fórmula de cuadratura sobre el soporte del integrando; sin embargo, la determinación exacta del soporte es muy complicada, razón por la cual la estrategia que seguimos es la determinación, en el rectángulo $[0, \pi] \times [0, 2\pi]$, del menor rectángulo que contiene el soporte. Encontrar ese rectángulo mínimo es mucho más sencillo y, una vez determinado, las integrales se calculan mediante la fórmula compuesta de los trapecios, con nodos equiespaciados, en dos dimensiones.

Los resultados numéricos que se presentan en la memoria consideran un dominio espacial cúbico Q. Asimismo, la condición de contorno es cero en toda la frontera excepto en una pequeña zona cuadrada de la cara superior, que representa la salida del acelerador lineal. Por esa pequeña zona cuadrada entra la radiación en el dominio. En primera instancia, la radiación se encuentra con aire y, en segunda instancia, con agua. Considerar agua

para simular tejidos del cuerpo humano es una técnica estándar en radioterapia cuando se piensa en ejemplos de prueba (*benchmark problems*), ya que las interacciones del agua con la radiación son similares a las que experimenta el tejido.

Una pieza importante del algoritmo es el cálculo del punto frontera. Dado un punto $\mathbf{r}$ interior al dominio Q y dada una dirección $\mathbf{\Omega}_\gamma \in S^2$, por punto frontera (asociado al par $(\mathbf{r}, \mathbf{\Omega}_\gamma)$) queremos decir el único punto $\mathbf{r}^* \in \partial Q$ que se encuentra al viajar en línea recta, desde $\mathbf{r}$, en la dirección $-\mathbf{\Omega}_\gamma$. Una vez obtenido $\mathbf{r}^\star$, basta aplicar una ley de decrecimiento exponencial, que se deriva de la ETB, para el cómputo de los fotones que no han sufrido *scattering*.

Para dominios diferentes al cubo o a un paralelepípedo rectangular, la adaptación del código desarrollado pasa por la programación de un método para el cálculo del punto frontera. En particular, como decíamos antes, la extensión es factible al caso de dominios convexos generales.

Resumen del capítulo 5. Un esquema de diferencias finitas para un problema de valor final degenerado.

Puesto que el método para resolver la ETB para fotones, de expansión en órdenes de *scattering*, no es aplicable a la ETB para electrones y, por otra parte, la resolución directa de la misma es muy costosa, es lógico que exista investigación con el objetivo de buscar otras formas de calcular la densidad angular de electrones ψ_{e}. Una alternativa a la resolución directa de la ETB para electrones es resolver en su lugar la llamada ecuación de Fokker–Planck. Dicha ecuación se obtiene, mediante desarrollos asintóticos, de la ETB bajo las hipótesis de pequeños ángulos de *scattering* y de pequeñas pérdidas de energía en los choques, que son dos conocidas características de los electrones.

El capítulo 5 incluye los primeros pasos dados en la búsqueda de un esquema de diferencias finitas para resolver la ecuación de Fokker–Planck para electrones. Una de las singularidades de esta ecuación es que es degenerada en la variable angular $\mu_{\mathrm{e}} \in [-1, 1]$ (ver ecuación (5.4) de esta memoria), debido a que el coeficiente del operador de Laplace en la esfera $(1 - \mu_{\mathrm{e}}^2)$ se anula en la frontera del dominio $[-1, 1]$. En consecuencia, no son necesarias condiciones de contorno en esa variable. Por otra parte, la condición con respecto a la variable energética ϵ_{e} no es inicial sino final. Esto es, no se da la solución para $\epsilon_{\mathsf{e}} = 0$, sino para $\epsilon_{\mathsf{e}} = \infty$ o, cuando se buscan aproximaciones numéricas, para ϵ_{e} igual a un valor suficientemente grande.

Desde una perspectiva *naïf*, es decir, a partir del único conocimiento de las fórmulas de derivación numérica de tipo interpolatorio polinómico, se busca una discretización con diferencias finitas apropiada a la situación. En concreto, se resuelve el siguiente problema de valor final para una EDP que retiene los operadores que en Fokker–Planck efectúan la derivación con respecto a μ_{e}, que pasa a ser x, y a ϵ_{e}, que pasa a ser t:

$$\frac{\partial u}{\partial t}(t,x) + \frac{\partial}{\partial x}\left[(1-x^2)\frac{\partial u}{\partial x}\right](t,x) = M(t,x) \quad \text{para } (t,x) \in (0,T)\times(-1,1), \tag{5.41}$$

$$u(T,x) = u_T(x) \quad \text{para } x \in (-1,1). \tag{5.42}$$

Las inhomogeneidades M y u_T, que pueden calcularse para $u(t,x)$ dada, sirven para disponer de problemas con solución exacta conocida, que nos permiten comparar los valores exactos con los valores aproximados.

Se proporciona un esquema de diferencias finitas para resolver el anterior problema de valor final. De acuerdo con lo esperado de las aproximaciones empleadas, se obtienen órdenes numéricos de convergencia iguales a 1 en t y a 2 en x.

Bibliography

[1] Ahnesjö, A.; Aspradakis, M. M., 1999, Dose calculation for external photon beams in radiotherapy *Phys. Med. Biol.*, **44** R99-R155.

[2] Alpen, E. L. , 1990, Radiation Biophysics (Englewood Cliffs: Prentice-Hall).

[3] Andreo, P., 1991, Monte Carlo Techniques in medical radiation physics *Phy. Med. Biol.*, **36** 861-920.

[4] Bell, G. I.; Glasstone, S., 1970, Nuclear Reactor Theory (Van Nostrand Reinhold).

[5] Boman, E., 2006, Forward and Inverse Problem Applying Boltzmann Transport Equation *Kuopio University Publication C. Natural and Environmental Sciences.*

[6] Börgers, C.; Larsen, E.W., *Asymptotic derivation of the Fermi pencil-beam approximation*, Nuclear Sci. Eng., 2123(1996), pp. 343-357.

[7] Davisson, C. M.; Evans, R. D., 1952, Gamma-ray absorption coefficients *Rev. Mod. Phys.* **24** 79-107.

[8] Duderstadt, J. J.; Martin, W. R., 1979, Transport Theory (Wiley-Interscience).

[9] Edward, L. A., 1998, Radiation Biophysics Second Edition, *Academic Press*, USA.

[10] Eyges, L., 1948, Multiple scattering with energy loss *Phys. Rev.* **74** 1534-35.

[11] Fano, U.; Spencer, L. V.; Berger, M. J., 1959, Penetration and diffusion of X rays *Handbuch der Physik* **vol** XXXVIII/2 ed S Flügge(Berlin: Springer).

[12] Gel'fand, I. M.; Shilov, G. E. (1966, second printing; first printing dated 1964; original Russian edition dated 1958) *Generalized Functions. Volume I: Properties and Operations.* Academic Press, New York (NY) [etc.].

[13] Gustafsson, A.; Lind, B. K.; Brahme, A., 1994, A generalized pencil beam algorithm for optimization of radiation therapy *Med.Phy.*, **21** 343-56.

[14] Hämmertin, G.; Hoffmann, K. H., *Numerical Mathematics*, Grundwissen Mathematik 7, Springer-Verlag, 1989.

[15] Hensel, H.; Iza-Teran, R.; Siedow, N., *Deterministic model for dose calculation in photon radiotherapy*, *Phys. Med. Biol.*, **51** (2006) 675-693.

[16] Henyey, L. G.; Greenstien, J. L., 1941, Diffuse radiation in the galaxy, Astrophys. J.**93** 70-83.

[17] Hogstrom, K. R.; Mills, M. D.; Almond, P. R., 1981, Electron beam dose calculation *Phys. Med. Biol.* **26** 445-59.

[18] Johns, E. J.; Cunningham, J. R., 1983, The Physics of Radiology (Springfield: Charles C. Thomas Publisher).

[19] Karimov, U. U., 2010, *A Deterministic Model for Computing the Radiation Dose in Cancer Treatment.* Master Project, Master in Mathematical Engineering, UDC-USC-UVIGO.

[20] Kawrakew, I.; Rogers, D. W. O., 2002, *The EGSnrc Code System (Ottawa: NRCC Report PIRS-701).*

[21] Khan, F. M., Treatment Planning in Radiation Oncology. 2nd Edition, *Lippincott Williams and Wilkins.*

[22] Lehmann, C., 1977, *Interaction of Radiation With Solids and Elementary Defect Production* (Amsterdam: North Holland).

[23] López López, J.A., 2008, *Aspectos médico-biológicos y físicos de la radioterapia como tratamiento del cáncer. Modelo determinista para el cálculo de la dosis absorbida.* Proyecto Fin de Máster, Master in Mathematical Engineering, UDC-USC-UVIGO.

[24] Mott, N. F.; Massey, H. S. W., 1965, *The Theory of Atomic Collisions(Oxford: Clarendon).*

[25] Nachtmann, O., 1986, Elementarteilchenphysik, Phänomene and Konzepte (Braunschweig:Vieweg).

[26] Olbrant, E. ; Frank, M., *Application of generalized Fokker-Planck theory of electron and photon transport in tissue*, arXiv:0912.1821V1 [*Physics. Med-Ph.*], 9 Dec 2009.

[27] Pomraning, G. C., 1992, The Fokker-Planck operator as sn asymptotic limit *Mathematical Model and Mrthods in Applied Sciences* **Vol.2, No.1**21-36.

[28] Przybylski, K.; Ligou, J., 1982, Numerical analysis of the Boltzmann equation including Fokker-Planck terms, *Nuclear Sci. Engrg.* **81** 92-109.

[29] Rainville, E. D., 1960, Special Function (Macmillan).

[30] Rossi, B.; Greisen, K., 1941, Cosmic-ray theory. *Rev. Mod. Phys.*, **13** 340-309. Fermi's work given on pp. 265-68.

[31] Syed, N. A., *Physics and Engineering of Radiation Detection*, 2007, first edition, *Academic Press Inc.*

[32] Tervo, J.; Kolmonen, P.; Vauhkonen, M. ; Heikkinen, L. M.; Kaipio, J. P. , 1999, A finite-element model of electron transport in radiation therapy and related inverse problem *Inverse Problems* **15** 1345-61.

[33] Tervo, J.; Kolmonen, P., 2002, Inverse radiotherapy treatment planning model applying Boltzmann-transport equation *Math. Models Methods Appl. Sci.* **12** 109-41.

[34] Ulmer, W.; Harder, D., 1995, A triple Gaussian pencil beam model for photon beam treatment planning Z. *Med.Phys.*, **5** 25-30.

[35] Williams, M. M. R., 1979, The role of the Boltzmann transport equation in radiation damage calculation *Prog. Nucl. Energy 31-65.*

[36] Zerby, C. D. ; Keller, F. L., 1967, Electron transport theory, calculation and experiments *Nucl. Sci. Eng.***27** 190-218.

[37] Zhengming, L.; Chengjun, G.; Zhangwen, W., 2004, Characteristic line theory of photon transport *Proc. of the 14th Int. Conf. on the Use of Computers in Radiation Therapy(Seoul)* 658-63.

[38] http://en.wikipedia.org/wiki/Management_of_cancer.

[39] http://rcwww.kek.jp/research/egs/docs/pdf/iccr_1994.pdf.

[40] http://www.cs.otago.ac.nz/cosc453/student_tutorials/monte_carlo.pdf.

[41] http://info.cancerresearchuk.org/cancerandresearch/all-about-cancer/what-is-cancer/treating-cancer/history-of-radiotherapy/radiotherapy3.

[42] http://en.wikipedia.org/wiki/History_of_radiation_therapy.

[43] http://www.brachytherapy.com/.

[44] http://www2.dailyprogress.com/lifestyles/cdp-lifestyles/2011/apr/03/radiation-therapy-falls- under-three-main-types-ar-944153/

[45] Biological Effects of Radiation, USNRC Technical Training Center. Internet cite: http://www.nrc.gov/reading-rm/basic-ref/teachers/09.pdf.

[46] http://www.cancer.org/Treatment/TreatmentsandSideEffects/TreatmentTypes/Radiation/RadiationTherapyPrinciples/radiation-therapy-principles-how-does-radiation-work.

[47] http://www.cancernews.com/data/Article/295.asp.

[48] http://staff.jccc.net/pdecell/celldivision/cellcycle.html.

[49] http://www.rare-earth-magnets.com/t-conductors-and-insulators.aspx.